Development and Application of a Wearable Device for Real Time Potentiometric Determination of Electrolytes in Sweat

By

Thomas (Tom) Glennon (B.Sc., M.Sc.)
Thesis submitted for the Degree of **Master of Science**

Dublin City University

Supervisor:
Prof. Dermot Diamond
Co-Supervisor:
Prof. Jens Ducrée

School of Chemical Sciences

January 2017

Declaration

I hereby certify that this material, which I now submit for assessment on the programme of study leading to the award of Master of Science, is entirely my own work, and that I have exercised reasonable care to ensure that the work is original, and does not to the best of my knowledge breach any law of copyright, and has not been taken from the work of others save and to the extent that such work has been cited and acknowledged within the text of my work.

Signed: _____

Thomas Glennon

ID No.: 14211685

Date:

Acknowledgements

Initially I would like to thank Prof. Dermot Diamond for giving me the opportunity to develop my research experience and skills in the Insight Centre for Data Analytics and the National Centre for Sensor Research and for providing his support and guidance throughout.

I would also like those in the adaptive sensors group who have supported me throughout the past two years including Dr Margaret McCaul, Dr Giusy Matzeu, Dr Matthew Jacobs, Conor O'Quigley and Eoghan McNamara. You have all put a lot of work into this project and I will always be grateful to you for it. To all the other members of the group throughout the years thank you for your friendship and support particularly Dr Simon Coleman for always being on hand for advice and distraction when needed.

Also my first experiences in research and my reason for continuing within it came in the microfluidics group of Prof. Jens Ducrée and I would like to thank him for that opportunity. To everyone in that group thank you for your support and friendship throughout the years. I have also been lucky enough to work abroad in some great groups during my studies and for this I would like to thank Prof. Gordon Wallace and everyone in his group in the University of Wollongong as well as Dr Fernando Benito Lopez and everyone I was lucky enough to work with in CIC microGUNE in Arrasate-Mondragon.

I would like to thank all of my family and friends for their support in all my endeavours up to this point. To Mam and Dad, thank you for your unwavering pride and support, I will always try to live as you have thought me, even though I may need reminding every now and then.

Last but certainly not least I thank, with all my sincerity, Cliana Quirke for your support in every aspect of my life for the past six years, I hope I can pay back even half of what you have done for me. You have been a rock and an inspiration.

Publications

Relevant Publications:

Peer Reviewed Journal Articles:

1. **T. Glennon,** C. O'Quigley, M. McCaul, G. Matzeu, S. Beirne, G. G. Wallace, F. Stroiescu, N. O'Mahoney, P. White and D. Diamond. *'"SWEATCH": A Wearable Platform for Harvesting and Analysing Sweat Sodium Content'.* Electroanalysis, 28, no. 6 (1 June 2016): 1283–89. DOI:10.1002/elan.201600106.
2. G. Matzeu, C. O'Quigley, E. McNamara, C. Zuliani, C. Fay, **T. Glennon** and D. Diamond. *An Integrated Sensing and Wireless Communications Platform for Sensing Sodium in Sweat.* Analytical Methods, 8, no. 1 (23 October 2015), 64-71. DOI: 10.1039/C5AY02254A

Conference Contributions:

Oral Presentations:

1. **T. Glennon**, C. O'Quigley, M. McCaul, G. Matzeu, S. Beirne, G. G. Wallace, F. Stroiescu, N. O'Mahoney, P. White, J. Ducrée and D. Diamond, *'SWEATCH' A fully integrated wearable watch-type platform for real-time sweat analysis and collection*, ESEAC 2016, Assembly Rooms, Bath, United Kingdom, 14 June 2016

Poster Presentations:

1. **T. Glennon,** *SwEatch: A Fully Integrated Wearable Sweat Analysis Device.* 3rd Annual Insight Student Conference, DCU Dublin, 14 September 2016,
2. **T. Glennon,** Conor O'Quigley, M. McCaul, G. Matzeu, S. Beirne, G. G. Wallace, F. Stroiescu, N. O'Mahoney, P. White and D. Diamond, *'SWEATCH': Wearable, Real-Time Monitoring of Electrolyte Levels in Sweat,* CASi 2016, DCU Dublin, 14th April 2016

3. **T. Glennon,** C. O'Quigley, G. Matzeu, E. Mc Namara, K. Fraser, M. McCaul, J. Ducrée, S. Beirne, G. Wallace, F. Stroiescu, P. White and D. Diamond, *The Development of a Watch-Type Sensing Platform for Real-time Monitoring of Sodium Levels in Sweat,* 2nd Annual Insight Student Conference, NUIG Galway, 30 October 2015,

Other Publications:

Conference Contributions:

Oral Presentations:

1. **T. Glennon,** P. Floris, E. McNamara, C. O'Quigley, K. J. Fraser, Y. Yang, A. Smeaton, J. Ducrée and D. Diamond. *Development of a Sensitive, Low-Cost and User-Friendly Centrifugal Microfluidic Disc for Multi-Analyte Environmental Monitoring,* 10th Annual International Electromaterials Science Symposium, Wollongong, Australia, 11 - 13 February 2015.
2. **T. Glennon,** J. Saez-Castano, J. Ducrée, D. Diamond, and F. Benito-Lopez. Photo-switchable microvalve in a reusable lab-on-a-disc. 18th International Conference on Solid-State Sensors, Actuators and Microsystems (Transducers 2015), June 21–25, Anchorage, Alaska, USA, 2015.
3. **T. Glennon,** P. Floris, C. O'Quigley, E. Mc Namara, Y. Yang, K. J. Fraser, A. Smeaton, J. Ducrée, and D. Diamond. Development of a sensitive, low-cost and user-friendly centrifugal microfluidic cartridge for multi-analyte environmental monitoring. In Proceedings of the Conference on Sensors in the Environment 2014 in London, England, October 15-16, 2014.

Poster Presentations:

1. P. Floris, T. Glennon, C. O'Quigley, E. Mc Namara, Y. Yang, J. Ducrée, A. Smeaton, D. Diamond, and K. J. Fraser. *Development of a portable multi-parameter centrifugal microfluidic analysis system (CMAS) for water quality monitoring,* 2nd International Conference on MicroFluidic Handling Systems (MFHS 2014) in Freiburg, Germany, October 8 – 10, 2014.

2. T. Glennon, P. Floris, C. O'Quigley, E. Mc Namara, K. J. Fraser, Y. Yang, A. Smeaton, J. Ducrée, and D. Diamond. *CMAS: Environmental monitoring using a disk to data approach,* 1st Annual Insight Student Conference 2014, UCD Dublin, September 12, 2014.

List of Publications and Author Contribution

The work presented in this thesis was carried out by the candidate under the supervision of Prof. Dermot Diamond at Dublin City University, within the Insight Centre for Data Analytics and National Centre for Sensor Research.

Chapters 2, 3 and 4 present and expand on the work presented in a peer reviewed article. The candidate is a co-author and conceived, designed and performed the experiments with the other co-authors. The paper has been rearranged for the consistency of the thesis and is distributed, where relevant, among chapters 2, 3 and 4.

Paper	Chapter	Title	DOI
1	2,3,4	"SWEATCH": A Wearable Platform for Harvesting and Analysing Sweat Sodium Content	10.1002/elan.201600106

List of Abbreviations

API	Application Programming Interface
CAD	Computer Aided Design
CIM	Colloid-imprinted mesoporous
CMOS	Complementary metal-oxide-semiconductor
CNT	Carbon nanotube
CP	Conducting Polymer
ECG	Electrocardiogram
EIS	Electrochemical impedance spectroscopy
Emf	Electromotive force
EMG	Electromyography
FPCB	Flexible printed circuit board
FTIR	Fourier transform infrared
ICT	Information and communications technology
IL	Ionic liquid
ISE	Ion-selective electrode
ISF	Interstitial fluid
LED	Light-emitting diode
MCV	Multi-channel voltmeter
NFC	Near field communication
PCB	Printed circuit board
PDMS	Polydimethylsiloxane
PMMA	Poly(methylmethacrylate)
PSA	Pressure-sensitive adhesive
RE	Reference electrode
RFID	Radio frequency identification
SC	Solid contact
SEM	Scanning electron microscopy
SPE	Screen-printed electrode
SSB	Sodium sensor belt

Abstract

Development and Application of a Wearable Device for Real Time Potentiometric Determination of Electrolytes in Sweat
Tom Glennon

The most common methods of biomedical diagnosis are blood-based and therefore require invasive methods for acquiring a sample causing trauma and presenting a risk of infection. This has led to the development of sensors targeting minimally invasive bio-fluids such as interstitial fluid and non-invasive bio-fluids including saliva and sweat. The monitoring of sweat in electrolytes, for example, has a number of applications including determining the efficacy of drugs on the chloride and sodium levels in cystic fibrosis patients as well as the monitoring of hydration levels in athletes to detect non-symptomatic overhydration, dehydration and fatigue.

This work presents the development of a platform for harvesting and analysing the sodium content of sweat in real time. In chapter 2 miniaturised solid-state sodium-selective and reference electrodes are developed, characterized and optimised. In chapter 3 these sensors are then incorporated into a custom designed sampling and fluidic system allowing passive transfer of the sweat from a point of contact on the skin to a fluidic channel across the electrodes for analysis before transport to a sampling reservoir. Chapter 4 presents the integration and real-time on-body trials of the sensing and fluidic components with a custom-designed electronic circuit board and lithium battery.

Two platforms were developed, a 'watch' type format for wrist based analysis and a 'pod' format, arranged horizontally for adaptable monitoring in various regions of the body. The devices can be easily disassembled to replace the electrodes and the high capacity adsorbent material. The storage sweat is available for subsequent measurement of the total volume of sweat harvested and the average concentration of sodium over the period of use. Results obtained during trials over

a period of up to 60 minutes controlled exercise are consistent with previously published data, showing a gradual increase of the sodium concentration in the sweat during this period.

Table of Contents

Chapter 1 A Review of the Advances, Challenges and Opportunities in Wearable Technology for Chemical Analysis of Sweat

1.1 Introduction

The biomedical diagnostics industry is currently evolving from large expensive lab based devices to small portable systems allowing personal sensing and point of care analysis [1]. One of the key examples of this is in the integration of miniaturised chemical sensing with wearable technology, which is currently one of the fastest growing sectors in the world. A recent report estimates the wearable technology market to be currently worth $30 billion and predicts it to rise to $150 billion by 2026 [2], [3]. While in that report wearable technology encompasses all electronic products designed to be worn on the body it also specifies an expected compound annual growth rate of 32% for wearable chemical sensors for the next 10 years [3].

This economical and technological environment is providing great opportunities for the development of wearable sensors for a range of biomedical purposes from the monitoring of mobility in rheumatoid arthritis patients [4] to the monitoring of glucose levels in ocular fluid [5]. One of the main advantages of wearable chemical sensing is the ability to incorporate non-invasive sensing which uses readily available fluids such as saliva, sweat and tears to test for a target analyte instead of obtaining a blood sample by traditional methods, such as phlebotomy or finger prick which risk infection and trauma [6]. These sensors also allow real-time monitoring which allow collection of information about an individuals biochemical responses to certain activities such as exercise while they can also be employed to monitor exposure to chemicals in the environment including the levels of toxic volatile organic compounds at gas stations [7].

An application of wearable sensors currently drawing considerable interest is the monitoring of electrolyte levels in sweat as it has applications in monitoring

the performance of athletes as well as in providing information in medical conditions such as cystic fibrosis. While the fabrication and mode of action of wearable sensors can vary widely there are many common issues in their incorporation into wearable platforms including aesthetics, ergonomics, data analysis, wireless communication and an integrated power supply. This chapter reviews the advances, opportunities and challenges in the development of wearable sensors for monitoring electrolyte levels in real time. The first section focuses on the overall technology developed for wearable biomedical monitoring with emphasis on the application of this technology to non-invasive chemical monitoring before focusing on the values of sweat as a diagnostic medium. The second section looks at the development of ion selective electrodes (ISEs) and their use in wearable sensors. A third section focuses on advances in research contributing to the realisation of fully integrated wearable analysis systems.

1.2 Wearable Sensor Technology in Personal Sensing and Point of Care Diagnostics

Wearable sensors employing a range of technologies are being used for a range of applications in biomedical diagnostics. The best known physiological sensors are wearable fitness trackers which monitor physical activity such as speed, steps taken and heart-rate to provide constructive feedback to the user and are widely commercially available [8]–[10]. These devices have also helped monitor patients rehabilitation along with other more specialised sensors such as mobility monitors and sensors for monitoring cardiovascular and motor-neuron function through the analysis of electrical signals based on electrocardiogram (ECG) and electromyography (EMG) [11], [12]. Chemical sensors are used to detect specific analytes present on the wearer or in the surrounding environment.

One approach to wearable technology is the incorporation of electronics and interconnections into fabric to create smart textiles [13]. An example of this was developed by Paul *et al.* by screen printing electrodes directly onto a woven textile to create a chest band for ECG monitoring and a head band for facial EMG

monitoring (a, Figure 1-1) [14]. Smart textiles have also been developed incorporating conductive yarn into a flexible material giving it piezoresistive properties which provide an electrical response when submitted to a strain allowing collection of information about body movements [15], [16]. Coyle *et al.* used this approach to develop a glove to monitor the mobility in the finger joints and hands by employing stretch sensors alongside a 3 axis accelerometer connected to a 3D printed housing containing a microcontroller, Wi-Fi module and a Lithium Polymer battery (b, Figure 1-1) [4].

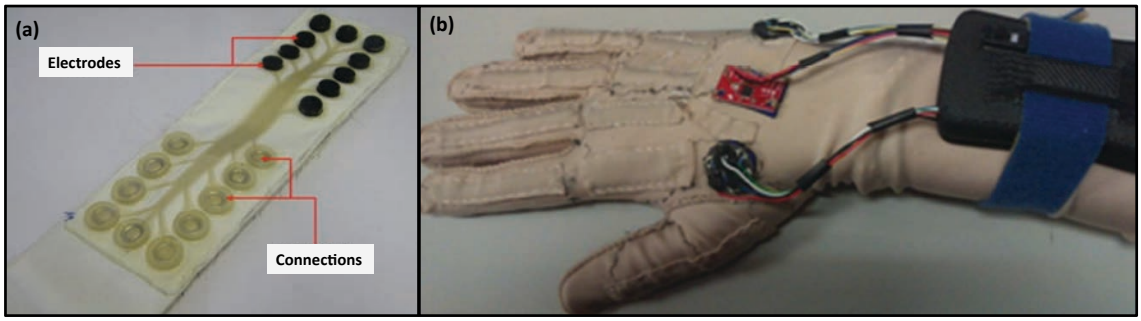

Figure 1-1: Two examples of smart textiles. (a) A facial EMG headband with screen-printed electrodes (adapted from Ref. [14]) and (b) a glove incorporated with piezoresistive fabric sensors to monitor the movement in the hand (adapted from Ref. [4]).

1.2.1 Minimal and Non-invasive Chemical Sensing

Wearable sensing provides an alternative to the traditional methods of diagnosis and biochemical monitoring which required a blood sample acquired through invasive methods causing physical trauma and risking infection [17]. This has led to the development of safer and less invasive alternatives which is particularly evident in the case of glucose monitoring in diabetics [18] with self monitoring required in individuals with both type 1 and type 2 diabetes [19], [20].

Alternative technologies to blood glucose can be minimally invasive, through monitoring of glucose levels in the interstitial fluid (ISF), or non-invasive which do not require any penetration of the skin barrier. Glucose levels in interstitial fluid are slower to rise than blood glucose levels with a mean lag time of 6.7 min [21], while ISF may show falling glucose levels before blood [18], [22]. An example of a commercially available minimally invasive wearable ISF glucose

monitor is the Abbott Freestyle Libre which uses a 0.4 mm thick micro needle to access the interstitial fluid in the subcutaneous layer 5 mm beneath the skin surface allowing it to wirelessly monitor glucose levels over 14 days with the application of a single sensor [23]–[25]. ISF glucose monitoring has also been developed through non-invasive means such as using reverse iontophoresis to cause uncharged and charged species to pass through the dermis with the application of a low electric current [26]. This approach was employed in the electrochemical glucose monitor GlucoWatch® Automatic Glucose Biographer, before it was withdrawn from the market due to reports of skin irritation [27], [28]. Lee *et al.* have reported a non-invasive sweat-based glucose and pH monitoring also incorporating a minimally invasive controlled transcutaneous drug delivery system through biodegradable temperature responsive microneedles [29].

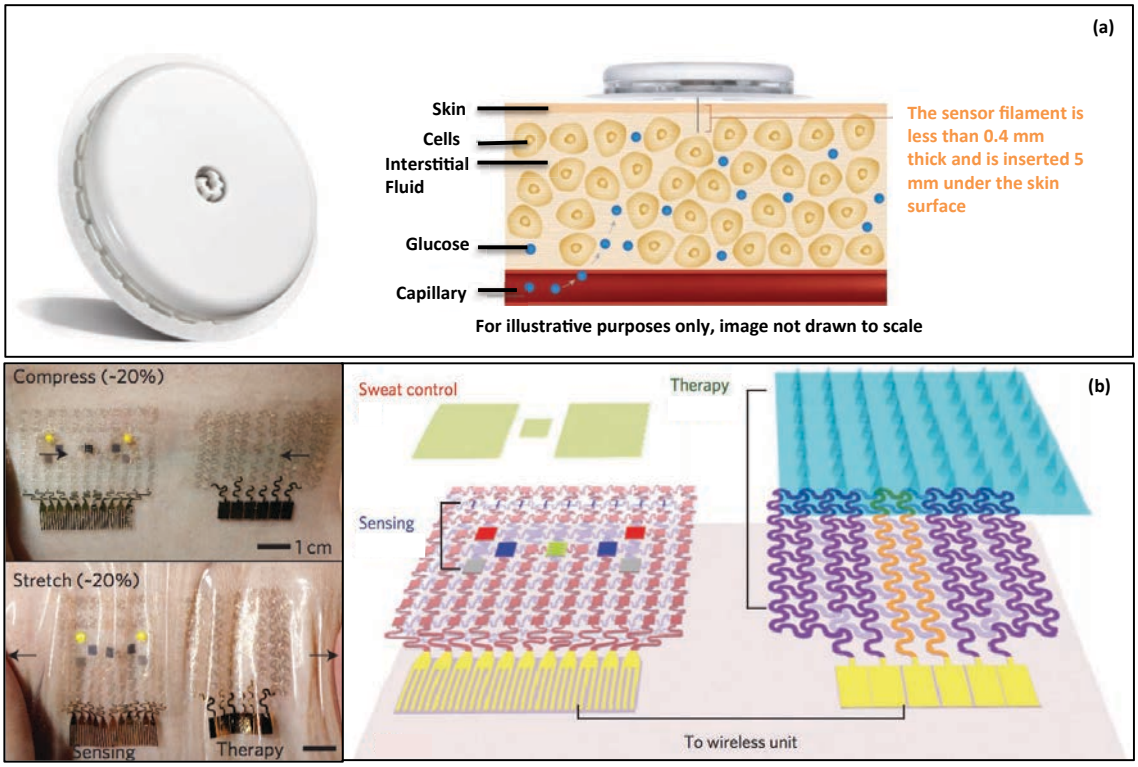

Figure 1-2: Wearable glucose monitoring. (a) The Abbott Freestyle Libre sensor with a schematic showing mechanism of entry to subcutaneous layer (adapted from Ref. [23], [30]) . (b) A combined sweat glucose monitor and subcutaneous drug delivery system from Lee *et al.* in place on skin with a schematic showing the individual components including microneedle array (adapted from Ref. [29]).

Some progress has been made in non-invasive optical sensing with the development of BSXinsight, a commercially available wearable device which uses near infrared LED technology to measure gastrocnemius muscle oxygenation and predict lactate threshold in cyclists [31], [32]. However, the most common targets for non-invasive chemical sensing are readily available biofluids such as tears, saliva and sweat [6], [33], [34].

1.2.1.1 Ocular Fluid Based Wearable Sensors

Tear fluid is a source of many analytes of interest in medical diagnostics including glucose, lactate, Na^+, K^+, and urea [35]–[38]. Due to their well defined prolonged use in the eye contact lenses are being developed with embedded sensors to analyse this information rich fluid in real time as well as being investigated for drug delivery and for the delivery of stem cells to treat corneal blindness [39]–[41]. Electrochemical sensors are the most popular methods for incorporation into contact lenses due to the lack of a need for reagents and the ease of integrating electrodes onto polymer surfaces [35], [36]. Liao *et al.* developed a non-invasive contact lens for fully integrated electrochemical continuous glucose monitoring consisting of a glucose sensor with power management, readout circuitry, wireless communication interface, LED driver, and energy storage capacitors in a CMOS chip on a polymer substrate [42]. Optical methods for wearable analysis of tears such as the use of boronic acid based colorimetric glucose monitoring in contact lenses are also being investigated [43]–[45].

1.2.1.2 Wearable Saliva Based Sensing

Saliva is a popular medium for non-invasive diagnostics [34] as it is readily available and is a source of many analytes including glucose, lactate and phosphate as well as several enzymes, antibodies and hormones such as salivary alpha amylase, immunoglobulin g, cortisol and testosterone [46]–[49]. Disposable electrochemical sensors have been developed for salivary analysis with some being integrated into mouth guards for wearable analysis [50], [51].

One example of this is a screen-printed amperometric uricase/Prussian-blue based sensor integrated with an amperometric circuit board on a mouth guard developed by Kim *et al.* for real time wireless monitoring of salivary uric acid [52]. Another approach to wearable oral analysis was demonstrated by Mannoor *et al.* in the development of a parallel resonant circuit with a gold inductive coil for wireless transmission, and inter digitised capacitive electrodes integrated onto a graphene/silk film which is adhered directly to the tooth allowing wireless detection of bacteria on tooth enamel [53].

1.2.1.3 Wearable Sweat Based Sensors

Sweat has many applications in medicine as a source of many metabolites such as glucose and lactate and xenobiotics such as prescription drugs, alcohol, marijuana and cocaine [54]–[57]. Sweat electrolyte analysis has particular potential in the diagnosis of cystic fibrosis and monitoring performance levels in athletes [58], [59]. The development of sensors for wearable monitoring of sweat is particularly desirable because of the potential to integrate them with smart watches and similar devices.

Wearable sweat sensing is evolving rapidly as technology allows the fabrication of smaller electronic, fluidic and sensing systems. An early example of chemical sweat sensing is evident in a 2009 publication by Morris *et al.* [60] as a wearable textile based sensor integrating LEDs for paired emitter-detector diode [61] colorimetric determination of pH in sweat (a, Figure 1-3). A waistband was fabricated from a polyester/lycra blend material and Bromocresol purple, a pH sensitive dye, was immobilised within channels defined by a silicon sealant. As sweat accumulated on the skin it wicked through the fabric into the channel through the immobilised dye to an area directly under the LED system, connected to an electronic circuit allowing real-time monitoring of sweat pH in the relevant range of 5-7 [60], [62].

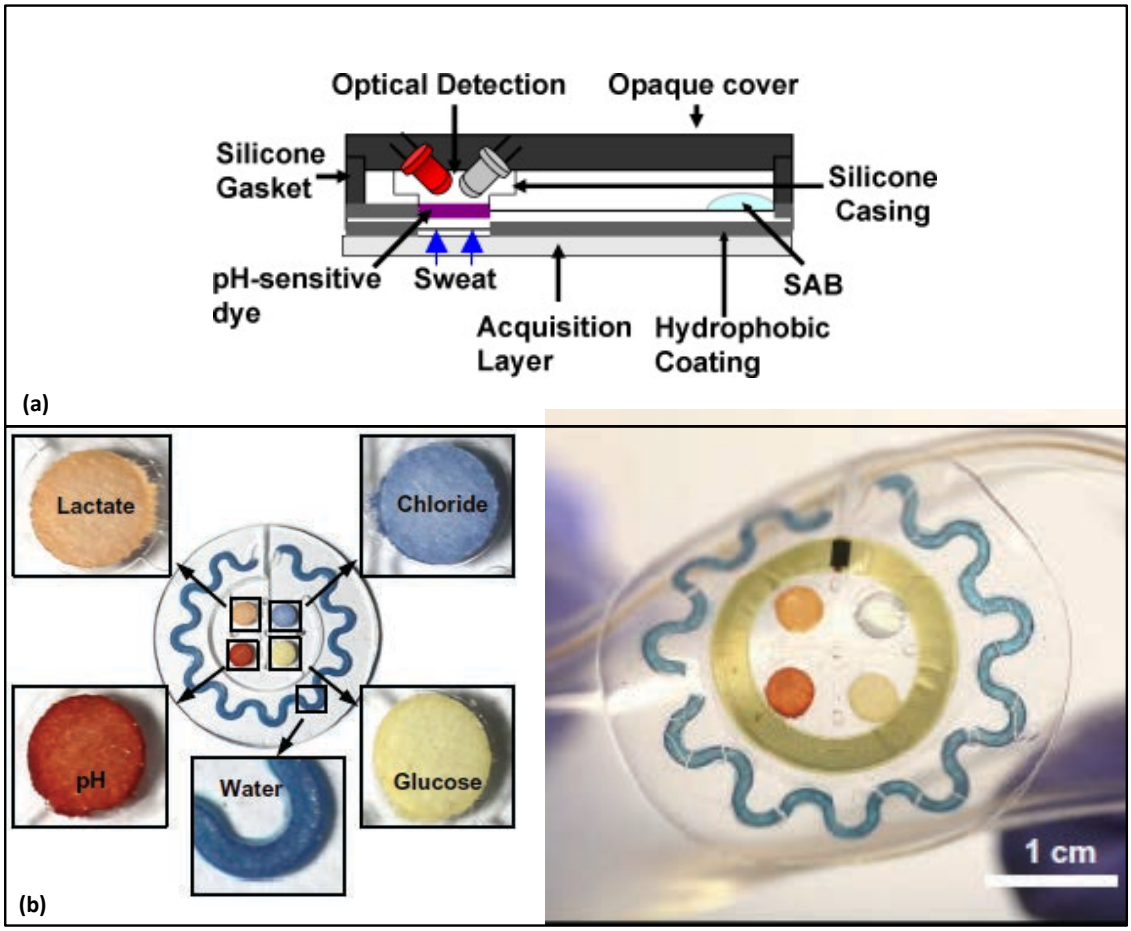

Figure 1-3: Advances in wearable colorimetric analysis of sweat. (a) Schematic showing the components for integrated wearable sweat sampling and pH determination (From Ref. [60]). (b) A soft microfluidic device with paper immobilised reagents for multi-analyte detection in sweat (Adapted from Ref. [63]).

The contribution of advanced technology to colorimetric sweat sensing devices in less than a decade is evident from the work of Koh *et al.* [63] who recently developed a multi-analyte wearable colorimetric platform for the determination of glucose, lactate, chloride and pH in sweat. A soft microfluidic device was fabricated from polydimethylsiloxane (PDMS) including channel geometries for movement of the sweat sample from the skin to four central reservoirs containing reagents immobilised on paper for the determination of the each of the analytes (b, Figure 1-3). Enzymatic assays utilising lactate dehydrogenase/diaphorase and glucose oxidase were employed for the determination of lactate and glucose respectively [64], [65] while a multi dye approach was used for pH monitoring and a 2,4,6-tris(2-pyridyl)-s-triazine (TPTZ) based chemical reaction was used for chloride detection [63], [66]. Smartphone technology was employed for wireless colorimetric analysis with

integrated NFC electronics and a control spot within the PDMS allowing proximity and colorimetric references for optimal results from the capture and analysis software employed.

Electrochemical sensors are of large interest in diagnostics due to their ease of fabrication, low cost, portability and simplicity [67]. Many wearable sweat sensors have been developed incorporating potentiometric sensors with simple fabrication techniques such as screen-printing. Schazmann *et al.* [68] developed the Sodium Sensor Belt (SSB), a wearable device for monitoring sodium levels in sweat. The platform was an elasticated belt incorporating a Na^+ ISE in plastic housing with an absorbent fabric acting as a passive pump for sweat transfer while a potentiometer was connected to the electrodes to monitor the potential in real time. The SSB was successfully used in on body trials in a comparative study of the sweat Na^+ concentrations of healthy individuals with those of individuals with cystic fibrosis.

Other approaches towards wearable sensing aim to analyse sweat by fabricating electrodes directly onto fabric for integration with clothing [13], [69]. When developing electrodes on new substrates especially flexible substrates it is important to define the effects of the material on the electrodes. Yang *et al.* compared screen printed carbon electrodes on three substrates, a plastic Mylar® material as a rigid reference alongside the elastic waistbands of two brands of underwear MERONA® and COVINGTON® [70]. Cyclic voltammetry showed similar initial responses to background phosphate buffer and 5 mM ferrocyanide. The effects of mechanical stress was assessed by monitoring the effect of four successive stretching and bending steps. Chronoamperometric analyisis showed minimal detrimental effect of bending and stretching upon measurements for NADH while enhanced signals were observed for chemical responses to hydrogen peroxide after mechanical stress.

Textile based sensors withstand stretching stress better than plastic sensors, however, they are limited in terms of the fabrics that can be used for optimal results [71] and the locations on the body they are in contact [72]. In 2012

Windmiller *et al.* presented the first example of a novel approach to wearable electrodes by screen-printing electrodes directly onto temporary tattoo paper allowing transfer of the flexible sensor directly onto the skin [73]. This technique has been employed for the analysis of the skin barrier including various analytes in sweat including pH, ammonium and lactate [74]–[76].

A tattoo based non-invasive wearable stripping-voltammetric detection of trace metals was demonstrated by Kim *et al.* [77]. They screen-printed pseudo-reference (Ag/AgCl), counter and working (carbon) electrodes and a transparent insulating layer on Papilio temporary transfer tattoo base paper before modification of the working electrode for Zn detection. The sensor was calibrated in Zn concentrations from 0.1 to 2 μg/ml reflecting the concentrations of 0.39 to 1.56 μg/ml [78] and was successfully used to monitor real time sweat Zn levels during on body trials. The effects on the electrodes of mechanical stress during physical activity was studied after exposing the electrodes to 100 stretching and bending cycles with no observable damage, while normal electrochemical response was retained under 30 cycles [77].

Commercial carbon fibres are also emerging as promising substrates for electrochemical sensing [79]–[81] with desirable qualities such as low weight, low cost and chemical and mechanical resistance [82]. A wearable potentiometric sodium sensor with integrated commercial carbon fibre based Na^+ ISEs and reference electrodes has been developed by Parrilla *et al.* [83]. ISE and reference membranes were polymerised onto one exposed end of separate carbon fibre bundles of 1 mm diameter and incorporated into plastic sleeves with a cotton strip providing passive flow of the sweat across the electrodes from the sampling area with the other ends of the fibre bundles providing electrical contacts for potentiometric monitoring. The sensors were successfully used for real time monitoring of sweat Na^+ levels in body trials.

As miniaturised electrochemical sensor technology is maturing the emphasis is continuing to shift to combining it with advanced technology from other disciplines to realise fully integrated wearable electrochemical sweat sensors. An

example of this was demonstrated by Rose *et al.* [84] in the development of a flexible wearable sweat Na^+ sensor incorporating ISE and reference electrodes with flexible circuitry incorporating RFID technology for wireless communication with smart devices. The components are positioned on a bandage like substrate while a vapour permeable membrane seals the top of the device (b, Figure 1-4).

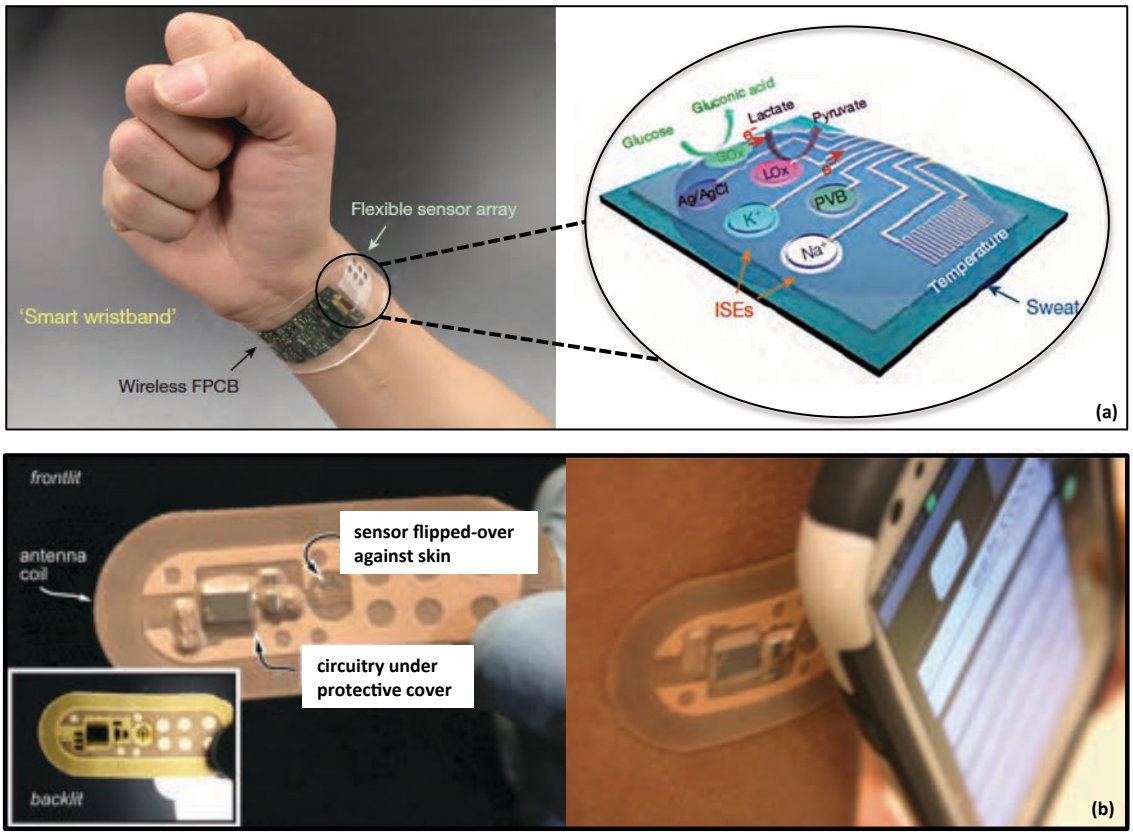

Figure 1-4: Fully integrated electrochemical sweat sensors. (a) A wearable wristband for real-time multi analyte monitoring in sweat (Adapted from Ref. [85]). (b) A bandage type sweat electrolyte device employing RFID for wireless communication of results (Adapted from Ref. [84]).

A fully integrated multi-analyte wearable smart band for monitoring temperature, glucose, lactate, Na^+ and K^+ levels in sweat has been developed by Gao *et al.* [85]. Two versions of the device were presented, a smart head band and a smart wrist band (a, Figure 1-4) both consisting of the same electronic and sensor configuration of amperometric sensors with a common Ag/AgCl reference for glucose and lactate monitoring, ISEs with a common polyvinyl butyral based reference for Na^+ and K^+ and a resistance based temperature sensor of Cr/Au micro wires integrated with a flexible printed circuit board

(FPCB). The FPCB incorporates modules allowing signal transduction, conditioning, processing and Bluetooth wireless transmission facilitating data collection analysis and communication powered by a single lithium ion polymer battery. The smart bands were used to analyse sweat during on body trials consisting of volunteers cycling on a stationary bicycle for up to 50 minutes and in a study to identify dehydration in prolonged outdoor running trials lasting ca. 100 minutes.

These integrated systems are a good utilisation of current technology and a very positive reflection of the advances being made currently in wearable sensor development. The limitations of these platforms include the lack of collection of sample fluid for prior analysis and the fact that sensing occurs directly on the skin, and thus potentially analyse the constituents of accumulated sweat rather than representing the constituents of the sweat in real-time. Therefore a platform that collects the sweat and pumps it indirectly across the electrodes to an excess reservoir may yield results more representative of real time sweat constituents.

1.3 Ion Selective Electrodes in Sweat Electrolyte Monitoring

As evident in previous sections ISEs are a popular category of electrochemical sensor for incorporation into wearable sensors. This section aims to evaluate the role of miniaturised solid state ISEs in sweat electrolyte determination by presenting the background and principles of the electrodes, their development and miniaturisation and their advances and current limitations.

1.3.1 Background and Principles of ISEs

In the early 20th century the development of the first H^+ responsive glass electrodes and their subsequent characterisation [86], [87] led to substantive interest in glass electrodes for ionic sensing resulting in the introduction of B_2O_3 in glass electrodes providing Na^+ sensitivity [88], [89]. In the late 1960s significant progress was made in ion sensing with the development of electrodes

for employing liquid ion-exchangers [90] and the fabrication of membranes incorporating ionophores for ionic detection [91] leading to the first ISEs, devices that allow the detection and quantification of a target ion by converting its activity into a measurable electrical signal.

Conventionally these potentiometric electrodes consist of an internal electrolyte solution between an ion selective membrane and reference electrode (a, Figure 1-5) to establish a constant phase boundary potential to govern the membrane response [92], [93]. A large range of ion selective membranes have been developed allowing the development of sensors for over 70 analytes for a wide range of applications [94], [95]. Though highly successful commercially, these liquid contact ISEs have many limitations including the possibility of internal solution evaporation, sensitivity to sample pressure and temperature delamination of the sensing membrane and large volume changes caused by osmotic pressure arising from ionic strength imbalance between internal and external solutions [96]. As a result these limitations combined with the fact that the internal solution makes miniaturising these electrodes difficult alternative strategies utilising solid state electrodes were developed [97].

1.3.2 The Development of Solid Contact ISEs

In 1971 Cattrall *et al.* [98] presented an approach for removing the need for an internal reference solution by coating a metal wire with a poorly soluble salt incorporating that metal and the ion of interest, for example Ag wire coated with AgCl for the detection of Cl^-. A polymer such as polyvinyl chloride (PVC) was used as a carrier of the salt to allow polymerisation to the wire. This work displayed a simple means of removing the internal solutions, however, the thermodynamically ill-defined ion selective membrane/electron conducting interface resulted in random potential changes [97], [99].

In order to stabilise the potential at the sensor interface intermediate layers, known as solid contact layers, were investigated to act as ion to electron transducers between the membrane and the electron conducting layers. One

strategy is to constrain an internal electrolyte within a hydrogel layer positioned between the membrane and conducting layers (b, Figure 1-5) [100]. Limitations of hydrogel based solid contact layers include sensitivity to dry storage and its tendency to absorb water leading to volume changes [97].

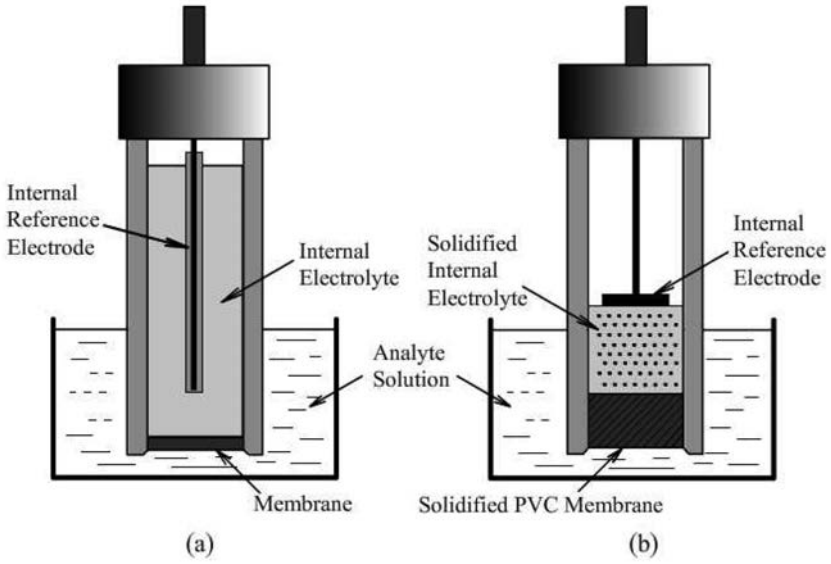

Figure 1-5: Schematic of (a) a liquid contact and (b) a solid contact ISE (From Ref. [101]).

A popular choice for solid contact layer are conducting polymers (CP) as they exhibit both electronic and ionic activity and are easily deposited on an electron-conducting layer by electrodeposition [96], [102]. Two of main types of CPs used in ISE development and fabrication are poly(pyrrole) (PPy) and polythiophenes [92], [103]. Michalska *et al.* [104] demonstrated the abilities of PPy as a solid contact for Na^+ and K^+ sensing by comparing two PPy configurations, one doped with hexacyanoferrate(II) and one with a chloride salt of the ion of interest, with liquid contact ISEs for both ions. In Na^+ sensing the PPy-Fe(CN) solid contact displayed Nernstian responses of 60 mV/decade which was more sensitive than the PPyCl solid contact with 58.3 mV/decade with both showing an improvement on the 56 mV/decade liquid contact ISE.

Poly(3-octylthiophene) (POT) and poly(3,4-ethylenedioxythiophene) (PEDOT) are two polythiophenes commonly used as solid contacts in ISEs [105], [106]. POT is usually used undoped and ion-free due to its high oxidation potential

making it less likely to react with ambient species [96]. Bobacka *et al.* [107] removed the need for both a plasticizer in the ISE membrane layer and a separate solid contact layer through the addition of POT in a K^+ ISE membrane. The study successfully proved the concept with K^+ detection yielding slopes of 49 mV/decade. Hu *et al.* have described how the addition of doping ions in the CP layer can help control whether anions or cations dominate the ion exchange at the ISE membrane/conducting polymer interface [96]. A large immobile polyelectrolyte such as poly(sodium 4-styrenesulfonate) (PSS) polyanion will lead to dominated cation exchange while doping the CP with a small anion will result in anion dominated exchange. This is reflected in K^+ sensing with many ISEs employing PEDOT: PSS in the solid contact layer [108]–[110].

In recent years nano-materials have been employed in scISE technology. Carbon nanotubes (CNT) have been incorporated into solid contact and ISE membrane layers to improve stability [111]–[113]. Highly stable scISEs have been presented by Hu *et al.* [114] incorporating colloid-imprinted mesoporous (CIM) carbon as solid contact achieving potential drift of 1.3 μV/h. Paczosa-Bator [115] investigated a carbon black/graphene mix based solid contact layer and observed a potential drift of less than 1 μV/h.

Solid contact reference electrodes (scRE) have also been developed enabling the development of single platform solid state combination ISE-RE sensing [116], [117]. Zuliani *et al.* [118] successfully used ionic liquids (IL) as a salt bridge in a PEDOT:IL solid contact layer in the development of scISEs and solid contact reference electrodes. Guinovart *et al.* [119] developed a PVB Ag/AgCl based solid state reference electrode for decentralized chemical measurements which have also been employed in a wearable sweat analysis platform [85].

1.3.3 Evaluating Solid Contact ISE Performance

Certain parameters are assessed to fully evaluate the performance of solid contact ISEs and/or their suitability for clinical use. These include the

reproducibility of the standard potential ($E°$) and the stability of electromotive force (emf) (the potential difference between the ISE and RE) [96], [120].

The reproducibility of the $E°$ is primarily defined by the redox potential of the CP layer which can be effected by various parameters including but not limited to crystallinity of the CP film and the ability of counter-ions to penetrate it, speed of conformational change and the dependence of film morphology on the fabrication process [96], [121]–[123]. Interpretation of the U.S. Code of Federal regulations [124] suggests that a commercial Na^+ ISE would have to achieve an $E°$ variation of less than 0.7 mV before it would be considered suitable for calibration free clinical use. The sensitivity of the CP redox potential to a range of parameters suggests it would be difficult to achieve such low $E°$ variation so calibration may be unavoidable in these sensors without further adaptation. Buhlmann *et al.* reported significant success in this area with the use of lipophilic redox buffers consisting of the Co(III) and Co(II) complexes and achieved a balanced ratio of the reduced and oxidized species leading to increased reproducibility with an $E°$ of 0.7 mV [125]–[127].

Emf stability is determined by the level of potential drift arising as a result of the sensors internal environment independent of sample concentration and constituents [96]. ISEs regularly display high levels of potential drift when initially in contact with a solution containing the target ion, this potential drift can be greatly reduced by conditioning the ISE in a solution containing a high concentration of the target ion until emf reaches equilibrium [120]. Analyte concentration and duration of conditioning step vary greatly in the literature but generally take multiple hours [128], [129].

Guzinski *et al.* [130] recently studied the effect of electron-conducting layer on conditioning time with a PEDOT:PSS solid contact layer and found equilibration times of 5-13 min with both glassy carbon and Au electron conducting layers while over 60 min was required for equilibration to be reached on a Pt electron-conducting layer. Another source of emf instability in solid contact ISEs can be the formation of an aqueous layer between the solid contact and ISE membrane

layer [131]–[133]. The prevention of aqueous layer formation can be achieved with careful selection of solid contact and membrane layer constituents [134]–[136], however, this may be restricted by the application and sensor requirements.

1.4 Technological Advances Contributing to Fully Integrated Wearable Systems

As previously mentioned, the ability to develop advanced wearable chemical sensors depends not only on developments in sensor research but also on advances in other disciplines such as flexible electronics and battery development. This section presents an insight into relevant recent advances which have the potential to contribute to the further development of fully integrated wearable devices.

1.4.1 Wearable Electronics

The rapid development of the smartphone and wearable device industries has contributed to a large amount of activity in the development of advanced electronics particularly in providing miniaturised flexible, low cost, low power high performance circuits for data processing and wireless communication [13], [137], [138]. Section 1.2.1.3 shows examples of advanced electronics already adapted into wearable sweat sensors with two fully integrated systems for sweat sensing wearable electronic circuitry in two configurations of flexible electronic components incorporating an RFID antenna coil integrated onto a bandage type substrate [84] and a flexible printed circuit board incorporating multiple modules for signal transduction, processing and wireless communication [85].

Bauer [139] recently presented an overview of electronic skins enabling the incorporation of electronic components and displays directly on the skin surface (a, Figure 1-6) [140], [141]. The development of these components are continue to benefit from materials research such as the use of silver nanowires [142] and carbon based nanomaterials such as CNTs [143] and graphene [144] in the

development of electrodes for flexible and stretchable electronics [137]. Another emerging field in wearable electronics is the production of circuits on fabric, also known as 'textile circuitry' [145] with a host of techniques such as e-broidery and fabric soldering [146], [147] being developed which will enhance the opportunities for wearable textile based sensors.

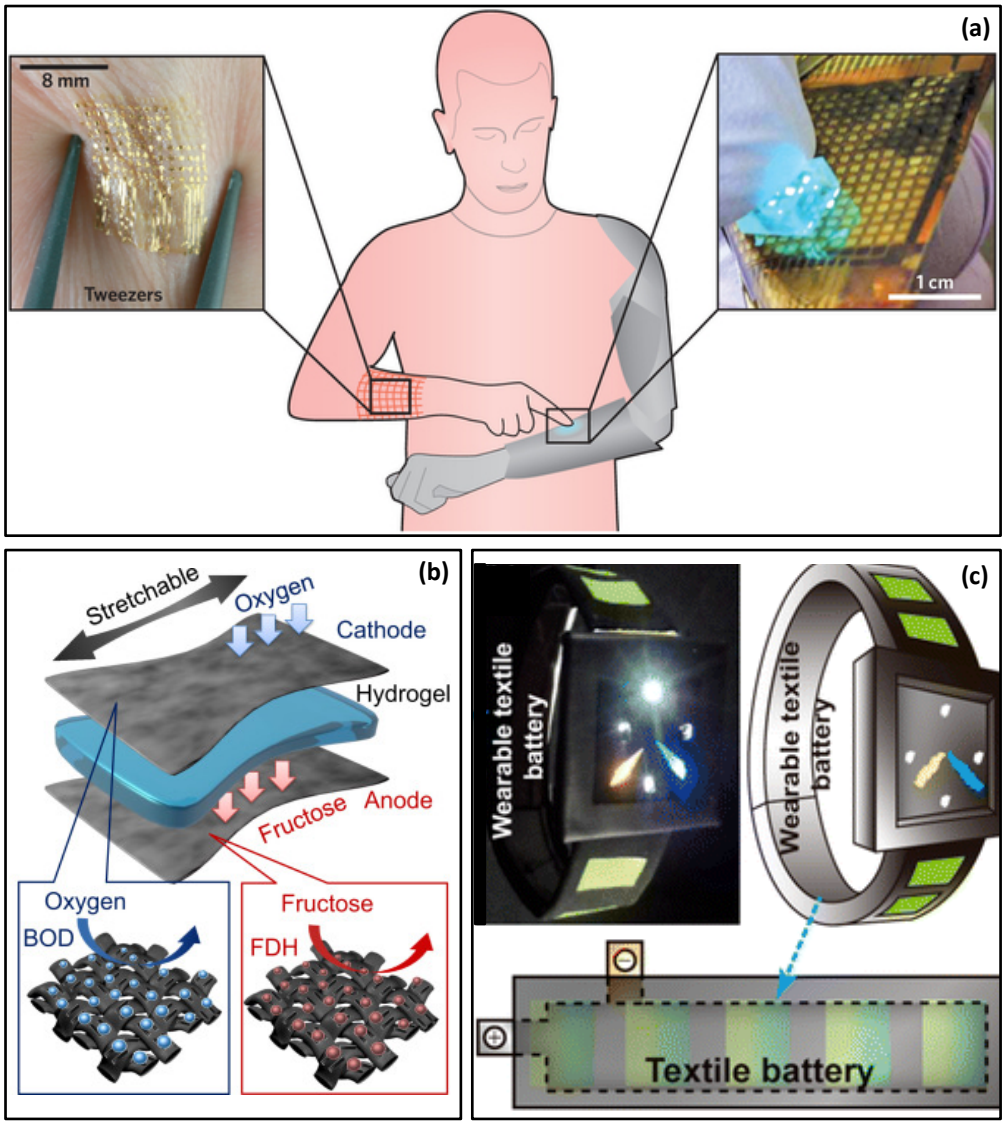

Figure 1-6: Advances in wearable technology. (a) Interpretation of the future of wear able devices with (left) ultrathin electronic films and (right) a wearable touch pad (From Ref. [139] incorporating images from Ref. [140], [141]). (b) A stretchable textile based biofuel cell utilising enzymatic reactions (From Ref. [148]). (c) A solar rechargeable textile battery (From Ref. [149])

1.4.2 Wearable Power Supply

Miniaturised sensors and electronic components and circuits are enabling the development of small and flexible wearable devices but the operation of these devices is often dependent on power supplies such as standard lithium ion or alkaline batteries which add considerable bulk and rigidity [150]. As shown in section 1.2.1.3 Rose *et al.* [84] developed a fully integrated wearable sweat sodium sensor incorporating an RFID transponder chip with energy harvesting capabilities allowing battery free operation. Battery free operation is not always an option meaning the development of advanced miniaturised batteries is required to fully realise the potential of miniaturised flexible wearable devices.

The development of printed battery technology is using a combination conventional battery chemistries and modern fabrication technologies to create thin and flexible power supplies [151]. Ostfeld *et al.* [152] have recently presented a flexible power source integrating a lithium ion battery and amorphous silicon solar module for power harvesting and supply to a wearable sensing device. Lee *et al.* [149] integrated nickel coated polyester yarn and polyurethane with lightweight solar cells to produce solar powered wearable textile batteries (c, Figure 1-6). An attractive approach to powering wearable devices is in the use of biofuel cells which could harvest energy directly from the user [150]. Ogawa *et al.* [148], [153] have demonstrated stretchable wearable biofuel cell utilising textile immobilised enzymes as anodes and cathodes (b, Figure 1-6). The further development of these and novel wearable batteries will provide a wealth of choices in the production of future wearable sensors.

1.5 Conclusion

This review presented an insight into the current state of wearable sensing technology with a focus on non-invasive chemical sensing. The quality and impact of the technology presented reflects an exciting time in sensor development and integration. In sweat sensing the fully integrated devices

beginning to emerge are but initial examples of the wide variety of advanced wearable platforms which will be realised in the coming decade. The continued emergence and success of non-invasive wearable platforms will depend on the further development and integration of low cost, simple and effective sensors such as ISEs with advanced technologies in fields such as electronics and materials science for the realisation of novel miniaturised wearable sensing devices.

1.6 References

[1] P. Yager, G. J. Domingo, and J. Gerdes, 'Point-of-Care Diagnostics for Global Health', *Annu. Rev. Biomed. Eng.*, vol. 10, no. 1, pp. 107–144, 2008.

[2] 'IDTechEx argues wearable tech market to exceed $30bn in 2016 and $150bn by 2026', *Wearable Tech News*. [Online]. Available: http://www.wearabletechnology-news.com/news/2016/nov/09/idtechex-argues-wearable-tech-market-exceed-30bn-2016-and-150bn-2026/. [Accessed: 09-Dec-2016].

[3] 'Wearable Sensors 2016-2026: Market Forecasts, Technologies, Players: IDTechEx', 01-Apr-2016. [Online]. Available: http://www.idtechex.com/research/reports/wearable-sensors-2016-2026-market-forecasts-technologies-players-000470.asp. [Accessed: 09-Dec-2016].

[4] S. Coyle *et al.*, 'Personal sensing wear: the role of textile sensors', in *Personal sensing wear: the role of textile sensors. In: International Workshop on Personalisation and Adaptation in Technology for Health (PATH 2015)*, TCD, Dublin, Ireland, 2015.

[5] R. Badugu, J. R. Lakowicz, and C. D. Geddes, 'A glucose-sensing contact lens: from bench top to patient', *Curr. Opin. Biotechnol.*, vol. 16, no. 1, pp. 100–107, Feb. 2005.

[6] A. J. Bandodkar and J. Wang, 'Non-invasive wearable electrochemical sensors: a review', *Trends Biotechnol.*, vol. 32, no. 7, pp. 363–371, Jul. 2014.

[7] F. Tsow *et al.*, 'A Wearable and Wireless Sensor System for Real-Time Monitoring of Toxic Environmental Volatile Organic Compounds', *IEEE Sens. J.*, vol. 9, no. 12, pp. 1734–1740, Dec. 2009.

[8] A. Lunney, N. R. Cunningham, and M. S. Eastin, 'Wearable fitness technology: A structural investigation into acceptance and perceived fitness outcomes', *Comput. Hum. Behav.*, vol. 65, pp. 114–120, Dec. 2016.

[9] K. M. Diaz *et al.*, 'Fitbit®: An accurate and reliable device for wireless physical activity tracking', *Int. J. Cardiol.*, vol. 185, pp. 138–140, Apr. 2015.

[10] J. Zheng, Y. Shen, Z. Zhang, T. Wu, G. Zhang, and H. Lu, 'Emerging Wearable Medical Devices Towards Personalized Healthcare', in *Proceedings of the 8th International Conference on Body Area Networks*, ICST, Brussels, Belgium, Belgium, 2013, pp. 427–431.

[11] S. Patel, H. Park, P. Bonato, L. Chan, and M. Rodgers, 'A review of wearable sensors and systems with application in rehabilitation', *J. NeuroEngineering Rehabil.*, vol. 9, p. 21, 2012.

[12] E. Nemati, M. J. Deen, and T. Mondal, 'A wireless wearable ECG sensor for long-term applications', *IEEE Commun. Mag.*, vol. 50, no. 1, pp. 36–43, Jan. 2012.

[13] M. Stoppa and A. Chiolerio, 'Wearable Electronics and Smart Textiles: A Critical Review', *Sensors*, vol. 14, no. 7, pp. 11957–11992, Jul. 2014.

[14] G. Paul, R. Torah, S. Beeby, and J. Tudor, 'The development of screen printed conductive networks on textiles for biopotential monitoring applications', *Sens. Actuators Phys.*, vol. 206, pp. 35–41, Feb. 2014.

[15] M. Pacelli, L. Caldani, and R. Paradiso, 'Performances evaluation of piezoresistive fabric sensors as function of yarn structure', in *2013 35th Annual International Conference of the IEEE Engineering in Medicine and Biology Society (EMBC)*, 2013, pp. 6502–6505.

[16] C.-T. Huang, C.-L. Shen, C.-F. Tang, and S.-H. Chang, 'A wearable yarn-based piezo-resistive sensor', *Sens. Actuators Phys.*, vol. 141, no. 2, pp. 396–403, Feb. 2008.

[17] K. A. Adal and B. M. Farr, 'Central venous catheter-related infections: A review', *Nutrition*, vol. 12, no. 3, pp. 208–213, Mar. 1996.

[18] N. S. Oliver, C. Toumazou, A. E. G. Cass, and D. G. Johnston, 'Glucose sensors: a review of current and emerging technology', *Diabet. Med.*, vol. 26, no. 3, pp. 197–210, Mar. 2009.

[19] American Diabetes Association, 'Consensus Statement on Self-Monitoring of Blood Glucose', *Diabetes Care*, vol. 10, no. 1, pp. 95–99, Jan. 1987.

[20] S. E. Inzucchi *et al.*, 'Management of Hyperglycemia in Type 2 Diabetes: A Patient-Centered Approach', *Diabetes Care*, vol. 35, no. 6, pp. 1364–1379, Jun. 2012.

[21] M. S. Boyne, D. M. Silver, J. Kaplan, and C. D. Saudek, 'Timing of Changes in Interstitial and Venous Blood Glucose Measured With a Continuous Subcutaneous Glucose Sensor', *Diabetes*, vol. 52, no. 11, pp. 2790–2794, Nov. 2003.

[22] V. Thomé-Duret *et al.*, 'Use of a subcutaneous glucose sensor to detect decreases in glucose concentration prior to observation in blood', *Anal. Chem.*, vol. 68, no. 21, pp. 3822–3826, Nov. 1996.

[23] 'How does the FreeStyle Libre system measure my glucose? | FreeStyle Blood Glucose Meters'. [Online]. Available: https://freestylediabetes.ie/freestyle-thinking/post/FreeStyle-Libre-system-measure. [Accessed: 14-Dec-2016].

[24] S. A. Beshyah and M. Haddad, 'Impact of Socializing, Fasting and Feasting on Day to Day Blood Glucose Profiles in Diabetes Elucidated by the FreeStyle® Libre™ System', *Ibnosina J. Med. Biomed. Sci.*, vol. 8, no. 4, pp. 114–119, Jul. 2016.

[25] P. R. Miller, R. J. Narayan, and R. Polsky, 'Microneedle-based sensors for medical diagnosis', *J. Mater. Chem. B*, vol. 4, no. 8, pp. 1379–1383, 2016.

[26] G. Rao, P. Glikfeld, and R. H. Guy, 'Reverse Iontophoresis: Development of a Noninvasive Approach for Glucose Monitoring', *Pharm. Res.*, vol. 10, no. 12, pp. 1751–1755, Dec. 1993.

[27] M. J. Tierney *et al.*, 'The GlucoWatch® biographer: a frequent, automatic and noninvasive glucose monitor', *Ann. Med.*, vol. 32, no. 9, pp. 632–641, Jan. 2000.

[28] S. K. Vashist, 'Non-invasive glucose monitoring technology in diabetes management: A review', *Anal. Chim. Acta*, vol. 750, pp. 16–27, Oct. 2012.

[29] H. Lee *et al.*, 'A graphene-based electrochemical device with thermoresponsive microneedles for diabetes monitoring and therapy', *Nat. Nanotechnol.*, vol. 11, no. 6, pp. 566–572, Jun. 2016.

[30] 'FreeStyle Libre'. [Online]. Available: https://www.freestylelibre.co.uk/. [Accessed: 14-Dec-2016].

[31] 'Wearable Muscle Oxygen Monitor & Lactate Threshold'. [Online]. Available: https://www.bsxinsight.com/. [Accessed: 15-Dec-2016].

[32] M. Driller, N. Borges, and D. Plews, 'Evaluating a new wearable lactate threshold sensor in recreational to highly trained cyclists', *Sports Eng.*, vol. 19, no. 4, pp. 229–235, Dec. 2016.

[33] N. M. Farandos, A. K. Yetisen, M. J. Monteiro, C. R. Lowe, and S. H. Yun, 'Contact Lens Sensors in Ocular Diagnostics', *Adv. Healthc. Mater.*, vol. 4, no. 6, pp. 792–810, Apr. 2015.

[34] R. S. P. Malon, S. Sadir, M. Balakrishnan, and E. P. Córcoles, 'Saliva-Based Biosensors: Noninvasive Monitoring Tool for Clinical Diagnostics', *BioMed Res. Int.*, vol. 2014, 2014.

[35] H. Yao, A. J. Shum, M. Cowan, I. Lähdesmäki, and B. A. Parviz, 'A contact lens with embedded sensor for monitoring tear glucose level', *Biosens. Bioelectron.*, vol. 26, no. 7, pp. 3290–3296, Mar. 2011.

[36] N. Thomas, I. Lähdesmäki, and B. A. Parviz, 'A contact lens with an integrated lactate sensor', *Sens. Actuators B Chem.*, vol. 162, no. 1, pp. 128–134, Feb. 2012.

[37] D. Harvey, N. W. Hayes, and B. Tighe, 'Fibre optics sensors in tear electrolyte analysis: Towards a novel point of care potassium sensor', *Contact Lens Anterior Eye*, vol. 35, no. 3, pp. 137–144, Jun. 2012.

[38] Á. Farkas, R. Vámos, T. Bajor, N. Müllner, Á. Lázár, and A. Hrabá, 'Utilization of lacrimal urea assay in the monitoring of hemodialysis: conditions,

limitations and lacrimal arginase characterization', *Exp. Eye Res.*, vol. 76, no. 2, pp. 183–192, Feb. 2003.

[39] L. W. Jones *et al.*, 'Revolutionary Future Uses of Contact Lenses', *Optom. Vis. Sci. Off. Publ. Am. Acad. Optom.*, vol. 93, no. 4, pp. 325–327, Apr. 2016.

[40] C. J. White, S. A. DiPasquale, and M. E. Byrne, 'Controlled Release of Multiple Therapeutics from Silicone Hydrogel Contact Lenses', *Optom. Vis. Sci. Off. Publ. Am. Acad. Optom.*, vol. 93, no. 4, pp. 377–386, Apr. 2016.

[41] S. Bobba and N. Di Girolamo, 'Contact Lenses: A Delivery Device for Stem Cells to Treat Corneal Blindness', *Optom. Vis. Sci. Off. Publ. Am. Acad. Optom.*, vol. 93, no. 4, pp. 412–418, Apr. 2016.

[42] Y. T. Liao, H. Yao, A. Lingley, B. Parviz, and B. P. Otis, 'A 3-μW CMOS Glucose Sensor for Wireless Contact-Lens Tear Glucose Monitoring', *IEEE J. Solid-State Circuits*, vol. 47, no. 1, pp. 335–344, Jan. 2012.

[43] R. Badugu, J. R. Lakowicz, and C. D. Geddes, 'Fluorescence sensors for monosaccharides based on the 6-methylquinolinium nucleus and boronic acid moiety: potential application to ophthalmic diagnostics', *Talanta*, vol. 65, no. 3, pp. 762–768, Feb. 2005.

[44] R. Badugu, J. R. Lakowicz, and C. D. Geddes, 'Boronic acid fluorescent sensors for monosaccharide signaling based on the 6-methoxyquinolinium heterocyclic nucleus: progress toward noninvasive and continuous glucose monitoring', *Bioorg. Med. Chem.*, vol. 13, no. 1, pp. 113–119, Jan. 2005.

[45] D. Bruen, R. Albatal, L. Florea, and D. Diamond, 'Contact lenses for real-time colorimetric sensing of glucose', presented at the Advanced Materials World Congress 2015, Stockholm, Sweden, 24-Aug-2015.

[46] U. M. Nater and N. Rohleder, 'Salivary alpha-amylase as a non-invasive biomarker for the sympathetic nervous system: Current state of research', *Psychoneuroendocrinology*, vol. 34, no. 4, pp. 486–496, May 2009.

[47] L. De Cock, V. Hutse, E. Verhaegen, S. Quoilin, H. Vandenberghe, and R. Vranckx, 'Detection of HCV antibodies in oral fluid', *J. Virol. Methods*, vol. 122, no. 2, pp. 179–183, Dec. 2004.

[48] J. S. Mitchell, T. E. Lowe, and J. R. Ingram, 'Rapid ultrasensitive measurement of salivary cortisol using nano-linker chemistry coupled with surface plasmon resonance detection', *Analyst*, vol. 134, no. 2, pp. 380–386, 2009.

[49] M. Yasuda *et al.*, 'Diagnostic significance of salivary testosterone measurement revisited: using liquid chromatography/mass spectrometry and enzyme-linked immunosorbent assay', *J. Mens Health*, vol. 5, no. 1, pp. 56–63, Mar. 2008.

[50] C. Zuliani, G. Matzeu, and D. Diamond, 'A potentiometric disposable sensor strip for measuring pH in saliva', *Electrochimica Acta*, vol. 132, pp. 292–296, Jun. 2014.

[51] J. Kim *et al.*, 'Non-invasive mouthguard biosensor for continuous salivary monitoring of metabolites', *Analyst*, vol. 139, no. 7, pp. 1632–1636, Mar. 2014.

[52] J. Kim *et al.*, 'Wearable salivary uric acid mouthguard biosensor with integrated wireless electronics', *Biosens. Bioelectron.*, vol. 74, pp. 1061–1068, Dec. 2015.

[53] M. S. Mannoor *et al.*, 'Graphene-based wireless bacteria detection on tooth enamel', *Nat. Commun.*, vol. 3, p. 763, Mar. 2012.

[54] J. Moyer, D. Wilson, I. Finkelshtein, B. Wong, and R. Potts, 'Correlation between sweat glucose and blood glucose in subjects with diabetes', *Diabetes Technol. Ther.*, vol. 14, no. 5, pp. 398–402, May 2012.

[55] J. M. Green, R. C. Pritchett, T. R. Crews, J. R. McLester, and D. C. Tucker, 'Sweat lactate response between males with high and low aerobic fitness', *Eur. J. Appl. Physiol.*, vol. 91, no. 1, pp. 1–6, Jan. 2004.

[56] J. Parnas, H. Flachs, L. Gram, and A. Wuurtz-JØrgensen, 'Excretion of antiepileptic drugs in sweat', *Acta Neurol. Scand.*, vol. 58, no. 3, pp. 197–204, Sep. 1978.

[57] M. A. Huestis, J. M. Oyler, E. J. Cone, A. T. Wstadik, D. Schoendorfer, and R. E. Joseph, 'Sweat testing for cocaine, codeine and metabolites by gas chromatography-mass spectrometry', *J. Chromatogr. B. Biomed. Sci. App.*, vol. 733, no. 1–2, pp. 247–264, Oct. 1999.

[58] A. Mishra, R. Greaves, and J. Massie, 'The Relevance of Sweat Testing for the Diagnosis of Cystic Fibrosis in the Genomic Era', *Clin. Biochem. Rev. Aust. Assoc. Clin. Biochem.*, vol. 26, no. 4, pp. 135–153, Nov. 2005.

[59] L. B. Baker, K. A. Barnes, M. L. Anderson, D. H. Passe, and J. R. Stofan, 'Normative data for regional sweat sodium concentration and whole-body sweating rate in athletes', *J. Sports Sci.*, vol. 34, no. 4, pp. 358–368, Feb. 2016.

[60] D. Morris, S. Coyle, Y. Wu, K. T. Lau, G. Wallace, and D. Diamond, 'Bio-sensing textile based patch with integrated optical detection system for sweat monitoring', *Sens. Actuators B Chem.*, vol. 139, no. 1, pp. 231–236, May 2009.

[61] M. O'Toole, K. T. Lau, R. Shepherd, C. Slater, and D. Diamond, 'Determination of phosphate using a highly sensitive paired emitter–detector diode photometric flow detector', *Anal. Chim. Acta*, vol. 597, no. 2, pp. 290–294, Aug. 2007.

[62] D. Granger, M. Marsolais, J. Burry, and R. Laprade, 'Na+/H+ exchangers in the human eccrine sweat duct', *Am. J. Physiol. Cell Physiol.*, vol. 285, no. 5, pp. C1047-1058, Nov. 2003.

[63] A. Koh *et al.*, 'A soft, wearable microfluidic device for the capture, storage, and colorimetric sensing of sweat', *Sci. Transl. Med.*, vol. 8, no. 366, p. 366ra165-366ra165, Nov. 2016.

[64] N. J. Hochella and S. Weinhouse, 'Automated assay of lactate dehydrogenase in urine', *Anal. Biochem.*, vol. 13, no. 2, pp. 322–335, Nov. 1965.

[65] A. W. Martinez, S. T. Phillips, M. J. Butte, and G. M. Whitesides, 'Patterned Paper as a Platform for Inexpensive, Low Volume, Portable Bioassays', *Angew. Chem. Int. Ed Engl.*, vol. 46, no. 8, pp. 1318–1320, 2007.

[66] E. B. de Jong, H. M. Goldschmidt, A. C. van Alphen, and J. A. Loog, 'An improved automated method for serum chloride', *Clin. Chem.*, vol. 26, no. 8, pp. 1233–1234, Jul. 1980.

[67] N. J. Ronkainen, H. Brian Halsall, and W. R. Heineman, 'Electrochemical biosensors', *Chem. Soc. Rev.*, vol. 39, no. 5, pp. 1747–1763, 2010.

[68] B. Schazmann *et al.*, 'A wearable electrochemical sensor for the real-time measurement of sweat sodium concentration', *Anal. Methods*, vol. 2, no. 4, pp. 342–348, Apr. 2010.

[69] S. Coyle *et al.*, 'BIOTEX--biosensing textiles for personalised healthcare management', *IEEE Trans. Inf. Technol. Biomed. Publ. IEEE Eng. Med. Biol. Soc.*, vol. 14, no. 2, pp. 364–370, Mar. 2010.

[70] Y.-L. Yang, M.-C. Chuang, S.-L. Lou, and J. Wang, 'Thick-film textile-based amperometric sensors and biosensors', *Analyst*, vol. 135, no. 6, pp. 1230–1234, 2010.

[71] M.-C. Chuang *et al.*, 'Textile-based Electrochemical Sensing: Effect of Fabric Substrate and Detection of Nitroaromatic Explosives', *Electroanalysis*, vol. 22, no. 21, pp. 2511–2518, Nov. 2010.

[72] A. J. Bandodkar, W. Jia, and J. Wang, 'Tattoo-Based Wearable Electrochemical Devices: A Review', *Electroanalysis*, vol. 27, no. 3, pp. 562–572, Mar. 2015.

[73] J. Ray Windmiller, A. Jairaj Bandodkar, G. Valdés-Ramírez, S. Parkhomovsky, A. Gabrielle Martinez, and J. Wang, 'Electrochemical sensing based on printable temporary transfer tattoos', *Chem. Commun.*, vol. 48, no. 54, pp. 6794–6796, 2012.

[74] K. De Guzman and A. Morrin, 'Screen-printed Tattoo Sensor towards the Non-invasive Assessment of the Skin Barrier', *Electroanalysis*, vol. Article in Press, Dec. 2016.

[75] T. Guinovart, A. J. Bandodkar, J. R. Windmiller, F. J. Andrade, and J. Wang, 'A potentiometric tattoo sensor for monitoring ammonium in sweat', *Analyst*, vol. 138, no. 22, pp. 7031–7038, 2013.

[76] W. Jia *et al.*, 'Electrochemical Tattoo Biosensors for Real-Time Noninvasive Lactate Monitoring in Human Perspiration', *Anal. Chem.*, vol. 85, no. 14, pp. 6553–6560, Jul. 2013.

[77] J. Kim *et al.*, 'Wearable temporary tattoo sensor for real-time trace metal monitoring in human sweat', *Electrochem. Commun.*, vol. 51, pp. 41–45, Feb. 2015.

[78] A. Crew, D. C. Cowell, and J. P. Hart, 'Development of an anodic stripping voltammetric assay, using a disposable mercury-free screen-printed carbon electrode, for the determination of zinc in human sweat', *Talanta*, vol. 75, no. 5, pp. 1221–1226, Jun. 2008.

[79] A. Periyakaruppan, R. P. Gandhiraman, M. Meyyappan, and J. E. Koehne, 'Label-Free Detection of Cardiac Troponin-I Using Carbon Nanofiber Based Nanoelectrode Arrays', *Anal. Chem.*, vol. 85, no. 8, pp. 3858–3863, Apr. 2013.

[80] E. Rand *et al.*, 'A carbon nanofiber based biosensor for simultaneous detection of dopamine and serotonin in the presence of ascorbicacid', *Biosens. Bioelectron.*, vol. 42, pp. 434–438, Apr. 2013.

[81] J. Fei, K. Wu, F. Wang, and S. Hu, 'Glucose nanosensors based on redox polymer/glucose oxidase modified carbon fiber nanoelectrodes', *Talanta*, vol. 65, no. 4, pp. 918–924, Feb. 2005.

[82] E. Frank, F. Hermanutz, and M. R. Buchmeiser, 'Carbon Fibers: Precursors, Manufacturing, and Properties', *Macromol. Mater. Eng.*, vol. 297, no. 6, pp. 493–501, Jun. 2012.

[83] M. Parrilla, J. Ferré, T. Guinovart, and F. J. Andrade, 'Wearable Potentiometric Sensors Based on Commercial Carbon Fibres for Monitoring Sodium in Sweat', *Electroanalysis*, vol. 28, no. 6, pp. 1267–1275, Jun. 2016.

[84] D. P. Rose *et al.*, 'Adhesive RFID Sensor Patch for Monitoring of Sweat Electrolytes', *IEEE Trans. Biomed. Eng.*, vol. 62, no. 6, pp. 1457–1465, Jun. 2015.

[85] W. Gao *et al.*, 'Fully integrated wearable sensor arrays for multiplexed in situ perspiration analysis', *Nature*, vol. 529, no. 7587, pp. 509–514, Jan. 2016.

[86] M. Cremer, *Über die Ursache der elektromotorischen Eigenschaften der Gewebe, zugleich ein Beitrag zur Lehre von den polyphasischen Elektrolytketten*. R. Oldenbourg, 1906.

[87] Z. Klemensiewicz, 'Über die Entstehung positiver Ionen an erhitzten Metallen', *Ann. Phys.*, vol. 341, no. 14, pp. 796–814, Jan. 1911.

[88] K. Horovitz, 'Der Ionenaustausch am Dielektrikum I. Die Elektrodenfunktion der Gläser', *Z. Für Phys.*, vol. 15, no. 1–2, pp. 369–398, Dec. 1923.

[89] G. Eisenman, 'Cation Selective Glass Electrodes and their Mode of Operation', *Biophys. J.*, vol. 2, no. 2 Pt 2, pp. 259–323, Mar. 1962.

[90] J. W. Ross, 'Calcium-Selective Electrode with Liquid Ion Exchanger', *Science*, vol. 156, no. 3780, pp. 1378–1379, Jun. 1967.

[91] R. Bloch, A. Shatkay, and H. A. Saroff, 'Fabrication and Evaluation of Membranes as Specific Electrodes for Calcium ions', *Biophys. J.*, vol. 7, no. 6, pp. 865–877, Nov. 1967.

[92] L. van de Velde, E. d'Angremont, and W. Olthuis, 'Solid contact potassium selective electrodes for biomedical applications – a review', *Talanta*, vol. 160, pp. 56–65, Nov. 2016.

[93] E. Lindner and R. E. Gyurcsányi, 'Quality control criteria for solid-contact, solvent polymeric membrane ion-selective electrodes', *J. Solid State Electrochem.*, vol. 13, no. 1, pp. 51–68, Jan. 2009.

[94] P. Bühlmann, E. Pretsch, and E. Bakker, 'Carrier-Based Ion-Selective Electrodes and Bulk Optodes. 2. Ionophores for Potentiometric and Optical Sensors', *Chem. Rev.*, vol. 98, no. 4, pp. 1593–1688, Jun. 1998.

[95] J. Bobacka, A. Ivaska, and A. Lewenstam, 'Potentiometric Ion Sensors', *Chem. Rev.*, vol. 108, no. 2, pp. 329–351, Feb. 2008.

[96] J. Hu, A. Stein, and P. Bühlmann, 'Rational design of all-solid-state ion-selective electrodes and reference electrodes', *TrAC Trends Anal. Chem.*, vol. 76, pp. 102–114, Feb. 2016.

[97] A. Michalska, 'All-Solid-State Ion Selective and All-Solid-State Reference Electrodes', *Electroanalysis*, vol. 24, no. 6, pp. 1253–1265, Jun. 2012.

[98] R. W. Cattrall and H. Freiser, 'Coated wire ion-selective electrodes', *Anal. Chem.*, vol. 43, no. 13, pp. 1905–1906, Nov. 1971.

[99] B. P. Nikolskii and E. A. Materova, 'Solid contact in membrane ion-selective electrodes', *Ion-Sel Electrode Rev*, vol. 7, no. 3, 1985.

[100] A. Michalska, M. Wojciechowski, E. Bulska, and K. Maksymiuk, 'Experimental study on stability of different solid contact arrangements of ion-selective electrodes', *Talanta*, vol. 82, no. 1, pp. 151–157, Jun. 2010.

[101] Y. Wang, H. Xu, J. Zhang, and G. Li, 'Electrochemical Sensors for Clinic Analysis', *Sensors*, vol. 8, no. 4, pp. 2043–2081, Mar. 2008.

[102] A. Michalska, J. Dumańska, and K. Maksymiuk, 'Lowering the Detection Limit of Ion-Selective Plastic Membrane Electrodes with Conducting Polymer Solid Contact and Conducting Polymer Potentiometric Sensors', *Anal. Chem.*, vol. 75, no. 19, pp. 4964–4974, Oct. 2003.

[103] A. Boyle, E. M. Geniès, and M. Lapkowski, 'Application of the electronic conducting polymers as sensors: Polyaniline in the solid state for detection of solvent vapours and polypyrrole for detection of biological ions in solutions', *Synth. Met.*, vol. 28, no. 1–2, pp. 769–774, Jan. 1989.

[104] A. Michalska, A. Hulanicki, and A. Lewenstam, 'All-Solid-State Potentiometric Sensors for Potassium and Sodium Based on Poly(pyrrole) Solid Contact', *Microchem. J.*, vol. 57, no. 1, pp. 59–64, 1997.

[105] J. Bobacka, 'Potential Stability of All-Solid-State Ion-Selective Electrodes Using Conducting Polymers as Ion-to-Electron Transducers', *Anal. Chem.*, vol. 71, no. 21, pp. 4932–4937, Nov. 1999.

[106] J. Bobacka, M. McCarrick, A. Lewenstam, and A. Ivaska, 'All solid-state poly(vinyl chloride) membrane ion-selective electrodes with poly(3-octylthiophene) solid internal contact', *Analyst*, vol. 119, no. 9, pp. 1985–1991, Jan. 1994.

[107] J. Bobacka, A. Ivaska, and A. Lewenstam, 'Plasticizer-free all-solid-state potassium-selective electrode based on poly(3-octylthiophene) and valinomycin', *Anal. Chim. Acta*, vol. 385, no. 1–3, pp. 195–202, Apr. 1999.

[108] M. Vázquez, J. Bobacka, A. Ivaska, and A. Lewenstam, 'Small-volume radial flow cell for all-solid-state ion-selective electrodes', *Talanta*, vol. 62, no. 1, pp. 57–63, Jan. 2004.

[109] T. Blaz, B. Baś, J. Kupis, J. Migdalski, and A. Lewenstam, 'Multielectrode potentiometry in a one-drop sample', *Electrochem. Commun.*, vol. 34, pp. 181–184, Sep. 2013.

[110] A. Michalska and K. Maksymiuk, 'All-plastic, disposable, low detection limit ion-selective electrodes', *Anal. Chim. Acta*, vol. 523, no. 1, pp. 97–105, Oct. 2004.

[111] Z. Mousavi, A. Teter, A. Lewenstam, M. Maj-Zurawska, A. Ivaska, and J. Bobacka, 'Comparison of Multi-walled Carbon Nanotubes and Poly(3-

octylthiophene) as Ion-to-Electron Transducers in All-Solid-State Potassium Ion-Selective Electrodes', *Electroanalysis*, vol. 23, no. 6, pp. 1352–1358, Jun. 2011.

[112] G. A. Crespo, S. Macho, and F. X. Rius, 'Ion-Selective Electrodes Using Carbon Nanotubes as Ion-to-Electron Transducers', *Anal. Chem.*, vol. 80, no. 4, pp. 1316–1322, Feb. 2008.

[113] F. X. Rius-Ruiz, D. Bejarano-Nosas, P. Blondeau, J. Riu, and F. X. Rius, 'Disposable Planar Reference Electrode Based on Carbon Nanotubes and Polyacrylate Membrane', *Anal. Chem.*, vol. 83, no. 14, pp. 5783–5788, Jul. 2011.

[114] J. Hu, X. U. Zou, A. Stein, and P. Bühlmann, 'Ion-Selective Electrodes with Colloid-Imprinted Mesoporous Carbon as Solid Contact', *Anal. Chem.*, vol. 86, no. 14, pp. 7111–7118, Jul. 2014.

[115] B. Paczosa-Bator, 'Ion-selective electrodes with superhydrophobic polymer/carbon nanocomposites as solid contact', *Carbon*, vol. 95, pp. 879–887, Dec. 2015.

[116] U. Guth, F. Gerlach, M. Decker, W. Oelßner, and W. Vonau, 'Solid-state reference electrodes for potentiometric sensors', *J. Solid State Electrochem.*, vol. 13, no. 1, pp. 27–39, Jan. 2009.

[117] M. W. Shinwari, D. Zhitomirsky, I. A. Deen, P. R. Selvaganapathy, M. J. Deen, and D. Landheer, 'Microfabricated Reference Electrodes and their Biosensing Applications', *Sensors*, vol. 10, no. 3, pp. 1679–1715, Mar. 2010.

[118] C. Zuliani, G. Matzeu, and D. Diamond, 'A liquid-junction-free reference electrode based on a PEDOT solid-contact and ionogel capping membrane', *Talanta*, vol. 125, pp. 58–64, Jul. 2014.

[119] T. Guinovart, G. A. Crespo, F. X. Rius, and F. J. Andrade, 'A reference electrode based on polyvinyl butyral (PVB) polymer for decentralized chemical measurements', *Anal. Chim. Acta*, vol. 821, pp. 72–80, Apr. 2014.

[120] C. Bieg, K. Fuchsberger, and M. Stelzle, 'Introduction to polymer-based solid-contact ion-selective electrodes—basic concepts, practical considerations, and current research topics', *Anal. Bioanal. Chem.*, pp. 1–17, Oct. 2016.

[121] J. Abad *et al.*, 'Molecular structure of poly(3-alkyl-thiophenes) investigated by calorimetry and grazing incidence X-ray scattering', *Sol. Energy Mater. Sol. Cells*, vol. 97, pp. 109–118, Feb. 2012.

[122] E. Csahók, E. Vieil, and G. Inzelt, 'In situ dc conductivity study of the redox transformations and relaxation of polyaniline films', *J. Electroanal. Chem.*, vol. 482, no. 2, pp. 168–177, Mar. 2000.

[123] M. Kobashi and H. Takeuchi, 'Inhomogeneity of Spin-Coated and Cast Non-Regioregular Poly(3-hexylthiophene) Films. Structures and Electrical and Photophysical Properties', *Macromolecules*, vol. 31, no. 21, pp. 7273–7278, Oct. 1998.

[124] '42 CFR 493.931 - Routine chemistry.' [Online]. Available: https://www.gpo.gov/fdsys/granule/CFR-2011-title42-vol5/CFR-2011-title42-vol5-sec493-931/content-detail.html. [Accessed: 20-Dec-2016].

[125] P. Buhlmann, X. U. Zou, X. V. Zhen, J. Hu, and A. Stein, 'Lipophilic Redox Buffers for Polymeric Solid-Contact Electrodes', *Meet. Abstr.*, vol. MA2016-02, no. 46, pp. 3360–3360, Sep. 2016.

[126] X. U. Zou, J. H. Cheong, B. J. Taitt, and P. Bühlmann, 'Solid contact ion-selective electrodes with a well-controlled Co(II)/Co(III) redox buffer layer', *Anal. Chem.*, vol. 85, no. 19, pp. 9350–9355, Oct. 2013.

[127] X. U. Zou, X. V. Zhen, J. H. Cheong, and P. Bühlmann, 'Calibration-Free Ionophore-Based Ion-Selective Electrodes With a Co(II)/Co(III) Redox Couple-Based Solid Contact', *Anal. Chem.*, vol. 86, no. 17, pp. 8687–8692, Sep. 2014.

[128] K. Y. Chumbimuni-Torres, N. Rubinova, A. Radu, L. T. Kubota, and E. Bakker, 'Solid Contact Potentiometric Sensors for Trace Level Measurements', *Anal. Chem.*, vol. 78, no. 4, pp. 1318–1322, Feb. 2006.

[129] A. Michalska and K. Maksymiuk, 'The influence of spontaneous charging/discharging of conducting polymer ion-to-electron transducer on potentiometric responses of all-solid-state calcium-selective electrodes', *J. Electroanal. Chem.*, vol. 576, no. 2, pp. 339–352, Mar. 2005.

[130] M. Guzinski, J. M. Jarvis, B. D. Pendley, and E. Lindner, 'Equilibration Time of Solid Contact Ion-Selective Electrodes', *Anal. Chem.*, vol. 87, no. 13, pp. 6654–6659, Jul. 2015.

[131] X. Li, S. Petrović, and D. J. Harrison, 'A novel spectroscopic method to image H2O distribution in ion-selective membranes', *Sens. Actuators B Chem.*, vol. 1, no. 1–6, pp. 275–280, Jan. 1990.

[132] M. Fibbioli, W. E. Morf, M. Badertscher, N. F. de Rooij, and E. Pretsch, 'Potential Drifts of Solid-Contacted Ion-Selective Electrodes Due to Zero-Current Ion Fluxes Through the Sensor Membrane', *Electroanalysis*, vol. 12, no. 16, pp. 1286–1292, Nov. 2000.

[133] R. D. Marco *et al.*, 'Evidence of a water layer in solid-contact polymeric ion sensors', *Phys. Chem. Chem. Phys.*, vol. 10, no. 1, pp. 73–76, Dec. 2007.

[134] F. Sundfors, T. Lindfors, L. Höfler, R. Bereczki, and R. E. Gyurcsányi, 'FTIR-ATR Study of Water Uptake and Diffusion through Ion-Selective Membranes Based on Poly(acrylates) and Silicone Rubber', *Anal. Chem.*, vol. 81, no. 14, pp. 5925–5934, Jul. 2009.

[135] J.-P. Veder *et al.*, 'Elimination of Undesirable Water Layers in Solid-Contact Polymeric Ion-Selective Electrodes', *Anal. Chem.*, vol. 80, no. 17, pp. 6731–6740, Sep. 2008.

[136] T. Lindfors, L. Höfler, G. Jágerszki, and R. E. Gyurcsányi, 'Hyphenated FT-IR-Attenuated Total Reflection and Electrochemical Impedance Spectroscopy Technique to Study the Water Uptake and Potential Stability of Polymeric Solid-Contact Ion-Selective Electrodes', *Anal. Chem.*, vol. 83, no. 12, pp. 4902–4908, Jun. 2011.

[137] D. Chen, J. Liang, and Q. Pei, 'Flexible and stretchable electrodes for next generation polymer electronics: a review', *Sci. China Chem.*, vol. 59, no. 6, pp. 659–671, Jun. 2016.

[138] T. Sekitani, 'Soft Biosensor Systems Using Flexible and Stretchable Electronics Technology', in *Stretchable Bioelectronics for Medical Devices and Systems*, J. A. Rogers, R. Ghaffari, and D.-H. Kim, Eds. Springer International Publishing, 2016, pp. 133–149.

[139] S. Bauer, 'Flexible electronics: Sophisticated skin', *Nat. Mater.*, vol. 12, no. 10, pp. 871–872, Oct. 2013.

[140] C. Wang *et al.*, 'User-interactive electronic skin for instantaneous pressure visualization', *Nat. Mater.*, vol. 12, no. 10, pp. 899–904, Oct. 2013.

[141] R. C. Webb *et al.*, 'Ultrathin conformal devices for precise and continuous thermal characterization of human skin', *Nat. Mater.*, vol. 12, no. 10, pp. 938–944, Oct. 2013.

[142] L. Li, Z. Yu, W. Hu, C. Chang, Q. Chen, and Q. Pei, 'Efficient Flexible Phosphorescent Polymer Light-Emitting Diodes Based on Silver Nanowire-Polymer Composite Electrode', *Adv. Mater.*, vol. 23, no. 46, pp. 5563–5567, Dec. 2011.

[143] M. W. Rowell *et al.*, 'Organic solar cells with carbon nanotube network electrodes', *Appl. Phys. Lett.*, vol. 88, no. 23, p. 233506, Jun. 2006.

[144] K. S. Kim *et al.*, 'Large-scale pattern growth of graphene films for stretchable transparent electrodes', *Nature*, vol. 457, no. 7230, pp. 706–710, Feb. 2009.

[145] L. M. Castano and A. B. Flatau, 'Smart fabric sensors and e-textile technologies: a review', *Smart Mater. Struct.*, vol. 23, no. 5, p. 53001, 2014.

[146] E. R. Post, M. Orth, P. R. Russo, and N. Gershenfeld, 'E-broidery: Design and fabrication of textile-based computing', *IBM Syst. J.*, vol. 39, no. 3.4, pp. 840–860, 2000.

[147] L. Buechley and M. Eisenberg, 'Fabric PCBs, electronic sequins, and socket buttons: techniques for e-textile craft', *Pers. Ubiquitous Comput.*, vol. 13, no. 2, pp. 133–150, Feb. 2009.

[148] Y. Ogawa, Y. Takai, Y. Kato, H. Kai, T. Miyake, and M. Nishizawa, 'Stretchable biofuel cell with enzyme-modified conductive textiles', *Biosens. Bioelectron.*, vol. 74, pp. 947–952, Dec. 2015.

[149] Y.-H. Lee *et al.*, 'Wearable Textile Battery Rechargeable by Solar Energy', *Nano Lett.*, vol. 13, no. 11, pp. 5753–5761, Nov. 2013.

[150] A. J. Bandodkar, 'Review—Wearable Biofuel Cells: Past, Present and Future', *J. Electrochem. Soc.*, vol. 164, no. 3, pp. H3007–H3014, Jan. 2017.

[151] R. E. Sousa, C. M. Costa, and S. Lanceros-Méndez, 'Advances and Future Challenges in Printed Batteries', *ChemSusChem*, vol. 8, no. 21, pp. 3539–3555, Nov. 2015.

[152] A. E. Ostfeld, A. M. Gaikwad, Y. Khan, and A. C. Arias, 'High-performance flexible energy storage and harvesting system for wearable electronics', *Sci. Rep.*, vol. 6, May 2016.

[153] Y. Ogawa *et al.*, 'Organic transdermal iontophoresis patch with built-in biofuel cell', *Adv. Healthc. Mater.*, vol. 4, no. 4, pp. 506–510, Mar. 2015.

Chapter 2 The Development and Characterisation of a Miniaturised Solid Contact Electrochemical Sensor for the Determination of Sodium Concentration in Sweat.

2.1 Introduction

In the last decade there has been considerable movement towards the application of microfluidics to miniaturise sensing platforms in order to develop low cost and portable devices for a range of applications including point of care, wearable and environmental monitoring [1]–[3]. The realisation of these miniaturised platforms is dependent on the development of miniaturised sensing technology, often employing colorimetric or electrochemical methods [4]–[6].

Ion selective electrodes (ISE) are an example of a type of electrochemical sensor commonly used in microfluidic platforms [7]. ISEs allow the quantification of a specific ion in a solution by converting ionic activity into electrical potential which can then be read and analysed. Conventionally these electrodes consist of an internal electrolyte solution between an ion selective membrane and reference electrode to establish a constant phase boundary potential to govern the membrane response [8], [9]. As the internal solution makes miniaturising these electrodes difficult alternative strategies utilising solid state electrodes were developed [10].

Solid contact ISEs (sc-ISE) employ a conducting substrate and a solid ion to electron transducer, removing the need for internal electrodes and electrolyte solutions [11]. One of the most common type of materials used in sc-ISEs are conducting polymers (CP) owing to a range of factors including ease of electrodeposition on a large amount of substrates and mixed electronic and ionic conductivity making them very effective ion to electron transducers [12]. ISEs have been developed to quantify over 70 analytes and used for a range of different applications from the the detection of heavy metals such as Pb^{2+} in

environmental samples to the determination of pH, Na^+ and K^+ levels in sweat and saliva [13]–[18].

As the number of publications utilising sc-ISEs has increased in recent years so too has the number of critical studies into their characteristics and limitations [9], [19]. The most commonly discussed criteria concerning sc-ISEs involve stability and reproducibility of the electrode potential. An important step in establishing stability of electrode potential is conditioning. When initially immersed in a solution containing the ion of interest ISEs will display a high level of potential drift, which decreases and stabilises to a state of equilibrium with prolonged exposure [11]. Therefore it is necessary to pre-condition ISEs in electrolyte solution for a period of time before calibration. The conditioning period can range from minutes to several hours depending on the electron conducting and solid contact materials used [20].

This work presents the miniaturisation, optimisation and characterisation of an ISE for the monitoring of Na^+ levels in sweat. The sensor is a screen printed electrode (SPE) consisting of a solid contact Na^+ ISE alongside an ionogel-based solid contact reference electrode [21], [22]. The study consisted of optimisation of the conditioning step, determination of the reproducibility of the electrodes and investigation of the stability of the electrodes during dry storage and during prolonged testing.

2.2 Experimental

2.2.1.1 Materials

The carbon and dielectric inks used in the preparation of the screen-printed electrodes, SPE's, were obtained from Gwent Inc. Pontypool, UK (product codes C2030519P4 and D50706D2, respectively). PET sheets (0.175mm thick HiFi, Dublin, Ireland) were used as the electrode substrate, while pressure-sensitive adhesive (86 μm, PSA-AR9808, Adhesives Research, Ireland) and PMMA (0.5 mm thick) was obtained from GoodFellow, UK.

Sodium chloride, 3,4-ethylenedioxythiophene (EDOT, 97%), high molecular weight poly(vinyl chloride) (PVC), tetrahydrofuran (THF, ≥99.5%), 4-tert-butylcalix[4]arene-tetraacetic acid tetraethyl ester (sodium ionophore X), potassium tetrakis(4-chlorophenyl)borate (KTFClPB), bis(2-ethylhexyl)sebacate, 2,2-dimethoxy-2-phenylacetophenone (DMPA, >99%), butyl-acrylate (>99%) and 1,6-hexanediol diacrylate (HDDA, 80%), all selectophore grade, where available, were purchased from Sigma-Aldrich (Dublin, Ireland). N-Decyl-methacrylate was obtained from Polysciences (Northampton, UK). 1-Ethyl-3-methylimidazolium bis(trifluoromethanesulfonyl)imide [emim][NTf_2], [emim] tris(pentafluoroethyl)trifluorophosphate [FAP] and 1-hexyl-3-methylimidazolium [hmim] [FAP] were obtained from VWR (Dublin, Ireland). All chemicals were used without any further purification. Milli-Q reagent-grade deionised water (resistivity 18.2 MΩ cm) was used for making all aqueous solutions.

2.2.1.2 Screen Printed Electrode Fabrication

The solid-state ISE (based on the calix[4]arene tetraester Na^+ ionophore X [23]), and RE were prepared on a conducting carbon layer insulated by a dielectric layer, before conducting polymer, ISE and RE layers were prepared (Figure 2-1).

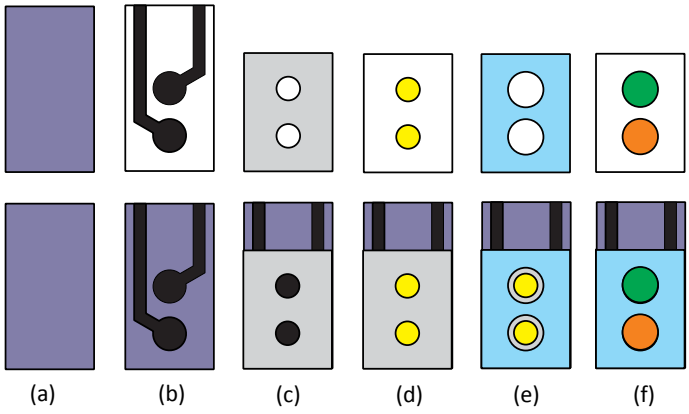

Figure 2-1: A schematic showing the individual components (top) in parallel to the cumulative assembly of the combination electrode (bottom). A PET substrate (a) was cleaned before conducting carbon (b) and insulating dielectric (c) layers were screen-printed respectively. A conducting polymer solid contact layer (d) was then electrodeposited before the addition of a 0.5 mm PMMA layer (e), adhered with PSA, to act as a reservoir for the dropcast ISE and photo-polymerised RE membranes (f).

The screens printed electrodes, SPEs, were designed using computer aided design, CAD, software and realized using a DEK 248 printer (Weymouth, UK).

Two layers of the D50706D2 dielectric ink were formed at the speed of 10 cm s^{-1} which represented a good compromise between the quality of the insulation, and time and materials spent for an additional print. The C2030519P4 carbon ink was printed at 30 cm s−1. The squeegee "pressure" value was adjusted to 14 and 10 kg, respectively, for the printing of D50706D2 and C2030519P4, and table/screen separation was the closest achievable with the instrument, i.e., ~ 1-2 mm. Each printed layer was annealed according to the supplier specifications, i.e., C2030519P4: 12 minutes at 80 °C, D50706D2: 30 minutes at 80 °C. In case of multiple prints with same ink, curing was repeated in between printing of individual layers.

A poly-3,4-ethylenedioxythiophene (PEDOT) solid contact layer was electrodeposited on the exposed carbon layers using 0.5M 3,4-ethylenedioxythiophene (EDOT, 97%, 483028 Aldrich) and [emim] tris-(pentafluoroethyl)trifluorophosphate [FAP] (VWR, Dublin, Ireland). Potentiostatic depositions were achieved applying a constant potential of 1.0 V vs. Ag wire for 576 seconds[21] .

0.5 mm PMMA was laser cut and used to create two separate 3.0 mm diameter reservoirs in which ISE and reference polymer membranes were prepared by drop casting (see below) and attached to the screen-printed layers using 86 µm pressure sensitive adhesive (PSA), from Adhesives Research, Ireland (Figure 2-2).

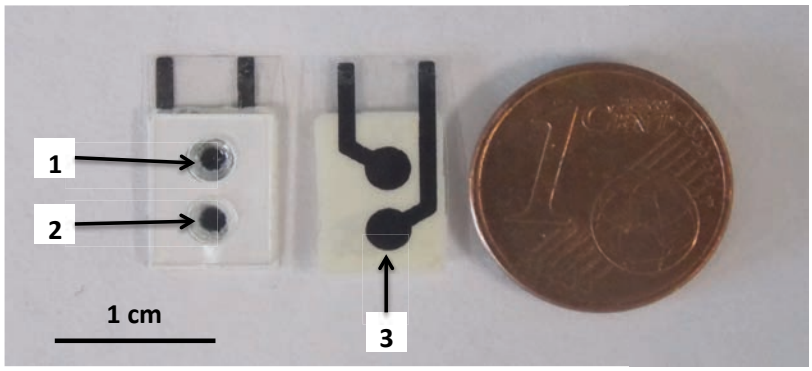

Figure 2-2: Front (left) and back (right) of the electrochemical sensor showing (1) the ISE, (2) the reference electrode and (3) the screen-printed conductive carbon layer.

For the Na^+ ISE a total of 30 µL Na^+ selective membrane material dissolved in THF30 was drop-cast into the reservoir above the solid-contact PEDOT layer in

the following sequence: 2.5 µL (once); 3 µL (5 times); 2.5 µL (once); 2 µL (twice); 1.5 µL (twice) and 1 µL (3 times) in order to build up polymer layers to fill the 3.5 µL reservoir meaning a maximum of 3.5 µL can be added per step with reductions in capacity with each subsequent addition. For the reference membrane, a cocktail was prepared of ionic liquid (IL) vortexed for 1 h with the acrylate monomer(s), the cross-linker and the photoinitiator. This was then photopolymerised within the 3 mm reservoir by irradiation for 32 minutes with a CL-1000 ultraviolet cross-linker UVP source.

2.2.1.3 Electrode Characterisation

A number of tests were carried out to assess the reproducibility and stability of the electrodes. The potentiometric responses of both the ISE and RE electrodes to changes in Na^+ concentration were monitored using the multi channel voltmeter, MCV, capabilities of an EMF-16 channel system from Lawson Labs (USA). Measurements were carried out against a double-junction Ag/AgCl reference electrode (Sigma-Aldrich, Dublin). A custom experimental setup was designed using CAD software to allow the lowering of four combination electrodes, each consisting of an ISE and RE electrode, in parallel in a single beaker.

In order to minimise potential drift, evident when the ISEs are initially exposed to a solution of the ion of interest, conditioning is required involving hydration in a solution of the target ion until equilibrium is reached the potential signal reaches a steady state indicating equilibrium has been reached. The electrodes were conditioned by being lowered into a solution of 10 mM NaCl and monitored using the MCV for a range of conditioning periods. 3 conditioning periods were investigated 16 hours (overnight), 2 hours and 1 hour. The sensors were then calibrated by lowering them into a solution of low NaCl concentration, 0.01 or 0.1 mM, before stepwise additions of 1M and 5M NaCl to increase Na^+ activities from 10^{-4} to 10^{-1} in decade intervals. Na^+ concentration was converted to ionic activity using its direct relationship with activity and the Na^+ activity coefficient calculated using the Debye-Huckel equation [24], [25]. Stability studies were

performed by calibrating the electrodes before and after dry storage of 13 to 19 days. After testing the electrodes were rinsed with 0.1 mM NaCl solution, dryed gently and stored in the dark at room temperature.

A study was also carried out to mimic sustained exposure to Na^+ concentrations commonly found in sweat and assess their effect on electrode performance. The procedure involved calibrating the electrodes with the method described above before exposing them to 10mM NaCl, representative of a low sweat sodium level, for 120 min followed by another calibration. This was followed by 120 min exposure to 50mM NaCl, representative of a high sweat sodium level before a final calibration.

2.3 Results and Discussion

2.3.1 Conditioning Studies

In order to evaluate the impact of conditioning duration on the electrode performance the electrodes were initially monitored during 15 hour conditioning before a four point calibration was carried out. These results were then compared with those of a reduced conditioning period of 2 hours.

2.3.1.1 Overnight Conditioning

Two combination electrodes were initially conditioned in 10 mM overnight while connected to the MCV to monitor potential response against an external Ag/AgCl reference electrode. The signal of 2 of the electrodes, ISE 2 and RE 1 appeared stable over the initial 300 min but began to drift steadily for the remaining 600 min (Figure 2-3). ISE 1 showed an initial increase in signal before exhibiting similar behaviour to ISE 2. RE 2 showed drift throughout starting at ca. 310 mV and drifting to ca. 180 mV at 900 min.

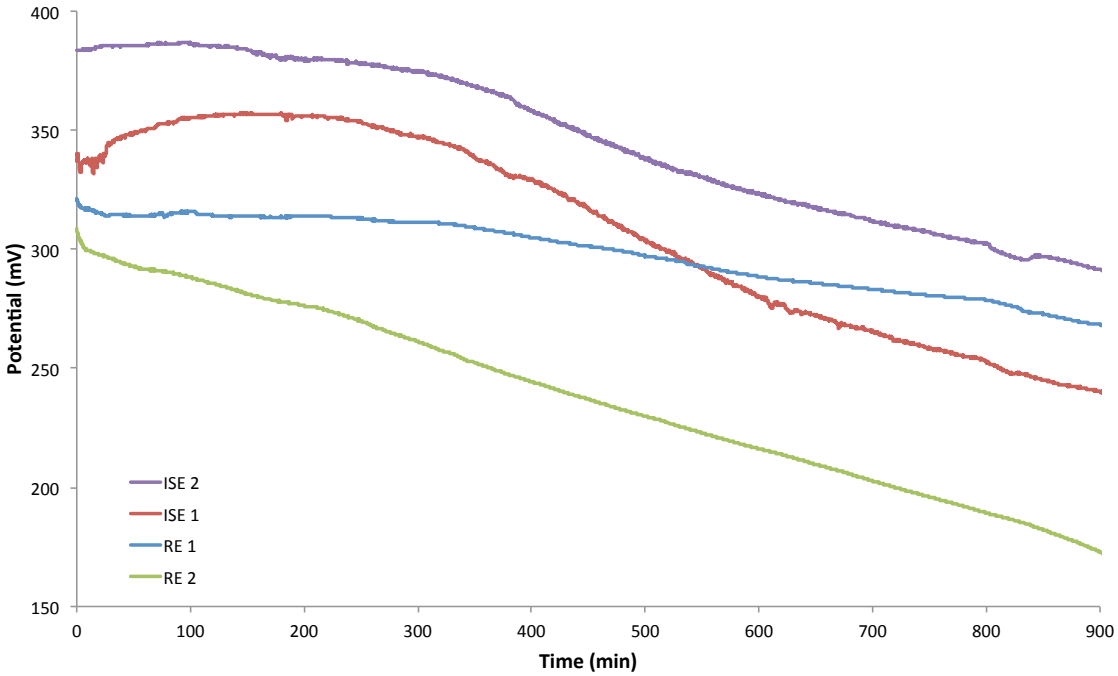

Figure 2-3: Potential of the ISE and RE of 2 combination electrodes over 15 hours exposure to 10mM NaCl.

When focusing on the first 120min of data a steady signal was observed for all four electrodes after ca. 40 min which suggest equilibrium was reached sometime during this period (Figure 2-4). This would suggest that conditioning steps above 120 minutes may be unnecessary.

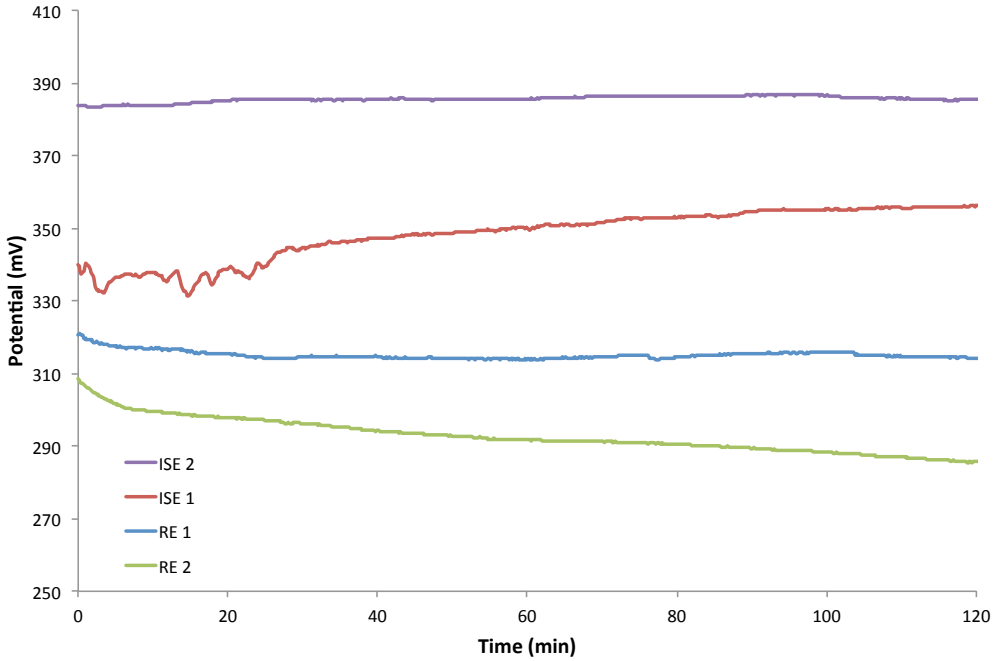

Figure 2-4: Initial 2 hours of 15 hour conditioning step of 2 combination electrodes.

A four point calibration, from Na^+ activities of 10^{-4} to 10^{-1} in decade intervals, of combination electrodes showed a sub-Nernstian response of ca. 49 mV/decade and R^2 values of 0.99 for the ISE's while the RE's were stable with slopes of ca. 1 mV/decade (Figure 2-5).

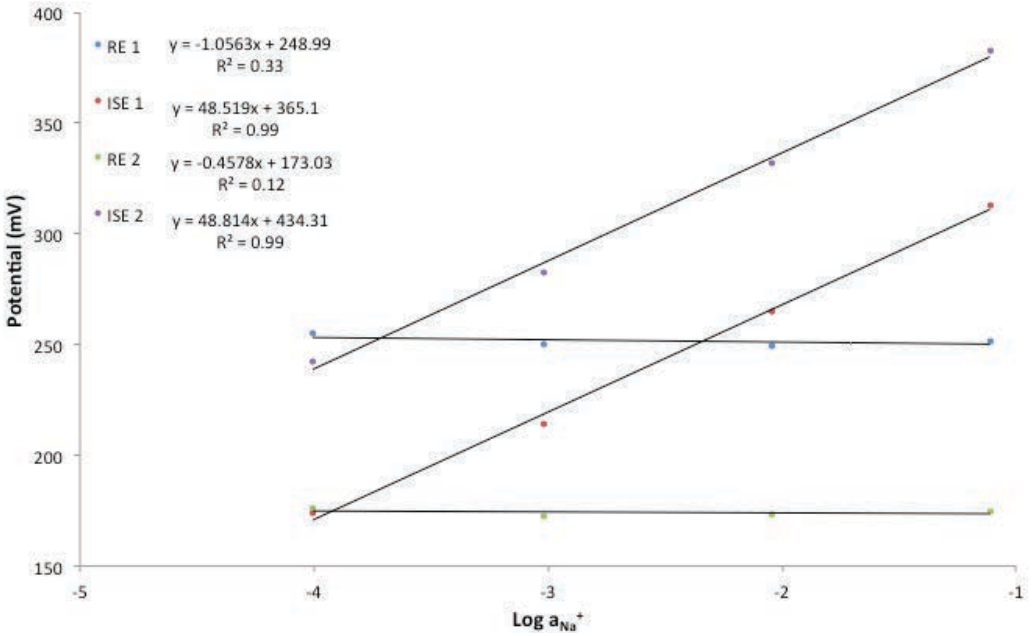

Figure 2-5: A four point calibration (0.1 to 100 mM) of a 2 ISE's and 2 RE's showing ion selectivity after a 15 hour conditioning step.

The low responses in potential to changes in Na^+ suggest that the prolonged conditioning protocols may not be optimal for these sensors. The results prompted investigation into the effects of a shorter conditioning period on Na^+ sensitivity.

2.3.1.2 Shortened Conditioning Studies

For the comparison study, two combination electrodes were conditioned in 10 mM NaCl for a shortened period of 2 hours. The RE's displayed a steady signal throughout while the ISE's fluctuated initially before equilibrium was reached ca. 40 min. Steady signals and improved Na^+ sensitivities were observed from the subsequent calibration (Figure 2-6). ISE 3 exhibited a super-Nernstian response of 62.9 mV/decade while ISE 4 displayed a Nernstian response of 59.5 mV/decade.

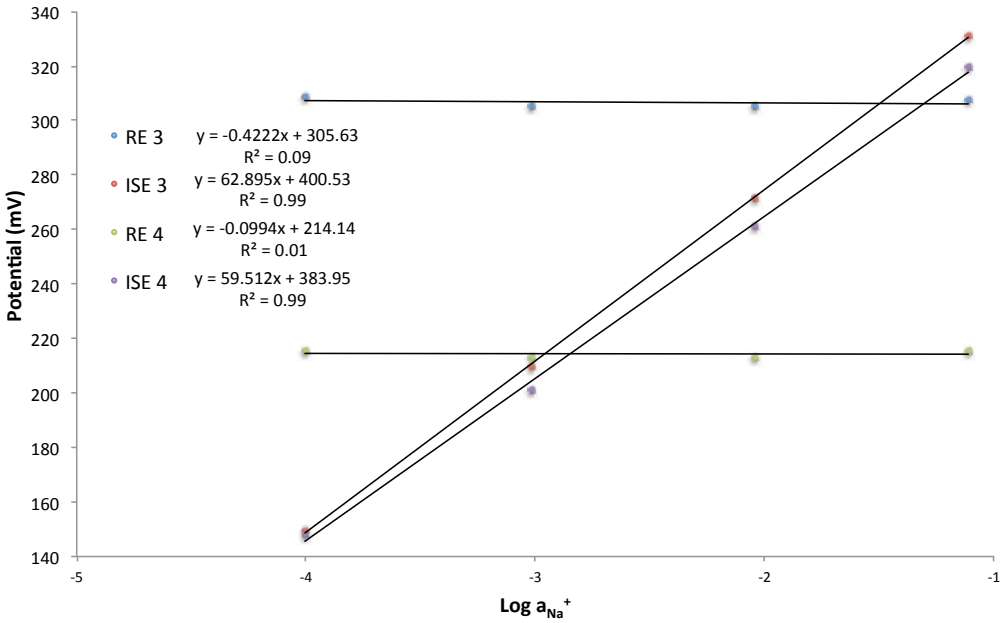

Figure 2-6: Four point calibration after a 2 hour conditioning step.

As superior Na^+ sensitivities were achieved, the shortened conditioning procedure was utilized in subsequent sensor characterisation steps.

2.3.2 Reproducibility Studies

Before progressing to on-body trials it was important to characterise the reproducibility of the sensors in order to define the necessary calibration protocol. The reproducibility of the electrodes was characterised by fabricating 10 combination electrodes fabricated in parallel prior to a 4 point calibration from 0.1 mM to 100mM NaCl. All electrodes were conditioned in 10 mM NaCl for 1 hour before use. The calibrations were carried out using the same protocol used for the conditioning studies.

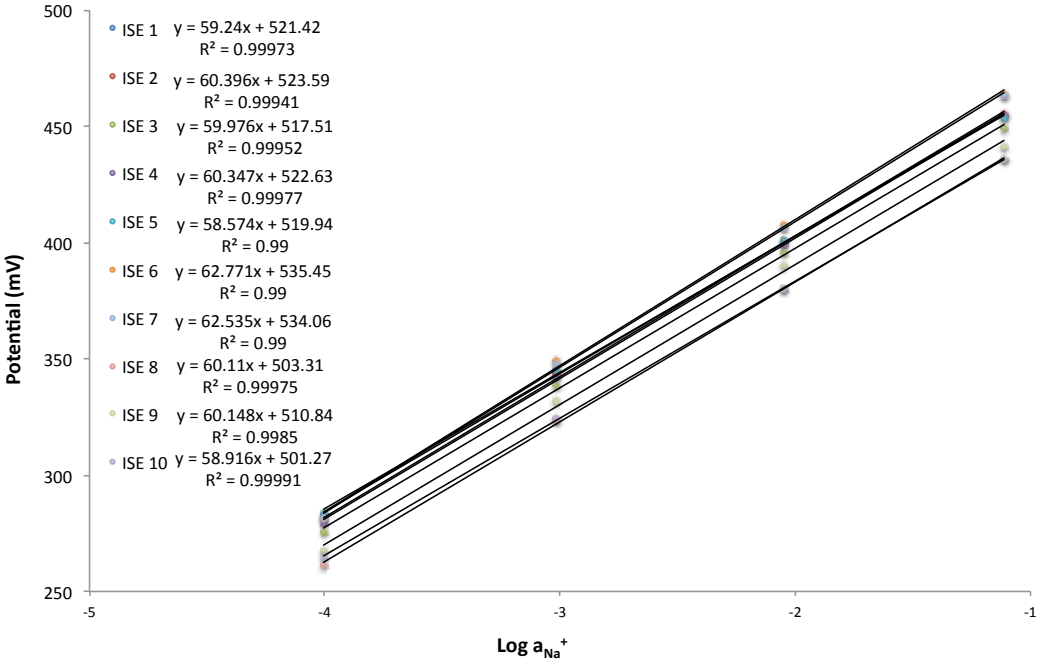

Figure 2-7: Calibration of ISEs (n=10) against an external Ag/AgCl reference electrode. The electrodes had been conditioned in 10^{-2} mM NaCl prior to calibration.

All 10 ISE electrodes exhibited ca. Nernstian responses with slopes ranging from 58.6 to 62.8 mV/decade (Figure 2-7). Although the electrodes displayed similar slopes higher variation could be observed in the baseline values, covering a range of 22 mV, 262-284 mV, in 0.1 mM NaCl and 28 mV, 436-464 mV in 100mM NaCl. As discussed in section 1.3.3 various strategies including the use of redox buffers and nanomaterials have been effective in studies by other groups in controlling interfacial potential resulting in reduced potential drift and increased reproducibility in standard potential [26]–[28]. Membrane thickness variations arising from the multilayer drop-casting fabrication method can also contribute to variations in standard potential [20].

A comparison of the 10 combination electrodes with the y intercept values subtracted allowed a more realistic comparison of sensor behaviour by removing the error caused by membrane height (Figure 2-8). These results show a standard deviation of 6.63, 4.47, 3.45 and 2.02 mV at 10^{-4}, 10^{-3}, 10^{-2} and 10^{-1} a_{Na^+} respectively while maintaining an average Na^+ sensitivity of 58.9 mV/decade ± 1.59 mV.

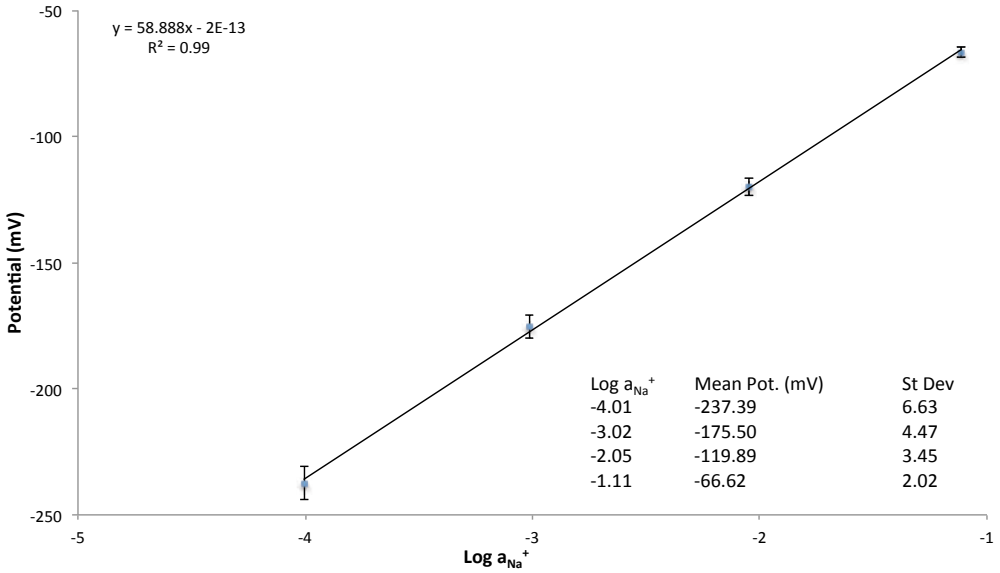

Figure 2-8: Calibration of combination electrodes (n=10), without systematic error, showing the responses when exposed to solutions containing log 10^{-4} to 10^{-1} a_{Na^+}. The error bars show a decreasing standard deviation with increases in Na^+ activity.

The highest 2 calibration solutions cover the range of sweat sodium found on the forearm of 14.4-54 mM [29]. The results from the 10 electrode study show that the standard deviation lowers with increasing concentrations reflecting higher reproducibility in the range of interest.

2.3.3 Stability Studies

2.3.3.1 Stability After Dry Storage

An investigation was carried out into the stability of the electrodes after being stored dry, at room temperature in the dark for periods of 13 and 19 days. The electrodes were conditioned at 10 mM NaCl for one hour and calibrated on the first final days to observe behavioural changes. Table 2-1 presents the comparison of the potential and sensitivities shown on Day 1 with those observed on the final day.

Table 2-1: Calibration data of 3 sensors tested before and after dry storage of 13 (sensors 1 and 2) and 19 days (sensor 3), with data from external reference vs solid contact ISE and RE beside the combination electrode (CE) values of the combined solid contact cell.

Sensor 1: 13 Day Stability Study

		Δ mV Between Days	
Log a_{Na}^+	**RE 1: Day 1 to 13**	**ISE 1: Day 1 to 13**	**CE 1: Day 1 to 13**
-4.01	+10	-26	-36
-3.02	+6	-31	-37
-2.05	+7	-33	-40
-1.11	+9	-30	-39
	Slope RE 1	**Slope ISE 1**	**Slope CE 1**
Day 1	1.98	60.97	58.99
Day 13	1.76	59.50	57.74

Sensor 2: 13 Day Stability Study

		Δ mV Between Days	
Log a_{Na}^+	**RE 2: Day 1 to 13**	**ISE 2: Day 1 to 13**	**CE 2: Day 1 to 13**
-4.01	-12	-30	-18
-3.02	-14	-35	-21
-2.05	-14	-36	-22
-1.11	-10	-35	-25
	Slope RE 2	**Slope ISE 2**	**Slope CE 2**
Day 1	1.05	61.91	60.85
Day 13	1.66	60.23	58.57

Sensor 3: 19 Day Stability Study

		Δ mV Between Days	
Log a_{Na}^+	**RE 3: Day 1 to 19**	**ISE 3: Day 1 to 19**	**CE 3: Day 1 to 19**
-4.01	-59	-18	+41
-3.02	-59	-38	+21
-2.05	-59	-45	+14
-1.11	-57	-47	+10
	Slope RE 3	**Slope ISE 3**	**Slope CE 3**
Day 1	1.35	68.35	67.00
Day 19	1.97	58.56	56.59

The difference in the potentiometric signals at each concentration for each electrode from the first and last day of testing varied according to each sensor. The REs showed the most variation between sensors with an increase of 10 and 9 mV for the lower and higher Na^+ concentrations respectively observed for RE1 while the other 13 day test RE 2 showed a decrease of 12 and 10 mV at the same concentrations. The variation shown by the RE of sensor 3, stored for 19 days, contrasts significantly more with a decrease of 59 and 57 mV observed at the higher and lower concentrations respectively. These varying changes in RE potential signal over time could be attributed to physical changes caused by drying and rehydration of the ionogel based reference membrane. Importantly, no major variation was observed for the responses of the REs between the four calibration solutions with initial and final slopes of 1.98 and 1.76 mV, 1.05 and 1.66 mV and 1.35 and 1.97 mV for sensors 1, 2 and 3 respectively.

The ISE potential signals between the first and last day varied significantly less than the RE when compared between the sensors. Sensors 1 and 2, both monitored after 13 days, showed changes of -26 and -30mV and -30 and -35 mV for the lowest and highest Na^+ concentrations respectively. The sensor stored for 19 days showed a smaller difference of -18 mV at the lowest concentration and a larger difference of -47 mV at the higher concentrations. The effects of storage on ISE sensitivity over 13 days displayed as a 2.41% decrease in slope for sensor 1 and a 2.71% decrease in sensor 2. The ISE of sensor 3, stored for 19 days, showed a more extensive change in sensitivity with a 14.32% decrease in slope.

The effects of storage on the whole Na^+ combination electrode system is observed by analysis of the combined electrode slopes, considering effects on both RE and ISE elements, representing the effect on Na^+ sensitivity (see Appendix Figures A-1 to A-3). Sensors 1 and 2, both stored dry for 13 days, showed 2.12 and 3.75% decrease in sensitivity. Sensor 3, stored dry for 19 days, showed a 15.54% decrease in sensitivity.

The potential drift and reduction in sensitivity suggest, in the case of dry storage, that a calibration should take place as near as possible or directly before an

electrode is to be used for the identification of unknown samples to optimise the accuracy of the test. Possible causes identified for drift in sc-ISEs include leaching of constituents from the membrane layer into the sample solution and the formation of a water layer between the ISE and solid contact layer [11]. Due to the small sample size this study can only give a brief insight into the effects of storage on the electrodes. A larger sample set and more extensive study would be needed to fully define the potential drift and determine the cause.

2.3.3.2 Stability After Prolonged Na^+ Exposure

The purpose of the Na^+ electrodes is to monitor sweat sodium levels in real time during exercise. For this, they will be exposed to the Na^+ concentration of the sweat for the duration of the test (30-120 min). To determine the effect that the normal range of sodium in sweat, 14.4-54 mM [29], has on the electrodes two electrodes were conditioned and calibrated as in the previous stability study. The electrodes were then immersed in 10mM NaCl for 120 min before a repeat calibration in order to simulate the long-term effects of a low Na^+ sweat sample on the electrode. This was then repeated with 50mM NaCl to simulate long term exposure to a high Na^+ sweat sample (see Appendix Figures A-4 and A-5).

Table 2-2 presents the changes in potential and sensitivity of the 2 sensors between the 3 calibrations. The changes in potential at the higher concentrations in the 2 sensors were more similar than those at the lower Na^+ activities. This is particularly evident from the initial calibration after the 120 min 10 mM exposure with a range of -3.10 to +0.02 at Log a_{Na^+} -4.01 comparing with -7.97 to -7.04 at Log a_{Na^+} -1.11. This reflects the observations made in section 2.3.2 that the electrodes show higher reproducibility at higher concentrations.

The potential varies more as a result of the 120 min exposure to the 50 mM than that of 10 mM Na^+. An example of this is at the Log a_{Na^+} -1.11 potential where sensor 1 shows a 7.97 mV decrease after the 10 mM exposure and a 12.76mV after the 50 mM exposure, while sensor 2 shows decreases of 7.04 mV and 14.75 mV at the same points. This variation in sensor behaviour when exposed to

different Na^+ concentrations emphasizes the need for further tests to fully define the behaviour so that it can be accounted for during real time analysis.

Table 2-2: Calibration data for 2 Na^+ combination electrodes over 3 calibrations monitoring the effect of prolonged exposure to 2 varying concentrations of Na^+. Cal A was after a 60 min conditioning step in 10mM NaCl before 120 min in 10 mM NaCl followed by Cal B and finally 120 min in 50 mM NaCl followed by Cal C. Also presented are the changes in potential from, initial calibration to 10 mM incubation (0-120 min), 10 mM to 50 mM incubation (120-240 min) and over the entire study period (0-240 min)

Sensor 1

	Potential (mV)			Δ mV Between Cals		
Log a_{Na}^+	Cal A	Cal B	Cal C	0-120	120-240	0-240
	0 min	120 min	240 min	min	min	min
-4.01	**-34.61**	**-37.71**	**-46.08**	**-3.10**	**-8.37**	**-11.47**
-3.02	**14.15**	**7.83**	**-2.12**	**-6.33**	**-9.95**	**-16.27**
-2.05	**65.04**	**57.81**	**46.46**	**-7.23**	**-11.35**	**-18.58**
-1.11	**117.05**	**109.08**	**96.31**	**-7.97**	**-12.76**	**-20.74**
Slope	**52.42**	**50.80**	**49.29**			

Sensor 2

	Potential (mV)			Δ mV Between Cals		
Log a_{Na}^+	Cal A	Cal B	Cal C	0-120	120-240	0-240
	0 min	120 min	240 min	min	min	min
-4.01	**-66.87**	**-66.84**	**-72.67**	**+0.02**	**-5.83**	**-5.80**
-3.02	**-12.03**	**-16.14**	**-25.31**	**-4.11**	**-9.17**	**-13.28**
-2.05	**42.15**	**36.60**	**23.71**	**-5.55**	**-12.89**	**-18.44**
-1.11	**95.53**	**88.49**	**73.74**	**-7.04**	**-14.75**	**-21.79**
Slope	**56.11**	**53.76**	**50.60**			

2.4 Conclusion

This work highlights the development of minituarised screen printed electrodes for monitoring of Na^+ levels in sweat samples. Initial electrodes submitted to an overnight conditioning step yielded low sensitivities while reduced conditioning time of < 120 min resulted in near-Nernstian sensitivities. The electrodes exhibited high reproducibility (section 2.3.2) but a preliminary study indicated potential drift and loss of sensitivity during dry storage and prolonged ion exposure (section 2.3.3).

The reproducibility of the electrodes suggest that they would be suitable for integration into a platform for real-time electrolyte monitoring of sweat and the subsequent generation of preliminary data for on-body testing. The stability tests, however, indicate the need for pre and post-trial calibrations in order to give the most accurate comparisons for trial analysis. This will allow the quantification of potential drift over the duration of the trial which can then be factored in when analysing Na^+ concentration to optimise the accuracy of the results.

To further enhance electrode behaviour a comprehensive study should be carried out to investigate optimal storage conditions and investigate possible aqueous layer formation at the metal-solid contact interface and possible leaching of the ISE membrane constituents [11], [19]. Aqueous layer formation can be investigated with the use of advanced techniques such as electrochemical impedance spectroscopy (EIS) and Fourier transform-infrared (FTIR) micro-spectroscopy [30], [31].

2.5 References

[1] E. K. Sackmann, A. L. Fulton, and D. J. Beebe, 'The present and future role of microfluidics in biomedical research', *Nature*, vol. 507, no. 7491, pp. 181–189, Mar. 2014.

[2] J. C. Jokerst, J. M. Emory, and C. S. Henry, 'Advances in microfluidics for environmental analysis', *Analyst*, vol. 137, no. 1, pp. 24–34, 2012.

[3] J. Chuan Yeo, Kenry, and C. Teck Lim, 'Emergence of microfluidic wearable technologies', *Lab. Chip*, vol. 16, no. 21, pp. 4082–4090, 2016.

[4] A. W. Martinez, S. T. Phillips, G. M. Whitesides, and E. Carrilho, 'Diagnostics for the Developing World: Microfluidic Paper-Based Analytical Devices', *Anal. Chem.*, vol. 82, no. 1, pp. 3–10, Jan. 2010.

[5] D. G. Rackus, M. H. Shamsi, and A. R. Wheeler, 'Electrochemistry, biosensors and microfluidics: a convergence of fields', *Chem. Soc. Rev.*, vol. 44, no. 15, pp. 5320–5340, 2015.

[6] K. N. Han, C. A. Li, and G. H. Seong, 'Microfluidic Chips for Immunoassays', *Annu. Rev. Anal. Chem.*, vol. 6, no. 1, pp. 119–141, 2013.

[7] J. Bobacka, A. Ivaska, and A. Lewenstam, 'Potentiometric Ion Sensors', *Chem. Rev.*, vol. 108, no. 2, pp. 329–351, Feb. 2008.

[8] L. van de Velde, E. d'Angremont, and W. Olthuis, 'Solid contact potassium selective electrodes for biomedical applications – a review', *Talanta*, vol. 160, pp. 56–65, Nov. 2016.

[9] E. Lindner and R. E. Gyurcsányi, 'Quality control criteria for solid-contact, solvent polymeric membrane ion-selective electrodes', *J. Solid State Electrochem.*, vol. 13, no. 1, pp. 51–68, Jan. 2009.

[10] A. Michalska, 'All-Solid-State Ion Selective and All-Solid-State Reference Electrodes', *Electroanalysis*, vol. 24, no. 6, pp. 1253–1265, Jun. 2012.

[11] C. Bieg, K. Fuchsberger, and M. Stelzle, 'Introduction to polymer-based solid-contact ion-selective electrodes—basic concepts, practical considerations, and current research topics', *Anal. Bioanal. Chem.*, pp. 1–17, Oct. 2016.

[12] J. Bobacka, 'Conducting Polymer-Based Solid-State Ion-Selective Electrodes', *Electroanalysis*, vol. 18, no. 1, pp. 7–18, Jan. 2006.

[13] I. A. Pechenkina and K. N. Mikhelson, 'Materials for the ionophore-based membranes for ion-selective electrodes: Problems and achievements (review paper)', *Russ. J. Electrochem.*, vol. 51, no. 2, pp. 93–102, Feb. 2015.

[14] M. B. Gumpu, S. Sethuraman, U. M. Krishnan, and J. B. B. Rayappan, 'A review on detection of heavy metal ions in water – An electrochemical approach', *Sens. Actuators B Chem.*, vol. 213, pp. 515–533, Jul. 2015.

[15] M.-R. Huang, Y.-B. Ding, and X.-G. Li, 'Combinatorial Screening of Potentiometric Pb(II) Sensors from Polysulfoaminoanthraquinone Solid Ionophore', *ACS Comb. Sci.*, vol. 16, no. 3, pp. 128–138, Mar. 2014.

[16] A. J. Bandodkar *et al.*, 'Epidermal tattoo potentiometric sodium sensors with wireless signal transduction for continuous non-invasive sweat monitoring', *Biosens. Bioelectron.*, vol. 54, pp. 603–609, Apr. 2014.

[17] W. Gao *et al.*, 'Fully integrated wearable sensor arrays for multiplexed in situ perspiration analysis', *Nature*, vol. 529, no. 7587, pp. 509–514, Jan. 2016.

[18] C. Zuliani, G. Matzeu, and D. Diamond, 'A potentiometric disposable sensor strip for measuring pH in saliva', *Electrochimica Acta*, vol. 132, pp. 292–296, Jun. 2014.

[19] J. Hu, A. Stein, and P. Bühlmann, 'Rational design of all-solid-state ion-selective electrodes and reference electrodes', *TrAC Trends Anal. Chem.*, vol. 76, pp. 102–114, Feb. 2016.

[20] M. Guzinski, J. M. Jarvis, B. D. Pendley, and E. Lindner, 'Equilibration Time of Solid Contact Ion-Selective Electrodes', *Anal. Chem.*, vol. 87, no. 13, pp. 6654–6659, Jul. 2015.

[21] G. Matzeu *et al.*, 'An integrated sensing and wireless communications platform for sensing sodium in sweat', *Anal. Methods*, vol. 8, no. 1, pp. 64–71, Dec. 2015.

[22] C. Zuliani, G. Matzeu, and D. Diamond, 'A liquid-junction-free reference electrode based on a PEDOT solid-contact and ionogel capping membrane', *Talanta*, vol. 125, pp. 58–64, Jul. 2014.

[23] D. Diamond, G. Svehla, E. M. Seward, and M. A. McKervey, 'A sodium ion-selective electrodebased on methyl p-t-butylcalix[4]aryl acetate as the ionophore', *Anal. Chim. Acta*, vol. 204, pp. 223–231, Jan. 1988.

[24] E. Lindner and B. D. Pendley, 'A tutorial on the application of ion-selective electrode potentiometry: An analytical method with unique qualities, unexplored opportunities and potential pitfalls; Tutorial', *Anal. Chim. Acta*, vol. 762, pp. 1–13, Jan. 2013.

[25] P. C. Meier, 'Two-parameter debye-hückel approximation for the evaluation of mean activity coefficients of 109 electrolytes', *Anal. Chim. Acta*, vol. 136, pp. 363–368, Jan. 1982.

[26] P. Buhlmann, X. U. Zou, X. V. Zhen, J. Hu, and A. Stein, 'Lipophilic Redox Buffers for Polymeric Solid-Contact Electrodes', *Meet. Abstr.*, vol. MA2016-02, no. 46, pp. 3360–3360, Sep. 2016.

[27] J. Hu, X. U. Zou, A. Stein, and P. Bühlmann, 'Ion-Selective Electrodes with Colloid-Imprinted Mesoporous Carbon as Solid Contact', *Anal. Chem.*, vol. 86, no. 14, pp. 7111–7118, Jul. 2014.

[28] B. Paczosa-Bator, 'Ion-selective electrodes with superhydrophobic polymer/carbon nanocomposites as solid contact', *Carbon*, vol. 95, pp. 879–887, Dec. 2015.

[29] R. M. Carr, 'Dietary Sodium Intake, Sweat Sodium, Salt Appetite and Exercise', Thesis, University of Otago, 2015.

[30] F. Sundfors, T. Lindfors, L. Höfler, R. Bereczki, and R. E. Gyurcsányi, 'FTIR-ATR Study of Water Uptake and Diffusion through Ion-Selective Membranes Based on Poly(acrylates) and Silicone Rubber', *Anal. Chem.*, vol. 81, no. 14, pp. 5925–5934, Jul. 2009.

[31] J.-P. Veder *et al.*, 'Elimination of Undesirable Water Layers in Solid-Contact Polymeric Ion-Selective Electrodes', *Anal. Chem.*, vol. 80, no. 17, pp. 6731–6740, Sep. 2008.

Chapter 3 The Design and Development of a Microfluidic System for the Collection and Analysis of Sweat in a Wearable Device

3.1 Introduction

Medical diagnosis often depends on the retrieval of a blood sample which is an intrusive process involving physical trauma and often poses the risk of infection. This has led to the development of non-invasive alternatives often targeting biofluids such as saliva, sweat and tears as readily available sources of relevant biomarkers [1]. Sweat is particularly interesting in this regard as it is an abundant source of information, with analytes such as sodium, potassium, lactate, glucose and ammonium, that is readily available for sampling from multiple sites in the body [2], [3].

Sweat analysis is currently evolving from sample collection and subsequent laboratory analysis to wearable devices which can analyse sweat in situ autonomously [2], [4]. Early sweat drug determination in the 1970s collected samples by rubbing the skin with cotton, gauze or towel or by applying an occlusive bandage consisting of three layers of filter paper [5], [6]. In the 1990s a patch designed by Pharmchem™ Laboratories (Menlo Park CA, USA) was used in many studies of drug presence in sweat [7], [8]. Advanced collection patches have been utilised for recent studies of sweat sodium levels [9], [10]. The Megaduct® and Macroduct® collection systems were developed by Wescor® Inc. (Logan, UT, USA) to harvest sweat by transferring it form the base of a plastic device to a length of tubing where it was collected by capillary action for use in the diagnosis of cystic fibrosis [11].

Wearable devices for sweat analysis have employed various strategies for sweat sampling. Textile based sweat sensing has seen sensors patterned directly onto clothing [12]–[14], while sensors have also successfully been incorporated onto plastic and temporary-transfer tattoo paper for detection of various analytes

including alcohol, sodium and pH [15]–[17]. Recently a fully integrated wearable device incorporating flexible electronics was developed for multi-analyte detection in sweat [18]. While these devices represent major advances in wearable biochemical sensing they involve direct contact between the skin and sensor. For medium-long term monitoring this could mean that the final sample present would not be indicative of the sweat produced at that time but rather an accumulation of the sweat generated throughout the trial.

A wearable device was recently developed which sampled sweat from the skin surface with an adapted macroduct® device and delivered it passively by capillary action to an adsorbent material which wicked the sample across the electrodes for real-time analysis to a reservoir containing cotton material which absorbed the excess sample [19]. This chapter presents the design, development and characterisation of a fluidic system combining adsorbent material and capillary channels for the collection delivery of a sweat sample over a minituarised Na^+ sensitive electrode presented in chapter 2. This system was designed for easy incorporation into a fully integrated wearable device for real time sweat analysis.

3.2 Experimental

3.2.1 Materials

Pressure-sensitive adhesive (86 μm, PSA-AR9808, Adhesives Research, Ireland) was used to bond the PMMA (0.3mm, 0.5 mm, 1.5 mm and 3.0 mm thick) obtained from GoodFellow, UK which was laser cut to form the walls of the fluidic chip. Two types of highly adsorbent material were obtained to provide assisted passive flow of the sample across the electrodes in a capillary channel. The first was a polypropylene/cellulose 'compo wipe' composite material (Superior Cleanroom Products, product number 87109) and the second was a 30% cotton, 70% cellulose Wettex® sponge cloth (http://www.vileda.com/au/wettex-traditional-sponge-cloth-3pk-3587.html, EAN 9325005000031). Cotton threads in the channel (removed from medical

bandages, W.O.W. Bandage BP, 5 cm × 5 cm) were used to facilitate flow in combination with the adsorbent material while ensuring contact between the sample and the device.

3.2.2 Electrochemical Sensors

The screen-printed combination electrodes were prepared on a PET substrate with the drop-cast Na^+ selective membrane and photo-polymerised reference membrane prepared on an electrodeposited PEDOT/IL solid contact layer as outlined in chapter 2.

3.2.3 Microfluidic Chip

3.2.3.1 Microfluidic Chip Generation 1

A microfluidic chip was designed using CAD software, specifically for incorporation into a fully integrated platform (chapter 4), to provide passive (pump-free) liquid flow ensuring the continued transfer of sample across the electrodes to a sampling reservoir. This was achieved using a PMMA based microfluidic chip (Figure 3-1) incorporating the highly adsorbent material and cotton thread. The multilayer system (Figure 3-2) was made using PSA and PMMA layers cut with a CO2-laser ablation system. The PMMA base (1, Figure 3-2) contained the inlet hole (for fluid transfer from the 3D-printed sweat harvesting baseplate). An 86 μm thick PSA layer was used to attach a 500 μm thick PMMA (2, Figure 3-2), cut to provide channels and location for the adsorbent material.

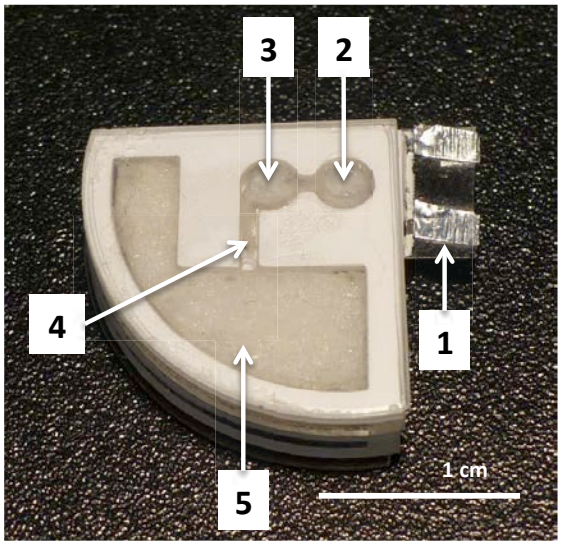

Figure 3-1: Electrode locations and fluidic system. The electrodes connect to the Shimmer electronics board through silver tape connections (1). The sweat passes from the skin through a short vertical channel to the ISE (2) and passes laterally to the reference electrode (3) (both the ISE and reference electrodes are 3 mm diameter with a 500 µm space above giving a volume of 3.53 mm3 and capacity of 3.53 µl over each), and through a short connecting channel (4) to the high capacity adsorbent material (5) for sample storage (total storage capacity of 344 µl Variation of the width of the connecting fluidic channel (4) enables the overall flow rate of the system to be modulated.

The adsorbent material was pre-washed with deionised water to remove any surfactant or ionic impurities, and dried at 65 °C. The material was laser cut in two patterns, 1; the shape of the electrodes and connecting channels (2, 3 and 4, Figure 3-1) in order to facilitate flow of the sample across the ISE and RE to the sampling reservoir and channel configuration (to cover the electrodes and fill the channels) and 2; the configuration of the sample collection reservoir (5, Figure 3-1) to wick the liquid into the reservoir maintaining a passive pumping system. The adsorbent material in the sampling reservoir can be easily removed for subsequent quantification of the total amount of sweat gathered during trials, and for analysis of the aggregated sweat sample using reference methods.

A cotton thread positioned underneath the adsorbent material across the electrodes is also used to facilitate fluid delivery across the electrodes. It protrudes 1 cm from the inlet to ensure sample contact with the adsorbent material and electrodes. A layer of 86 µm PSA was used to attach both the electrochemical-sensing chip (3, Figure 3-2) and the 3 mm PMMA sample

reservoir enclosure (4, Figure 3-2). An 86 µm PSA layer attached the final 500 µm PMMA (5, Figure 3-2) enclosing layer.

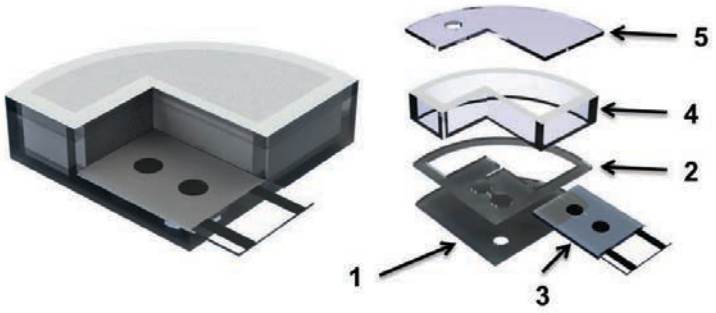

Figure 3-2: CAD images of full chip, left, and its individual components, right, consisting of (1) 500µm PMMA base and inlet layer, (2) 500µm PMMA layer with channels with identical PSA on both sides for adhesion to adjacent layers including (3) the electrochemical sensor and (4) 3 mm PMMA layer to house the adsorbent material. The device is sealed by (5) 500µm PMMA vented lid bonded to the device with PSA.

3.2.3.2 Adsorbent Material Comparison

The ability of the adsorbent material to maintain flow of the sample across the electrodes and provide an accurate reading of ionic concentration was monitored by applying varying concentrations of NaCl solution directly to the inlet of the fluidic chip (2, Figure 3-1). No thread was used during these tests as the solutions were added directly to the adsorbent material through the inlet.

The responses of the electrodes were monitored using the multi channel voltmeter, MCV, capabilities of an EMF-16 channel system from Lawson Labs (USA). Four concentrations, 0.1, 1, 10 and 100 mM NaCl were added in stepwise manner in increasing and decreasing cycles to test the ability of the fluidic system to maintain the transfer of the liquid while maintaining the ion concentration relevant to the solution across the electrodes. Two different adsorbent materials, a polypropylene cellulose 3 layer composite cleanroom wipe and a 70% cellulose 30% cotton Wettex® sponge cloth, were investigated as well as a fluidic chip with no material in the channel. Scanning electron

microscope (SEM) images of both materials were captured with a Hitachi S3400N SEM.

3.2.3.3 Microfluidic Chip Generation 2

A second fluidic chip was designed to expand the capacity of the sampling area and reduce the dead volume across the electrodes minimising the amount of sample needed and thus the amount of time needed to gain an initial sweat signal in an on body trial. In order to increase sample capacity the sampling reservoir (4, Figure 3-3) was expanded to encompass the areas both sides of the sensor and the height was increased from 3.5 mm to 5.5 mm. The dead volume was decreased by directing the fluid in a 1.2 mm wide channel across the centre of the ISE and RE (Figure 3-3) instead of covering the full 3 mm diameter of both electrodes. The potential response in the channel with full electrode coverage in the original fluidic chip was compared with partial electrode coverage in the new design by adding four concentrations 0.1, 1, 10 and 100 mM NaCl in a stepwise manner across the same sensor separately in both configurations.

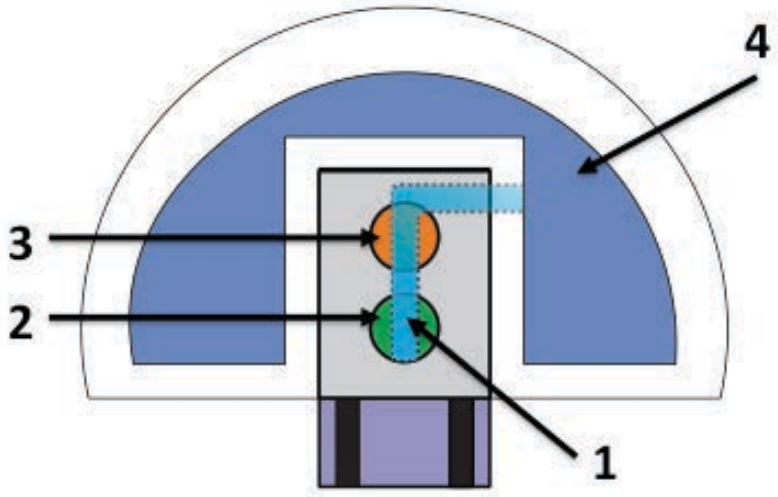

Figure 3-3: Illustration of the generation 2 fluidic chip employing a straight 1.2 mm wide channel (1) bringing the sample across the centre of the 3mm diameter ISE (2) and RE (3) electrodes to the larger capacity (ca. 800 µL) sample reservoir (4).

The flowrate in the new design was monitored in a custom PMMA setup with a loading reservoir to which the fluidic chip was attached to the PMMA base with PSA (Figure 3-4). Two conditions were investigated to observe the flow rates

where 1; the fluidic system worked correctly with the inlet fully filled with sweat directly in contact with the adsorbent material and 2; air blockages or a lack of contact with the skin would occur resulting in only partial filling of the reservoir with only thread providing sample to the adsorbent material and throughout the fluidic chip.

The flow rates of the thread and adsorbent material combination, simulating the contact between liquid and absorbent material when the capillary inlet of a harvester was filled with sweat, were observed by filling the loading reservoir with 700 µL so the liquid was in contact with both thread and adsorbent material. The flow rate in cases where liquid would fail to fill the capillary inlet, which could occur due to an air blockage or a break in contact between the harvester base and the skin, was monitored by only partially filling the loading reservoir with 300 µL liquid so that it was only in contact with the thread.

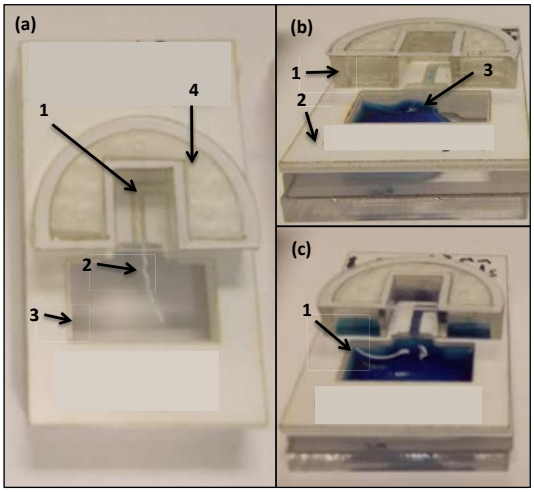

Figure 3-4: Generation 2 microfluidic chip fluidic testing setup. (a) gives the top view of the components testing the flowrate of (1) the 1.5mm wide channel with compo wipe adsorbent material and (2) cotton thread facilitating flow from (3) the inlet reservoir to (4) the sampling reservoir containing 8 layers of adsorbent material. (b) shows the side view of the components with the (1) sampling reservoir and (2) base layer at different heights, in this case the inlet reservoir is partially filled with liquid (3) to test flow rate when only the thread is in contact with the sample. (c) shows the experimental setup to test the flowrate by both thread and adsorbent material by filling the inlet reservoir with sample (1).

3.2.3.4 Flow Rate Studies

A sweat harvesting device (Figure 3-5) to collect sweat from the skin directly and transfer it to the fluidic chip was designed using CAD software and 3D printed

using the rigid polymer VEROWHITEPLUS RGD835 with a Stratasys Objet 260 Connex1 PolyJet 3D printer.

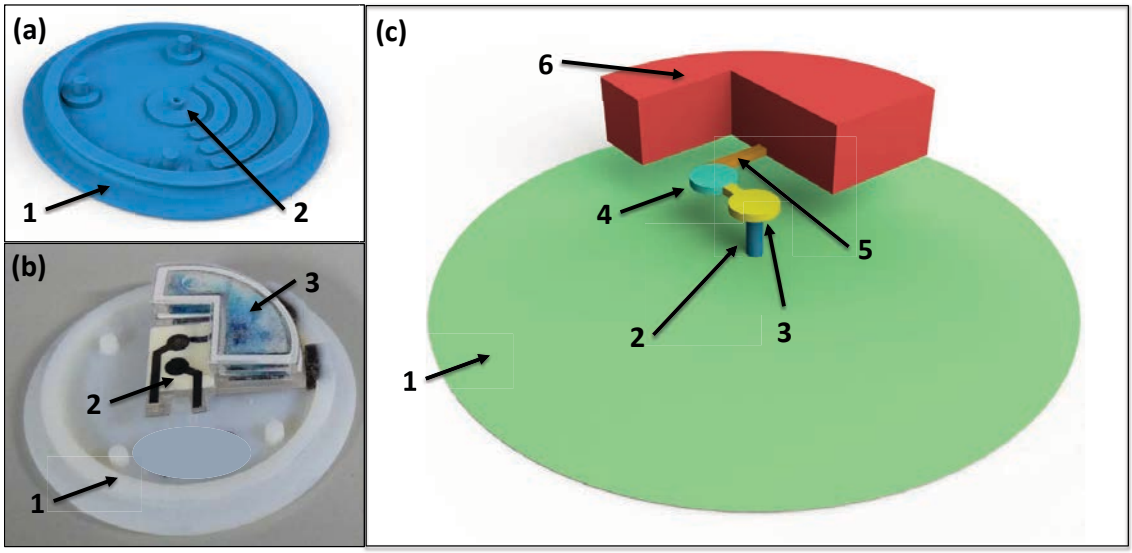

Figure 3-5: Outline of the fluid collection system showing (a) a CAD render of the sweat harvester design with a circular base (a1) focusing the liquid to the inlet capillary channel (a2) and (b) an image of the fluidic test setup with the 3D printed harvester (b1) having transferred blue test liquid across the electrodes (b2) to the absorbent material in the sample reservoir (b3). The path of the sample is shown in the liquid negative image (c) where it is collected from the 12.5cm^2 sampling area (c1) and focussed through the inlet capillary channel (c2) from where it is transported across the ISE (c3) and RE (c4) and delivered through an adjoining channel (c5) to the sampling reservoir (c6).

Control over the flow rate through the channel was achieved by adjusting the width of the connecting channel (4, Figure 3-1). Microfluidic chips in the generation 1 circular channel design were fabricated with 250 µm, 500 µm and 750 µm channel widths (4, Figure 3-1), and incorporated into the sweat harvesting devices for fluid transfer testing (b, Figure 3-5). A cotton thread was used alongside the adsorbent material to encourage flow from the base of the harvester through the inlet and fluidic channel into sampling reservoir. Each test rig was placed in contact with deionised water dyed with blue dye, and the mass of water transferred through the fluidic system was measured every 30 s.

3.3 Results and Discussion

3.3.1 Comparison of Fluid Transfer Strategies

The ability to provide passive fluid transfer across the electrodes in the 1st generation, circular channel, fluidic chip (Figure 3-1) was studied in three configurations one with an empty channel with transfer by capillary force and two with adsorbent materials, a polypropylene/cellulose/polypropylene composite 3 layer cleanroom wipe and a 30 % cotton 70% cellulose Wettex® sponge cloth. All configurations were with an identical shaped channel of 500 um height (Figure 3-1). The adsorbent materials were further characterised through SEM analysis. All tests were carried out on the same day with the same sensor, which was calibrated from 0.1 – 100 mM NaCl before incorporation into the fluidic chips (Figure 3-6).

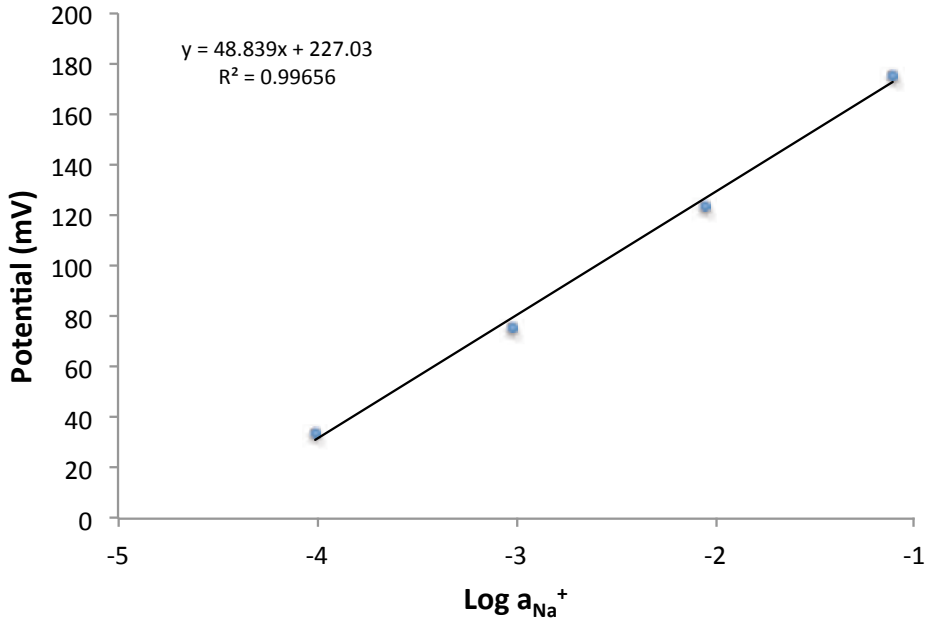

Figure 3-6: Calibration of an Na^+ sensor at of 10^{-4}, 10^{-3}, 10^{-2} and 10^{-1} a_{Na^+} with average potentials of 34, 76, 124 and 175 mV respectively.

3.3.1.1 Fluid Transfer by Capillary Action

The fluidic chip was initially tested with no adsorbent material in the channel above the electrodes. NaCl solutions were applied directly to the inlet at decade intervals from 0.1 mM to 100mM and back to 0.1 mM. Excess liquid in the sampling reservoir was actively removed throughout. The results (Figure 3-7) displayed a similar potential range, 36 – 174 mV, to that of initial calibrations, 34 – 175 mV (Figure 3-6).

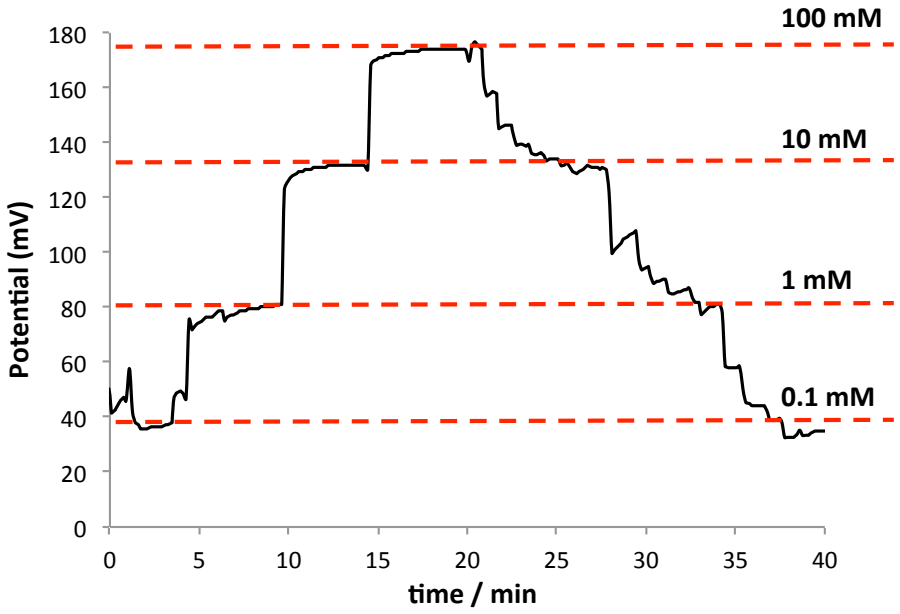

Figure 3-7: Response of an Na^+ electrode to exposures of 0.1 mM to 100 mM NaCl in a 500 µm capillary channel.

When increasing concentrations ca. 30 µL/decade NaCl was adequate to reach a stable response, however, when decreasing the concentration ca. 150 µL/decade was required. This suggests mixing was occurring in the channel, which raises concerns about the efficiency of this configuration in applications such as on body testing.

3.3.1.2 Fluid Transfer with Wettex® Sponge Cloth Material

The effect on electrode response of using the 30% cotton 70% cellulose adsorbent material to facilitate flow across the electrode was monitored by laser cutting the material to fit and placing it in the 500 µm channel above the

electrodes before following the same protocol as section 3.3.1.1. The responses to concentration increases observed with the sponge cloth material (Figure 3-8) were more gradual than the sharp increases observed without adsorbent material (Figure 3-7). There was a notable difference from the potentials displayed on the incline to those on the decline with the 10 mM solution only recovering to a 140 mV (after the addition of 600 µl of 10 mM NaCl) after an initial value of 127 mV, while the subsequent addition of 600 µl 1 mM NaCl resulted in 101 mV after 76 mV had been observed in the inclining step.

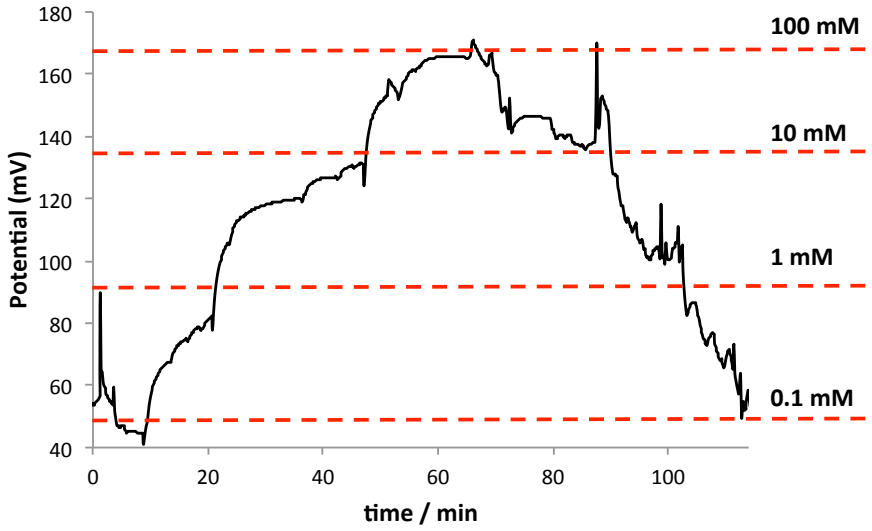

Figure 3-8: Response of an Na^+ electrode to exposures of 0.1 mM to 100 mM NaCl with Wettex® sponge cloth material facilitating fluid transfer across the sensor.

The potential range from 0.1 – 100 mM of 45-166 mV showed a narrowing on the calibration range of 34 – 175 mM. The results at 100 mM follow observations from the stability study in section 2.3.3.2 that exposure to higher concentrations can result in a drop in potential but the rise in potential at the low concentrations are not reflected in the same study. The SEM images at 65x and 250x magnification display a heterogenous network of pores ranging in size from ca. 40 (b2, Figure 3-9) to 200 µm in diameter (a1, Figure 3-9).

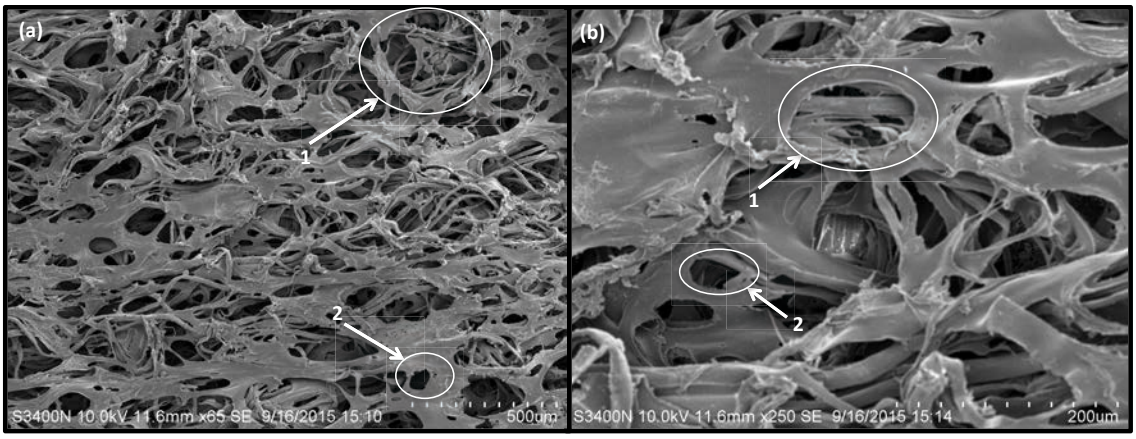

Figure 3-9: SEM image of Wettex® sponge cloth (30% cotton 70 % cellulose) at (a) 65x magnification showing pores ranging from ca. (1) 200 to (2) 50 µm diameter and (b) 250x magnification showing pores ranging from from ca. (1) 100 to (2) 40 µm diameter.

This large volumes of liquid required to go from a higher to lower concentration suggest that some Na^+ molecules were accumulating on the material surfaces before being washed through. This means that if Wettex® sponge cloth is used for fluid transfer in an on body trial the signal suggested by the Na^+ content on the material may not be indicative of the sweat Na^+ concentration at that exact time making the material unsuitable for real-time monitoring.

3.3.1.3 Fluid Transfer with Cleanroom Compo Wipe Material

Three layer cleanroom compo wipes were also laser cut and tested to facilitate sample flow across the electrodes. The material consists of a highly absorbent cellulose layer thermally bonded to two outer layers of abrasion resistant polypropylene layers. The results show that in this configuration the electrodes responded immediately to changes in Na^+ concentration with 20 µl sample enough to elicit the full relevant response to increasing or decreasing NaCl concentrations (Figure 3-10). The 0.1 mM reading of 37 mV is close to the calibration value of 34 mV while the reading of 165 mV is very similar to the 166 mV value achieved with the Wettex® sponge cloth material.

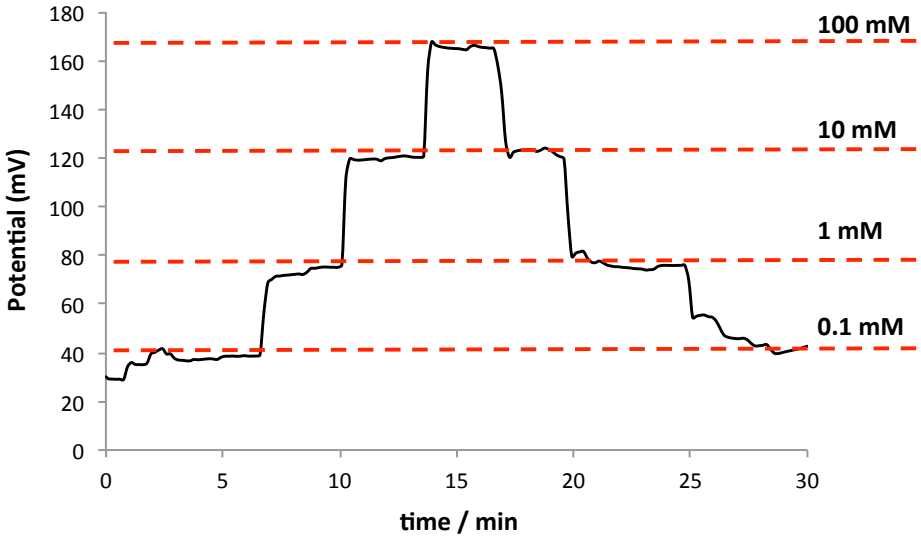

Figure 3-10: Response of an Na^+ electrode to exposures of 0.1 mM to 100 mM NaCl with cleanroom compo wipe material facilitating fluid transfer across the sensor.

The SEM images of the material show the polypropylene fibres above the cellulose layer (Figure 3-11). The wipes are designed so the surface of polypropylene fibers (a1, Figure 3-11) remain dry while the bulk of the liquid is absorbed by the inner cellulose layer (a2, Figure 3-11). The material is patterned by 1 mm diameter circles as a result of the thermal bonding process (b1, Figure 3-11).

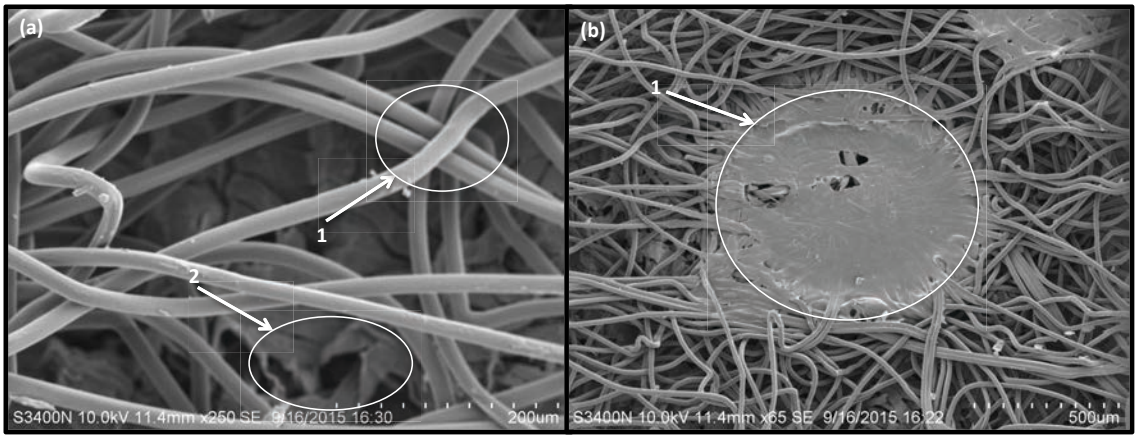

Figure 3-11: SEM images of cleanroom compo wipe of cellulose between polypropylene layers at 250x magnification showing (1) the top polypropylene fibres above (2) the cellulose layer and (b) 65x magnification showing (1) the ca. 1 mm diameter lamination point where the 3 layers are thermally bonded.

The problem of slow ion movement shown in the cellulose layer in the Wettex® material in section 3.3.1.2 is solved in the compo wipe configuration by the separation of the cellulose layer from the electrodes by the polypropylene layer.

The flow is maintained by the cellulose layer while the excess liquid moves through the polypropylene, layers filling the 500 µm channel and moving across the electrodes allowing real-time determination of the Na^+ content (Figure 3-11). The compo wipe facilitated fluid transfer also requires far less sample to elicit a response than in the other two configurations tested making it the best candidate for further fluidic trials.

3.3.2 Microfluidic Chip Generation 1 Flow Rate Studies

The compo wipe incorporation in the generation 1, circular channel, microfluidic chip was continued for fluidic studies where the effect on flow rate of altering the width of the channel to the sampling area (4, Figure 3-1) was investigated. Three channel widths of 750, 500 and 250 µm were investigated by measuring the volume of liquid delivered into the chip through the sweat harvesting device (Figure 3-5) every 30 seconds for up to 28 minutes. Flow rates of 38.2, 21.48 and 6.61 µL/min were obtained for the 750, 500 and 250 µm channels, respectively (Figure 3-12).

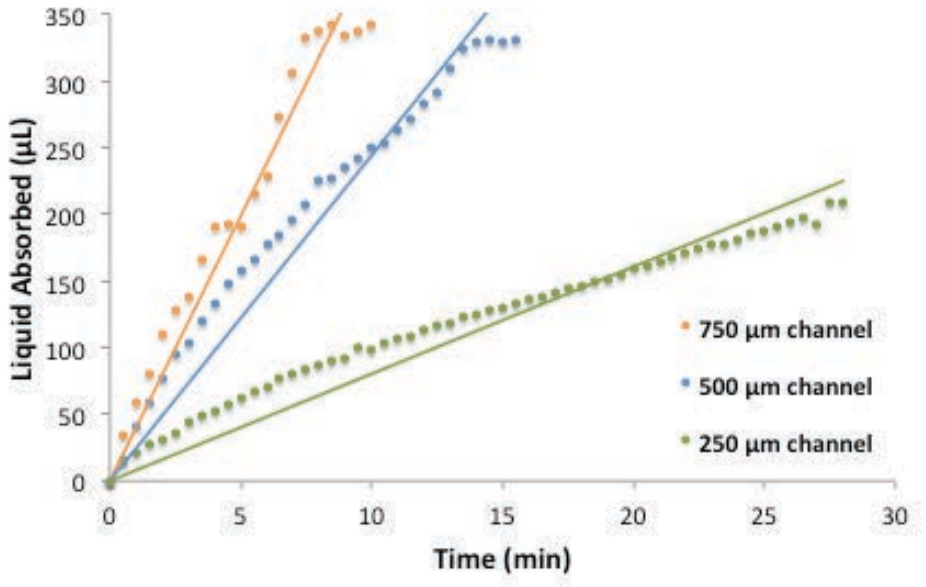

Figure 3-12: Modulation of platform flow rate by varying the width of the connecting fluidic channel. The average flowrates of each channel over the period of the experiments were 38.2 µL/min ± 1.34 for the 750 µm channel, 21.48 µL/min ± 0.57 for the 500 µm channel and 6.61µL/min ± 0.11 for the 250 µm channel. Capacity of ca. 340 µL was reached at ca. 8.5 and 14 min for the 750 µm and 500 µm channels respectively.

These results show that the sweat flow rate through the device can be controlled through applying a constriction within the fluidic system, and the flow rate is linear for all three channel widths throughout the durations of the experiments.

3.3.3 Microfluidic Chip Generation 2

3.3.3.1 The Effect of Partial Masking on Electrode Performance

An alternative microfluidic chip was developed to minimise dead volume and maximise sample capacity in the sampling reservoir (Figure 3-3). Instead of the channel encompassing the area of the electrodes (2, 3, Figure 3-1) a straight 1.2mm channel (1, Figure 3-3) was designed to bring the sample across an exposed 1.2mm central section of the electrodes while the remaining areas are covered by the PMMA layer. The effect of partially masking the electrodes was investigated by comparing the responses of a single sensor to changes in Na^+ concentrations from 0.1 to 100 mM in decade intervals in the first generation fluidic chip with those obtained with the masked configuration in the second generation fluidic chip. Cleanroom compo wipe material was used to facilitate flow in both tests. The electrodes exhibited very similar responses in both configurations at each concentration of 0.1, 1, 10 and 100 mM NaCl (Figure 3-13).

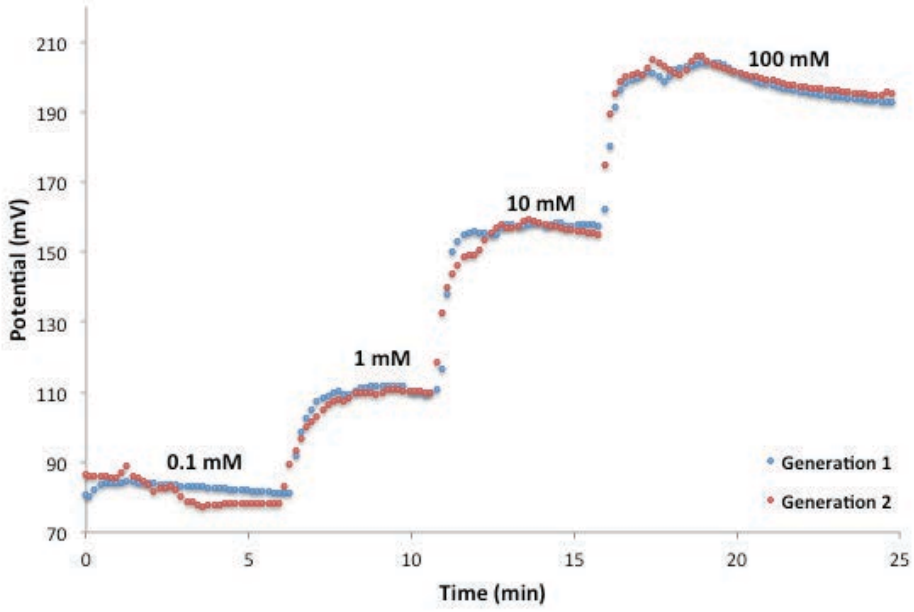

Figure 3-13: A comparison in response to Na+ concentrations between electrode surfaces in full contact with the sample in circular channels (Generation 1) and with partial contact with the sample in a straight channel (Generation 2)

The above results suggest partially covering the electrodes has no substantive effect on the electrode response so masking the electrodes can be employed as a strategy for narrowing the channels and reducing the volume of the channel across the electrodes.

3.3.3.2 Microfluidic Chip Generation 2 Flow Rate Studies

The channel in the first generation, circular channel, microfluidic chip (Figure 3-1) had a volume of 7.1 μL across the electrodes, this was reduced to 4.7 μL in the second generation design with the 1.2 mm straight channel (Figure 3-3). After the electrode area over the channel a turn was designed so the channel restrictions investigated in section 3.3.2 could be applied in future tests where necessary. The fluidics were tested with cotton thread and cleanroom compo wipe material facilitating flow from the inlet to the sampling reservoir (Figure 3-4). In all tests the thread across the channel extended 10 mm into the inlet reservoir and 45 mm around the base of the sampling reservoir under the adsorbent material layers.

The flow rate was investigated in two conditions, 1; full contact between the source sample and the adsorbent material and 2; contact only between the source sample and the cotton thread to simulate the conditions in the case of failure to fill the sweat harvester capillary (Figure 3-5) which could be caused lack of a seal around the harvester base or in the case of an air block.

In the thread-only contact tests the assembled components were weighed initially and every 15 minutes thereafter to record the amount of liquid absorbed. The liquid from the inlet reservoir was removed before weighing and replaced to continue the experiment. Each test showed great linearity in flow rate with R^2 values of 0.99 in all tests but the flow rate varied between tests (Figure 3-14). The average flow rate was 2.03 µL/min ± 0.38. The variation in flow rate could be explained by differences in the adsorbent material caused by the presence or absence of lamination points caused by thermal bonding patterned throughout the material (Figure 3-11). The compressed material at these points may impede the flow in the channel.

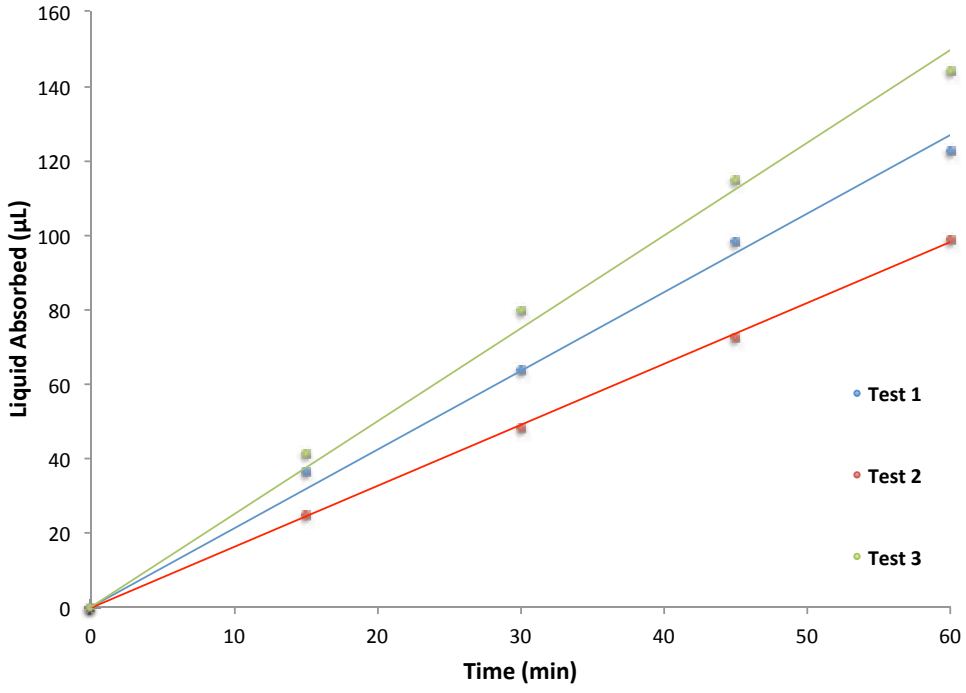

Figure 3-14 A comparison of three tests measuring the flow rate over a channel in the gen 2 microfluidic chip with only thread in contact with the sample source. Tests 1, 2 and 3 displayed flow rates of 2.05, 1.65 and 2.4 µL/min respectively, with an average flow rate of 2.03 µL/min ± 0.38.

In the case where adsorbent material was in direct contact with the source sample the flow rate was much faster meaning the duration of the experiment was reduced from 60 to 20 min with volumes recorded at 10, 15 and 20 min. The fastest flow rates for each of the three tests performed were recorded in the first 10 minutes with tests 1, 2 and 3 showing flow rates of 56.41, 61.11 and 48.99 µL/min respectively with an average flow rate of 55.5 µL/min ± 6.11. The flow rate slowed as the sampling reservoir began to fill (Figure 3-15). This is evident in the 10-15 min period where test 2, the test showing the fastest flow rate previously, slowed to 22.16 µL/min where tests 1 and 3 showed flow rates of 39.64 and 42.42 µL/min respectively. At 15 minutes tests 1, 2 and 3 were nearing capacity with volumes of 762.3, 721.1 and 787.9 µL respectively with flow rates slowing to 8.06, 6.04 and 17.18 µL for the final 5 minutes before reaching final volumes of 802.6, 752.1 and 787.9 µL (Figure 3-15).

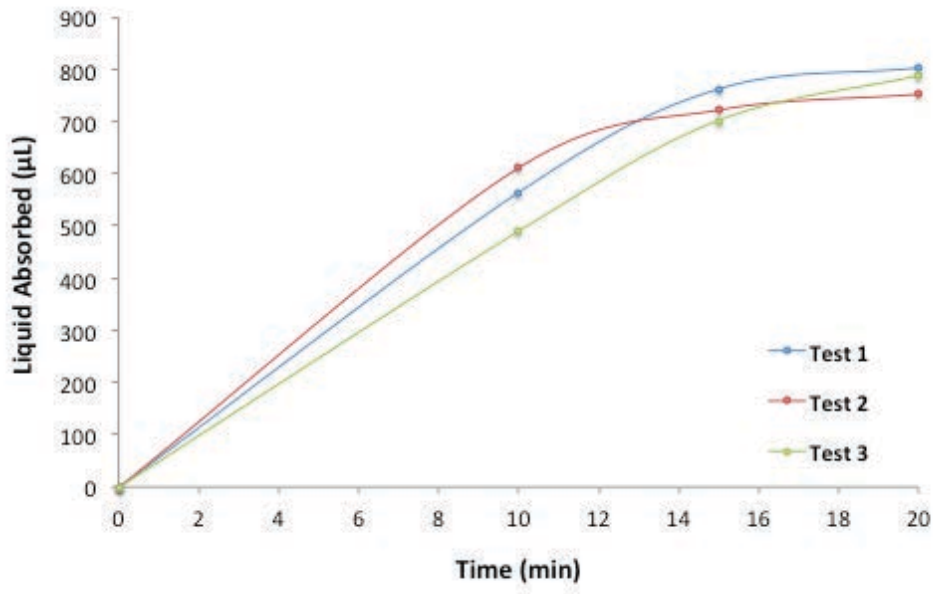

Figure 3-15: Flow rates produced with microfluidic chip generation 2 in 3 tests with the adsorbent material in direct contact with the sample source. Average flow rates observed were 55.5 µL /min ± 6.11 for the initial 10 minutes, 34.74 µL /min ± 10.98 from 10 – 15 min and 10.43 µL /min ± 5.94 for the final 5 minutes as the sampling reservoir reached capacity.

As the channel with the adsorbent material is situated at the top of the source reservoir, as the sample level lowers the level of contact sustained with the adsorbent material depends on many factors including surface interactions at the wall of the reservoir and the position of the thread in respect to the wall. This

could explain the variation in flow rate particularly in the first 10 minutes where there was a 12.12 µL/min difference between the fastest and slowest results.

As these flow rates are well beyond sweat flow rates suggested in the literature this fluidic chip was deemed suitable for sampling and maintaining the flow of sweat produced during on body trials [20].

3.4 Conclusion

This work resulted in the successful fluid handling system consisting of a 3D printed sweat harvester and a microfluidic chip utilising capillary action and adsorbent material for continuous fluid sampling and collection. Cleanroom compo wipe material was selected as the best means of facilitating sample flow across the electrodes after comparison with configurations using sponge cloth material to wick the sample, and sole capillary action in an empty channel. The initial design of the chip was successfully adapted to increase maximum sampling capacity from 342 to 803 µL while the volume of the channel across the electrodes was reduced from 7.1 to 4.7 µL.

The sensor and fluidic system have been shown to successfully collect a sample continuously while monitoring the Na^+ content in real-time. The system was therefore deemed ready for incorporation into an integrated wearable platform for real time electrolyte monitoring in sweat.

3.5 References

[1] A. J. Bandodkar and J. Wang, 'Non-invasive wearable electrochemical sensors: a review', *Trends Biotechnol.*, vol. 32, no. 7, pp. 363–371, Jul. 2014.

[2] A. Mena-Bravo and M. D. Luque de Castro, 'Sweat: A sample with limited present applications and promising future in metabolomics', *J. Pharm. Biomed. Anal.*, vol. 90, pp. 139–147, Mar. 2014.

[3] D. Diamond, S. Coyle, S. Scarmagnani, and J. Hayes, 'Wireless Sensor Networks and Chemo-/Biosensing', *Chem. Rev.*, vol. 108, no. 2, pp. 652–679, Feb. 2008.

[4] J. R. Windmiller and J. Wang, 'Wearable Electrochemical Sensors and Biosensors: A Review', *Electroanalysis*, vol. 25, no. 1, pp. 29–46, Jan. 2013.

[5] I. Ishiyama, T. Nagai, T. Nagai, E. Komuro, T. Momose, and N. Akimori, 'The significance of drug analysis of sweat in respect to rapid screening for drug abuse', *Z. Für Rechtsmed.*, vol. 82, no. 4, pp. 251–256, Mar. 1979.

[6] J. Parnas, H. Flachs, L. Gram, and A. Wuurtz-JØrgensen, 'Excretion of antiepileptic drugs in sweat', *Acta Neurol. Scand.*, vol. 58, no. 3, pp. 197–204, Sep. 1978.

[7] P. Kintz, A. Tracqui, C. Jamey, and P. Mangin, 'Detection of Codeine and Phenobarbital in Sweat Collected with a Sweat Patch', *J. Anal. Toxicol.*, vol. 20, no. 3, pp. 197–201, May 1996.

[8] B. M. R. Appenzeller, C. Schummer, S. B. Rodrigues, and R. Wennig, 'Determination of the volume of sweat accumulated in a sweat-patch using sodium and potassium as internal reference', *J. Chromatogr. B*, vol. 852, no. 1–2, pp. 333–337, Jun. 2007.

[9] N. Hamouti, J. D. Coso, J. F. Ortega, and R. Mora-Rodriguez, 'Sweat sodium concentration during exercise in the heat in aerobically trained and untrained humans', *Eur. J. Appl. Physiol.*, vol. 111, no. 11, pp. 2873–2881, Mar. 2011.

[10] R. M. Carr, 'Dietary Sodium Intake, Sweat Sodium, Salt Appetite and Exercise', Thesis, University of Otago, 2015.

[11] G. Mastella, G. Di Cesare, A. Borruso, L. Menin, and L. Zanolla, 'Reliability of sweat-testing by the Macroduct® collection method combined with conductivity analysis in comparison with the classic Gibson and Cooke technique', *Acta Pædiatrica*, vol. 89, no. 8, pp. 933–937, Aug. 2000.

[12] Y.-L. Yang, M.-C. Chuang, S.-L. Lou, and J. Wang, 'Thick-film textile-based amperometric sensors and biosensors', *Analyst*, vol. 135, no. 6, pp. 1230–1234, 2010.

[13] K. Malzahn, J. Ray Windmiller, G. Valdés-Ramírez, M. J. Schöning, and J. Wang, 'Wearable electrochemical sensors for in situ analysis in marine environments', *Analyst*, vol. 136, no. 14, pp. 2912–2917, 2011.

[14] S. Coyle *et al.*, 'Textile sensors to measure sweat pH and sweat-rate during exercise', in *2009 3rd International Conference on Pervasive Computing Technologies for Healthcare*, 2009, pp. 1–6.

[15] A. J. Bandodkar *et al.*, 'Epidermal tattoo potentiometric sodium sensors with wireless signal transduction for continuous non-invasive sweat monitoring', *Biosens. Bioelectron.*, vol. 54, pp. 603–609, Apr. 2014.

[16] J. Kim *et al.*, 'Noninvasive Alcohol Monitoring Using a Wearable Tattoo-Based Iontophoretic-Biosensing System', *ACS Sens.*, vol. 1, no. 8, pp. 1011–1019, Aug. 2016.

[17] A. J. Bandodkar, W. Jia, and J. Wang, 'Tattoo-Based Wearable Electrochemical Devices: A Review', *Electroanalysis*, vol. 27, no. 3, pp. 562–572, Mar. 2015.

[18] W. Gao *et al.*, 'Fully integrated wearable sensor arrays for multiplexed in situ perspiration analysis', *Nature*, vol. 529, no. 7587, pp. 509–514, Jan. 2016.

[19] G. Matzeu *et al.*, 'An integrated sensing and wireless communications platform for sensing sodium in sweat', *Anal. Methods*, vol. 8, no. 1, pp. 64–71, Dec. 2015.

[20] C. J. Smith and G. Havenith, 'Body mapping of sweating patterns in male athletes in mild exercise-induced hyperthermia', *Eur. J. Appl. Physiol.*, vol. 111, no. 7, pp. 1391–1404, Jul. 2011.

Chapter 4 The Development of SWEATCH, a Fully Integrated Wearable Device for Real Time Monitoring of Electrolyte Levels in Sweat

4.1 Introduction:

Interest in real-time monitoring of biochemical parameters using wearable/on-body sensors is a rapidly growing area of research [1], due in part to the convergence of interest of major economic sectors in applications based on new types of information. ICT companies like Apple and Google are exploring ways to access biochemical information as a means to move beyond the mature sensor technologies currently employed in exercise and sports apps that track a users location, body movements, temperature, energy expenditure and so on. These are typically based on physical transducers or imaging technologies embedded within wristbands or smart phones. However, employing similar approaches that depend on time-series data to the domain of biochemical sensing is much more difficult, due to the complex challenges associated with access to representative samples (typically a body fluid) and the less predictable behaviour of chemical sensors and biosensors over time.

Since the exciting developments of the 1980's, the application of biochemical sensing to real-time monitoring of the human condition has scarcely advanced in terms of the performance of the sensors. Today, the use-model has almost entirely shifted away from the early over-optimistic promise of implantable sensors that are in continuous contact with blood [2], to devices sited outside the body that somehow can access an information rich body fluid, like sweat [3], [4] or saliva [5]. For the past several decades, the predominant use model for health related diagnostics has been the disposable single-shot sensor combined with a finger prick access to blood samples.

Examples of use models that involve real-time monitoring of body fluids (albeit over relatively short periods typically at most up to several days) include the

integration of biosensors with contact lenses that can sample and report on the composition of ocular fluid, which is in turn reflective of the systemic blood composition [6]. Perhaps the best-known example of this is the collaborative venture between Google and Novartis [7], based on Parvis's work on glucose sensing [6]. Printable, conformable biosensors have recently been integrated onto the contact lens platform, and the use model is attractive in that the lens is disposable, typically being replaced on a daily basis [8].

Biochemical sensors have also been employed on skin, either through physical attachment such that the sensors access sweat induced by exercise or iontophoresis [9], or interstitial fluid accessed through the skin using microneedles [10]. The recently published sweat-band that can track the wearer's temperature, glucose, lactate, potassium and sodium from exercise induced sweat appears to be a significant advance [11]. The Abbott 'Libre' interstitial glucose sensor can be attached to the shoulder or other body locations using a customized applicator that simultaneously punctures the skin to access interstitial fluid. The device can be left in position for up to 2 weeks according to the specifications [12]. The group of Rogers has been particularly active in the development of conformable printable electronics and sensors that are produced in a tattoo format that can be transferred to the skin [13]. A more complete overiew of non-invasive electrochemical wearable sensors can be seen in a review by Bandodkar and Wang [14].

As in all analytical methods, access to a representative sample is vital. With biochemical on-body sensing this is compounded by difficulties associated with the need for invasive sampling through the skin to access blood or interstitial fluid. Sweat and ocular fluid are particularly attractive analytical media as access is non-invasive. Sweat is obtained either through exercise or induced locally using techniques like pilocarpine iontophoresis. Important applications for sweat analysis relate to monitoring of personal hydration status for athletes and persons exposed to extreme conditions [15] and for certain clinical conditions like cystic fibrosis, in which the normal range of electrolyte composition of sweat becomes significantly unbalanced. Monitoring of sweat electrolytes could also

play an important role in qualifying the efficacy of new therapeutic treatments for conditions like Cystic Fibrosis, as these are typically designed to restore the normal intra- and extra-cellular electrolyte balance, which in turn should be manifested as a return to more normal sodium levels in sweat [14].

This work presents two platforms designed to harvest and analyse sweat continuously as it emerges through the skin. Data generated is accessible remotely using via wireless Bluetooth connectivity.

4.2 Experimental

4.2.1 ISEs and Microfluidic Chip

The screen-printed combination electrodes were prepared on a PET substrate with the drop-cast Na^+ selective membrane and photo-polymerised reference membrane prepared on an electrodeposited PEDOT/IL solid contact layer as outlined in chapter 2. The electrodes were integrated into the microfluidic chip designed with CAD software for integration with a fluidic custom made sweat harvester and fabricated from laser ablated PMMA and PSA layers incorporating adsorbent material for sample transport and storage (chapter 3).

4.2.2 Platform Design

The sweat-monitoring platform is designed to allow close, direct skin contact for sweat sampling while protecting the individual device components within a custom-designed enclosure. Two platform designs have been investigated, a 'watch' type design in which the electronics and fluidics components are arranged vertically (a, Figure 4-1), and a 'pod' like design in which the electronics and fluidics components are arranged horizontally in separate compartments (b, Figure 4-1).

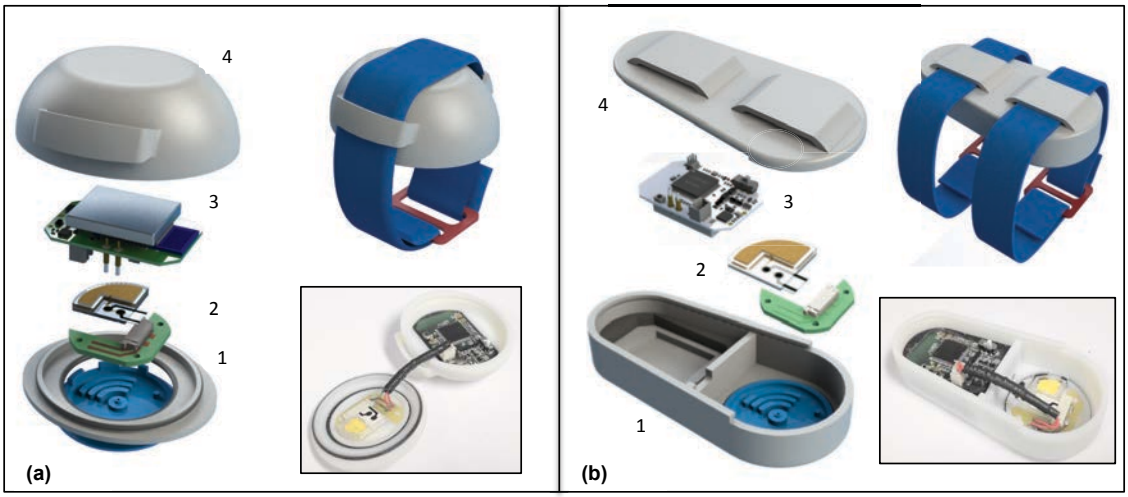

Figure 4-1: "Watch" type (a) with vertical arrangement and "Pod" type platform (b) with horizontal arrangement of electronic and fluidic components consisting of 1: sweat harvesting device in 3d-printed platform base, 2: fluidic sensing chip, 3: electronic data logger and battery, and 4: 3d-printed upper casing.

Each platform incorporates a miniaturized wireless data logging circuit protected by a 3D printed dual polymer casing. The main body of the casing is produced using the rigid polymer VEROWHITEPLUS RGD835. This is printed simultaneously with the softer polymer TANGOBLACKPLUS FLX980 (both from Stratasys, UK) to provide flexibility and sealing between the assembled components. The components include a sweat harvesting base plate with a centrally located sweat entry point, screen-printed ion-selective (ISE) and reference (RE) electrodes, incorporated in a microfluidic chip for Na^+ sensing, an electronic board for data logging and wireless communications (Shimmer), and a rechargeable lithium battery. The Shimmer board is custom designed, and includes high impedance inputs to ensure the ISE potentials are tracked accurately.

4.2.3 Data Collection, Processing and Communication

The prototype platforms incorporate a custom-designed electronics board provided by Shimmer for accurate measurement of the ISE-RE potential (Figure 4-2). The board incorporates high impedance inputs necessary for ISE monitoring and a Bluetooth module for wireless communication with a desktop or laptop computer, smart phone or tablet. Along with the Shimmer hardware,

an application programming interface (API) for Matlab was created which allowed the results to be visualised and processed remotely.

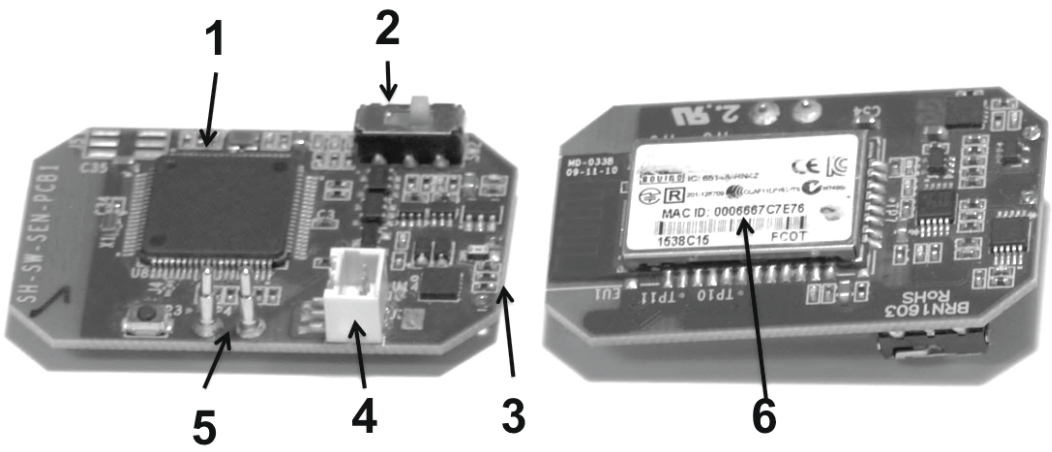

Figure 4-2: Top (left) and bottom (right) views of the custom-designed electronics. 1: MSP 430 microcontroller (Texas Instruments); 2: power switch; 3: battery connections; 4: molex sensor connections; 5: battery charging pins; and 6: bluetooth module.

The performance of the Shimmer board was evaluated by direct comparison with a Lawson Lab multi channel voltmeter (MCV). Both devices were connected in parallel to a Na^+ sensor and a four point calibration was performed with NaCl solutions from 0.1 to 100 mM in decade intervals.

4.2.4 Real-time On-body Sweat Sodium Monitoring Trials

Healthy male athletes with moderate to high fitness levels participated in indoor exercise trials using stationary cycles (average room temperature of 25 °C) and a cycle ergometer (Monark Exercise, Sweden) at an intensity load high enough to induce sweating. The sampling area was cleaned prior to positioning the prototype platforms on the upper arm. The 'pod' type platform was located on the upper arm and held in position using elastic straps incorporating Velcro for easy adjustment. Water was provided and the volunteers were free to hydrate at their choosing.

In all trials cleanroom compo wipe material (Superior Cleanroom Products http://superiorcleanroomproducts.com/index.html, product number 87109) was used in the microfluidic chip to facilitate flow across the electrodes in

combination with cotton thread, as shown in section 3.3.1.3. This material was also cut, with a CO2 laser, to the shape of the sampling reservoir, and placed to act as collection pads, which could be removed for subsequent analysis. The pads were cleaned with DI water and dried before use. The weight of the pads used in each trial was taken before and after the trial to estimate the volume of sweat collected.

All experiments involving human subjects were performed in compliance with Irish Law and Institutional Guidelines, see https://www4.dcu.ie/researchsupport/research ethics/guidelines.shtml, and were approved by DCU Research Ethics Committee. Informed consent was obtained for all experiments involving human subjects. Trials lasted from 15 to 60 min.

4.3 Results and Discussion

4.3.1 Electronics Evaluation

A direct comparison between the MCV and the Shimmer board was carried out to evaluate the performance and suitability of the latter for integration into a wearable device. Near-Nernstian calibration slopes were obtained from the solid-state ISE-RE combination using the MCV bench and Shimmer board in parallel, with excellent correlation between the two measurement systems, suggesting that the electrodes and the Shimmer customized electronics board were functioning satisfactorily (Figure 4-3).

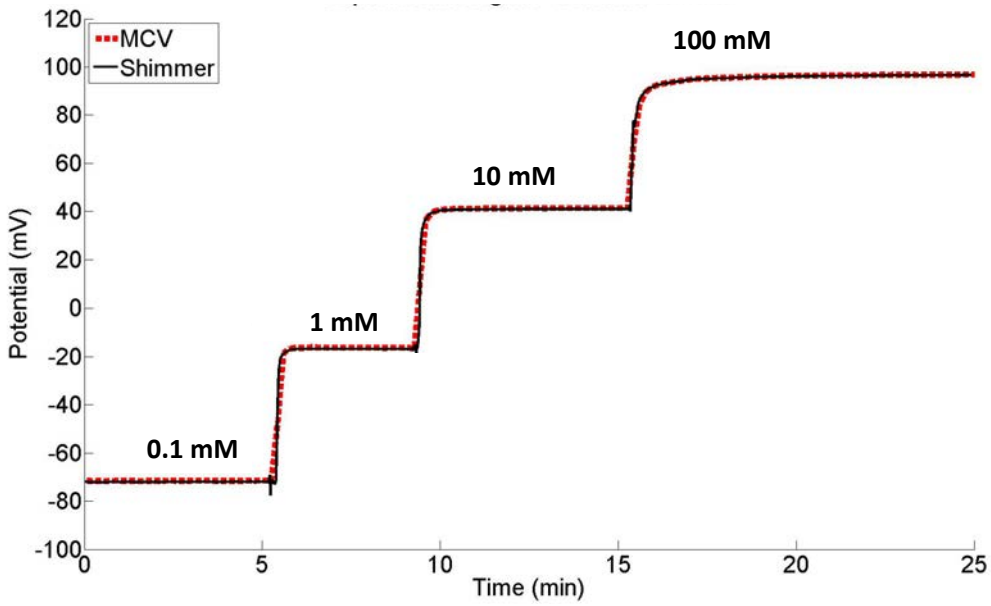

Figure 4-3: Data showing a calibration of a Na^+ ISE with the MCV and Shimmer electronics simultaneously with four solutions from 0.1 to 100 mM NaCl. The MCV and Shimmer readings gave near-Nernstian slopes of 56.238 and 56.287 mV respectively, with an R^2 value of 0.99 on both systems.

4.3.2 On Body Trials

Calibrations (Figure 4-4) of the combined solid-state ISE-RE pairs integrated within the prototype platform were performed using 10^{-4} to 10^{-1} M NaCl standard solutions, prior to commencing on-body trials. The solutions were pipetted through the inlet onto the absorbent material, which wicked the liquid across the electrodes to the sample collection reservoir. The total volume from inlet to sample collection, with the 1st generation microfluidic chip, with curved channels, (section 3.3.2) with 500 µm channel used in the first 2 trials was 10.28 µL while the 2nd generation fluidic chip, with straight channels, used in the third trial had a total volume of 9.81 µL meaning slightly more than 10 µL of an added concentration should be sufficient to entirely displace the preceding solution in both configurations. The platforms were pre-primed before use with 10^{-4} M NaCl by injecting enough volume to provide full contact with the electrodes and establish a stable baseline that would enable arrival of the more concentrated sweat to be observed through a rapid increase in the signal.

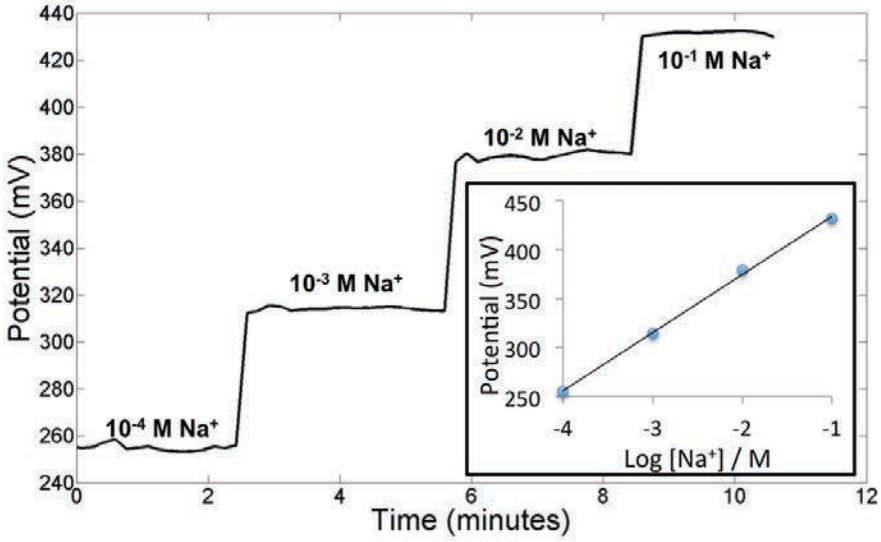

Figure 4-4: Calibration of a Na+-ISE and RE output signal using the Shimmer board, giving a slope of 56.98mV and an R2 value of 0.99.

The SWEATCH prototype (pod design, Figure 4-5) was positioned on a volunteer's arm before a 5 min warm up period of exercise on a stationary bicycle. In the initial trials the 1st generation fluidic chip with channels ensuring full coverage of the ISE and RE (Figure 3-1) was used in the device while the 2nd generation design using a straight channel across the centre of the ISE and RE masking portions of the electrodes (Figure 3-3) was utilised for the last trial presented. Prior to positioning the device, the sampling location was cleaned with a sterile wipe. The volunteer continued to exercise while the output signal of the platform was recorded wirelessly in real-time.

Figure 4-5: SWEATCH device in place on a volunteer's arm during a trial on a stationary exercise bicycle.

4.3.2.1 Trial 1

In the first trial a 28-year-old male of moderate fitness level cycled for 15 minutes with the 'pod' design in position on the upper arm. After approximately 4 min the signal began to increase rapidly indicating the accumulation of sweat underneath the sweat harvesting device (1, Figure 4-1) and the subsequent arrival of the initial sweat at the electrodes (Figure 4-6). Thereafter, a steady increase in signal was observed until approximately 10 min at which point the signal stabilised until the end of the trial after 15 min. From comparisons with the pre-trial and post-trial calibrations, the steady-state potential of ca. 330 mV is equivalent to a sodium concentration of ca. 44 mM, which is consistent with concentrations [3], [11] found in previous studies. Interestingly, a recent analysis by Traeger *et al.* of 13,785 sweat tests performed over a period of 23 years found a mean sodium concentration of 33.8 ± 15.7 mM of 204 Cystic Fibrosis negative patients over the age of 18 years [16].

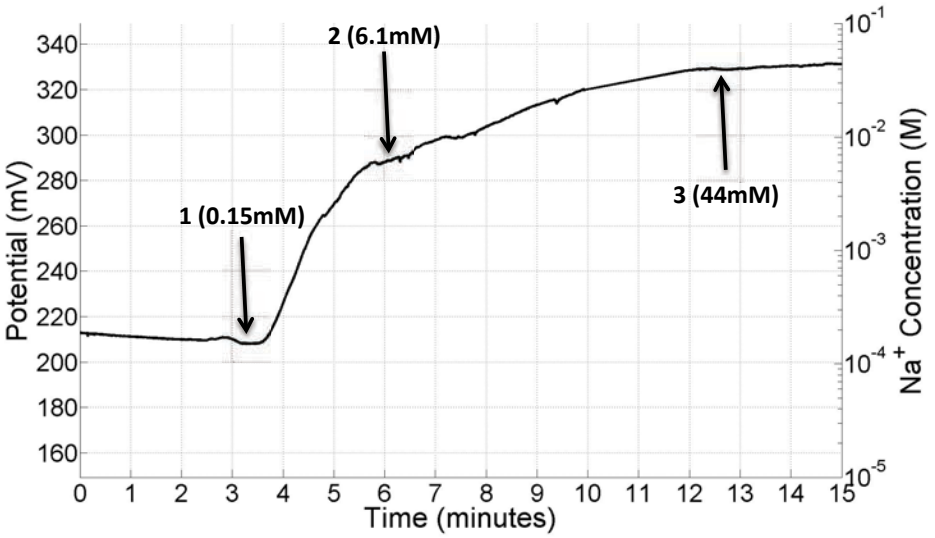

Figure 4-6: Real-time data obtained during a trial including a 5 min warm up period. The initial signal up to (1) reflects the 10^{-4}M NaCl conditioning solution which is initially in contact with the electrodes. After ca. 4 minutes, sweat reaches the electrodes, which results in a rapid increase in the signal. By point (2), any residual conditioning solution has been washed away from the electrodes and the signal is now representative of the sweat. From (2) to (3) the signal increases gradually to a steady state of ca. 44 mM Na^+.

After this trial, the amount of sweat recovered from the adsorbent material was 87.45 mg. Allowing for the fluidic system dead-volume (10.28 μL) and assuming

a density of 1 mg/μL, the total amount of sweat gathered was ca. 100 μL. It is difficult to say exactly when the sweat began to flow through the fluidic system during the initial 4 min period, but, assuming it was flowing for the entire 15 minute period, we can estimate the average sweat flow rate to be ca. 6.5 μL/min.

4.3.2.2 Trial 2

In the second trial sweat was sampled with the pod design and 1st generation, circular channel, fluidic chip from the upper arm of a 29 year old male for a period of 30 min including a 5 minute warm up with data being recorded for the entire duration. After an initial stable signal intermittent noise was evident from 5.25 to 18 min (inset, Figure 4-7) before steadying for the remainder of the trial. This noise suggests the device was highly sensitive to movement, which was not observed in the previous trial, meaning the connection may have been loose. After the trial this data was processed with the Matlab API to remove the noise and give a signal more representative of Na^+ concentrations throughout the trial.

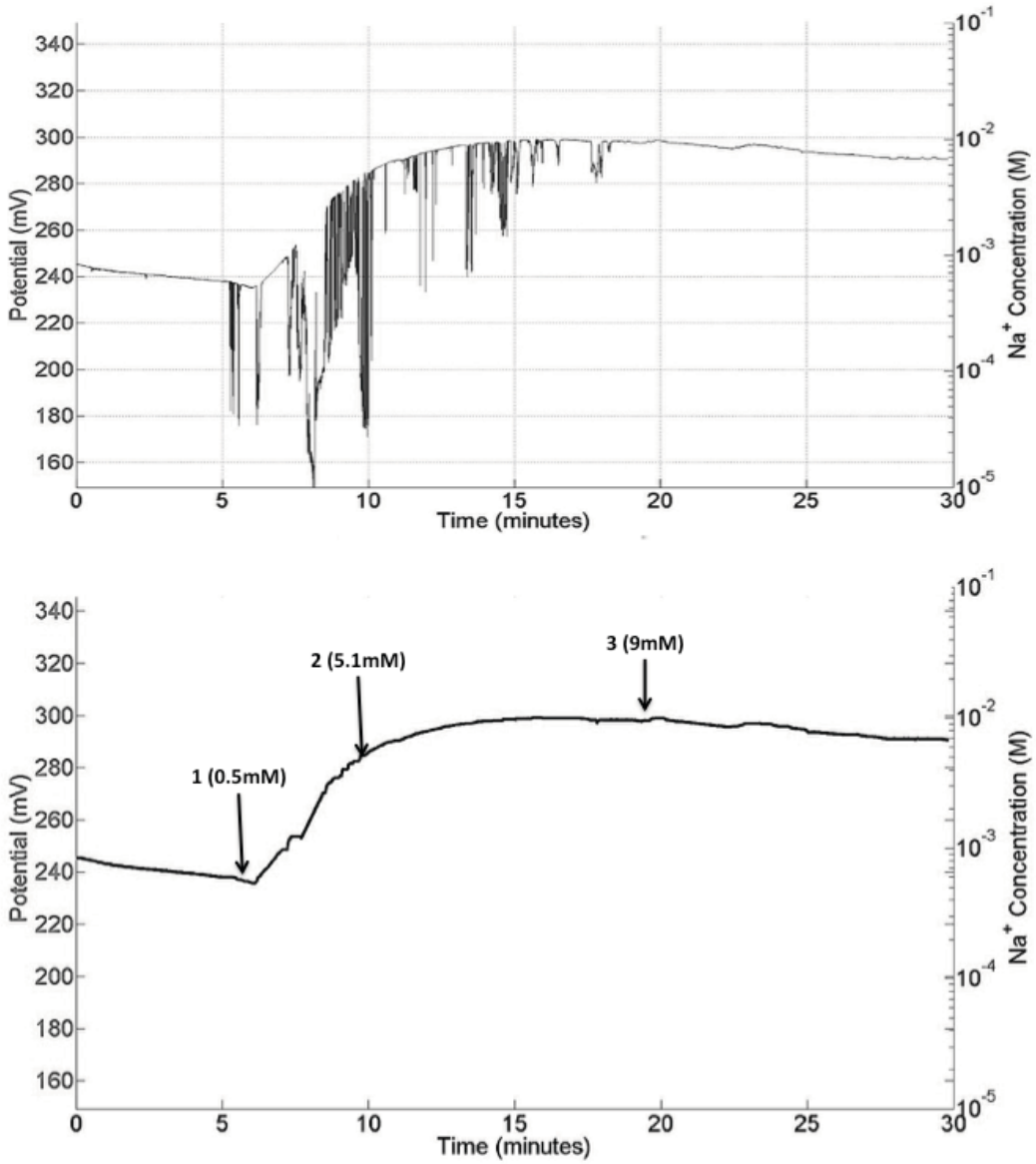

Figure 4-7: Trial data before (top) and after (bottom) processing with Matlab to remove noise (inset). The sweat started to displace the priming solution (1) at ca. 6.5 min, the signal rose steadily to 5.1 mM at 10 min (2) before steadying at 14 min to a concentration of ca. 9 mM (3) where it stayed until the end of the trial.

The sweat initially started to displace the priming solution at 6.5 min causing a sharp increase in potential to a value representative of 5.1 mM (2, Figure 4-7) when compared with the calibrations. The increase in Na^+ concentration slowed before stabilising at 14 min to ca. 9 mM (3, Figure 4-7). This concentration is half the 18.1 mM lower value suggested in the literature [16] suggesting depleted sodium levels indicating asymptomatic exercise associated hyponatraemia which can be caused by fluid intake at rates exceeding sweating rate [17].

41.7 μL sweat was collected from the sampling reservoir at the end of the 30 minute trial suggesting a flow rate of 1.39 μL/min. This value is less than the flowrate of 2.03 μL/min ± 0.38 observed when only thread is in direct contact with the sweat sample (Figure 3.13) suggesting that the capillary inlet was not filled with enough sweat to contact the adsorbent material directly. Since large volumes of sweat were observed on the volunteer and around the sampling area throughout the trial it suggests insufficient contact to cause a seal between the sweat harvesting device and the test area. This could be an alternative explanation for the noise between 5.25 and 18 min (inset, Figure 4-7) if loss of contact occurred during this period due to movement of the device causing intermittent contact with the electrodes.

4.3.2.3 Trial 3

An hour-long trial with the pod design and straight channel, generation 2, microfluidic chip was carried out on a moderately fit 28 year old male. The sweat began to displace the priming solution at 10 min before reaching a stable signal representative of 19 mM Na^+ at 25 min (3, Figure 4-8). The volunteer lifted his arm at 47 minutes which was followed by an immediate drop in potential from ca. 50 mV to 12 mV before stabilising at 38 mV for the last 12 minutes. This movement artefact is an issue as this could cause errors in the interpretation of the Na^+ concentration. The cause of this shift might be due to movement of the electrodes inside the device which needs to be prevented in future trials.

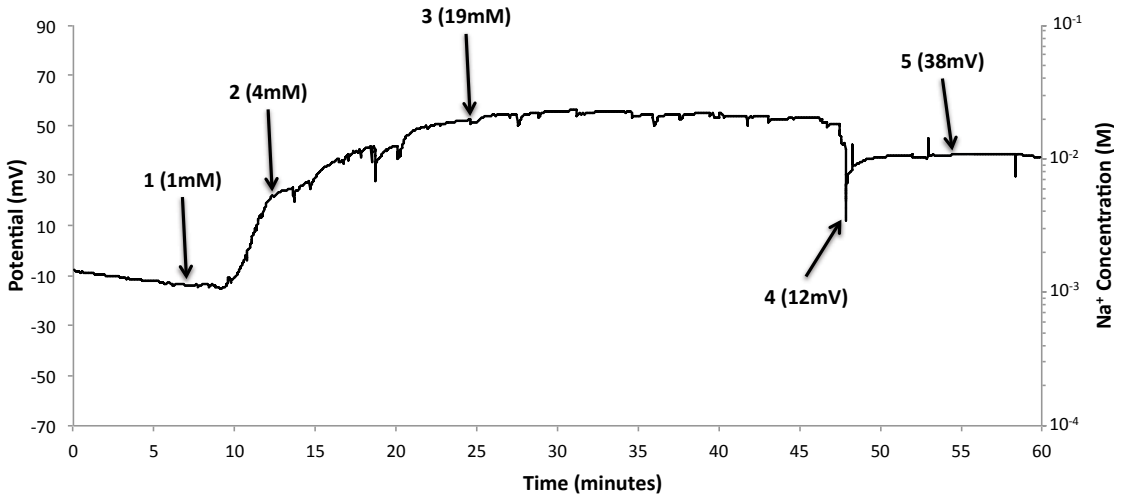

Figure 4-8: A 60 minute on body trial showing the baseline value provided by the priming solution (1) before entry of sweat across the electrodes began at 10 min leading to a sharp rise to 4 mM Na^+ at 12 min (2) before slowing to gradual rise to 19 mM at 25 min (3) where it stabilised for 22 min before movement of the arm caused a drop in potential to 12 mV (4) before partially recovering to 38 mV (5) where it stabilised for the remainder of the trial.

The concentration of 19 µL suggested by comparison with calibration data is at the lower end of the 33.8 ± 15.7 mM normal range suggested by Traeger *et al.* [16]. 358 µL of sweat, under half the maximum capacity of the sampling reservoir (Figure 3.14), was collected from the device suggesting a flow rate of ca. 6 µL/min. This correlates with the 6.5 µL/min of the first trial and further emphasises the probability of a contact issue causing the low 1.39 µL/min flow rate observed in trial 2.

4.4 Conclusion

Despite recent advances and increasing focus by industry and academic research teams, gathering personalised biochemical information in real time remains very challenging, as outlined in the introduction. The two designs investigated have the same contributing components (sampling baseplate, fluidic system, electrochemical sensors, sample storage and capillary driven movement, electronics and power) albeit with pros and cons associated with the designs. For example, the watch-design is more compact and less intrusive for the wearer, while the pod-design enables the electronics and fluidics components to

be physically separated, and allows for larger sample storage volumes (and therefore use periods) due to the increased footprint.

This work has demonstrated a wearable prototype platform that can:

- Harvest sweat from a pre-selected location on the body during exercise trials;
- Transport the sweat from the skin to electrodes that measure the Na^+ concentration in the sweat;
- Further transport the sweat to an in-device storage area for subsequent analysis post-trial;
- Make the measured data available in real-time using Bluetooth wireless connectivity.

The trials show the ability of the platform to continuously monitor real-time sweat across the device via the integration of the sensing and fluidic elements with 3D printed housing, custom-built electronics and a customised application programming interface (API). This allowed the monitoring of sweat during exercise for up to 60 minutes with the initial sweating pattern and continuous Na^+ levels observed. Varying levels of noise were evident during the trials suggesting the need to better secure the internal fluidic and electronic components and to optimise contact at the skin/SWEATCH interface in future iterations of the device. The ability of the API to remove significant amounts of noise and allow valuable data to be retrieved was evident in trial 2 showing the importance of user interface and data processing and collection.

These platforms can be developed further to incorporate detection for a range of relevant analytes such as K^+ and other relevant analytes. In addition, constricting the width of the fluidic channel can vary the sampling flow rate through the device. This work has presented very preliminary results from three limited trials. Batches of these platforms are currently being fabricated for further characterisation and use in scaled up trials that should enable a clearer picture of how the Na^+ concentration in sweat varies during exercise trials to emerge.

4.5 References

[1] G. Matzeu, L. Florea, and D. Diamond, 'Advances in wearable chemical sensor design for monitoring biological fluids', *Sens. Actuators B Chem.*, vol. 211, pp. 403–418, May 2015.

[2] H. G. DeYoung, 'Biosensors: The Mating of Biology and Electronics', *High Technol.*, pp. 41–49, Nov. 1983.

[3] B. Schazmann *et al.*, 'A wearable electrochemical sensor for the real-time measurement of sweat sodium concentration', *Anal. Methods*, vol. 2, no. 4, pp. 342–348, Apr. 2010.

[4] A. J. Bandodkar *et al.*, 'Epidermal tattoo potentiometric sodium sensors with wireless signal transduction for continuous non-invasive sweat monitoring', *Biosens. Bioelectron.*, vol. 54, pp. 603–609, Apr. 2014.

[5] J. Kim *et al.*, 'Non-invasive mouthguard biosensor for continuous salivary monitoring of metabolites', *Analyst*, vol. 139, no. 7, pp. 1632–1636, Mar. 2014.

[6] H. Yao, A. J. Shum, M. Cowan, I. Lähdesmäki, and B. A. Parviz, 'A contact lens with embedded sensor for monitoring tear glucose level', *Biosens. Bioelectron.*, vol. 26, no. 7, pp. 3290–3296, Mar. 2011.

[7] 'Smart contact lenses move closer to reality: Novartis and Google announce partnership to develop the new glucose-sensing technology', *diaTribe*, 15-Jul-2014. [Online]. Available: https://diatribe.org/issues/65/new-now-next/11. [Accessed: 28-Nov-2016].

[8] Y. S. Rim *et al.*, 'Printable Ultrathin Metal Oxide Semiconductor-Based Conformal Biosensors', *ACS Nano*, vol. 9, no. 12, pp. 12174–12181, Dec. 2015.

[9] A. Lynch, D. Diamond, and M. Leader, 'Point-of-need diagnosis of cystic fibrosis using a potentiometric ion-selective electrode array', *Analyst*, vol. 125, no. 12, pp. 2264–2267, Jan. 2000.

[10] B. Chua, S. P. Desai, M. J. Tierney, J. A. Tamada, and A. N. Jina, 'Effect of microneedles shape on skin penetration and minimally invasive continuous glucose monitoring in vivo', *Sens. Actuators Phys.*, vol. 203, pp. 373–381, Dec. 2013.

[11] W. Gao *et al.*, 'Fully integrated wearable sensor arrays for multiplexed in situ perspiration analysis', *Nature*, vol. 529, no. 7587, pp. 509–514, Jan. 2016.

[12] 'Abbott's FreeStyle Libre – Transforming Glucose Monitoring Through Utter Simplicity, Fingersticks Aside!', *diaTribe*, 09-Jan-2015. [Online]. Available: https://diatribe.org/abbott-freestyle-libre-transforming-glucose-monitoring-through-utter-simplicity-fingersticks. [Accessed: 28-Nov-2016].

[13] X. Huang *et al.*, 'Stretchable, Wireless Sensors and Functional Substrates for Epidermal Characterization of Sweat', *Small*, vol. 10, no. 15, pp. 3083–3090, Aug. 2014.

[14] A. J. Bandodkar and J. Wang, 'Non-invasive wearable electrochemical sensors: a review', *Trends Biotechnol.*, vol. 32, no. 7, pp. 363–371, Jul. 2014.

[15] M. H. Rosner and J. Kirven, 'Exercise-Associated Hyponatremia', *Clin. J. Am. Soc. Nephrol.*, vol. 2, no. 1, pp. 151–161, Jan. 2007.

[16] N. Traeger, Q. Shi, and A. J. Dozor, 'Relationship between sweat chloride, sodium, and age in clinically obtained samples', *J. Cyst. Fibros.*, vol. 13, no. 1, pp. 10–14, Jan. 2014.

[17] S. J. Montain, S. N. Cheuvront, and M. N. Sawka, 'Exercise associated hyponatraemia: quantitative analysis to understand the aetiology', *Br. J. Sports Med.*, vol. 40, no. 2, pp. 98–105, Feb. 2006.

Chapter 5 Conclusions and Future Work

5.1 Summary of SWEATCH Platform Development

The recent successes in mobile and wearable technologies including smart phones and smart watches have driven investors such as Google and Novartis to look for the next technological breakthroughs in the world of non-invasive chemical sensing [1]. The arising economical and technological environment is creating optimal circumstances for research in areas such as chemical sensing to be combined, in a multidisciplinary approach, with others to realise products which may thrive in clinical and commercial settings such as non-invasive wearable sensing [2], [3].

As outlined in Chapter 1 there are many areas within non-invasive sensing for which wearable technologies can and are being developed including ocular fluid, saliva and sweat based sensing [4]–[6]. Sweat based sensing is especially desirable as it can be used to develop devices worn on many areas of the body and these devices can be based on or combined with strategies already employed in wearable devices such as fitness trackers. One example of this is the development of sensors for real time electrolyte monitoring in athletes as a means of identifying the non-symptomatic early stages of dehydration and fatigue [7], [8].

The work presented in Chapters 2 to 4 aimed to develop a fully integrated platform for Na^+ detection in sweat. The work incorporated 3 main elements, the development of a miniaturised potentiometric sensor incorporating solid contact Na^+ ISE and RE electrodes, the design and development of a fluidic system for the sampling of sweat from the skin and its delivery across the electrodes and finally, the integration of these elements with electronics and 3D-printed housing for the realisation of a fully integrated platform for electrolyte testing in sweat.

The miniaturised potentiometric sensor, presented in chapter 2, consisted of a PET substrate with 3 functional layers, 1; a screen-printed electron conducting carbon layer, 2; an electrodeposited PEDOT/Ionic-liquid solid contact ion to electron transduction layer and 3; reference or ion selective capping membrane layers. A calixarene based compound was used for Na^+ sensitivity in the dropcast ISE membrane [9] while an ionogel based photopolymerised membrane was used for the RE [10]. A test of ten of the combination ion sensitive/reference electrodes showed reproducible Nernstian responses of 58.9 mV/decade ± 1.59 mV over a range of 10^{-4} to 10^{-1} a_{Na^+}.

A custom designed fluidic system was developed with 2 primary components, a 3D printed sweat harvester and a PMMA based microfluidic chip (see chapter 3). A capillary inlet in the harvesting device directs the sample into the microfluidic chip through a channel across the ISE and RE and into a sampling reservoir. Three strategies were investigated for passive fluid transfer in the microfluidic channel with optimal results observed using a cotton thread and a cellulose/polypropylene adsorbent material to assist flow in the capillary channel. This configuration was shown to maintain flow across the electrodes while maintaining an accurate representation of sample Na^+ activity in real time. Flow rate can be varied by changing the width of the connecting channel from the electrodes to the sampling reservoir.

Chapter 4 presented SWEATCH, the end result of the platform development, a wearable fully integrated sweat electrolyte monitoring device in two designs one, 'watch' for sweat sampling from the wrist and a 'pod' shaped system for adaptive wearing on multiple sites. A custom designed electronic circuit board, powered by a rechargeable lithium battery, provided data collection, processing and wireless communication via a Bluetooth module. 3D-printed housings were designed to hold the sensing, fluidic and electronic components and keep the sweat harvesting component in contact with the skin during trials with a stretchable elastic band.

Preliminary on body trials (see chapter 4) were carried out with the 'pod' device positioned on the upper arm displayed the ability of the device to collect and analyse sweat sample in real time for periods of up to 60 minutes. The three trials presented showed the initial entry of sweat after ca. 4 to 10 minutes cycling before reaching a steady state reflecting sodium concentration at between ca. 10 and 25 minutes with both flow rate and concentration varying among the three volunteers.

5.2 Future Work

Future trials will include more extensive studies with 'pod' and 'watch' (Figure 5-1) designs modified for more compact positioning of the electronic, fluidic and sensor components while ensuring maximum constant contact with the skin to minimise movement artefacts observed in trials and outlined in section 4.3.2. The ability to successfully sample excess sweat from the skin and across electrodes for continuous indirect sensing should be compared with sensing directly on the skin to properly evaluate the two strategies.

Figure 5-1: Improved SWEATCH 'watch' type platform with a render (left) showing the individual components including; fluidics and potentiometric sensing (1), electronics (2), lithium polymer battery (3) and 3D-printed housing beside a render of the enclosed system (left) with strap and a photo of the realised device (right)

The preliminary stability studies in chapter two suggest that to optimise electrode performance the electrodes may benefit from investigation of other strategies such as incorporation of nano-materials in the solid contact layer to

minimise potential drift. Strategies have been employed by Hu *et al.* [11] and Paczosa-Bator [12] incorporating colloid-imprinted mesoporous (CIM) carbon and a carbon black/graphene mix as solid contact, in two separate studies, achieving potential drift of 1.3 μV/h and less than 1 μV/h respectively.

The platform can also be developed further to incorporate multi-analyte sensing adding analytes such as K^+ and Cl^- to provide further information about the wearer [13], [14]. The incorporation of added sensors for these analytes can be achieved by the addition of more electrode tracks on the screen-printed layer (Figure 5-2) and the incorporation of the relevant ion selective membranes in a similar strategy as the Na^+ sensor in Chapter 4. For example, incorporating a valinomycin-based sensor for K^+ sensing instead the calixarene based Na^+ ionophore employed in the electrodes developed in Chapter 2.

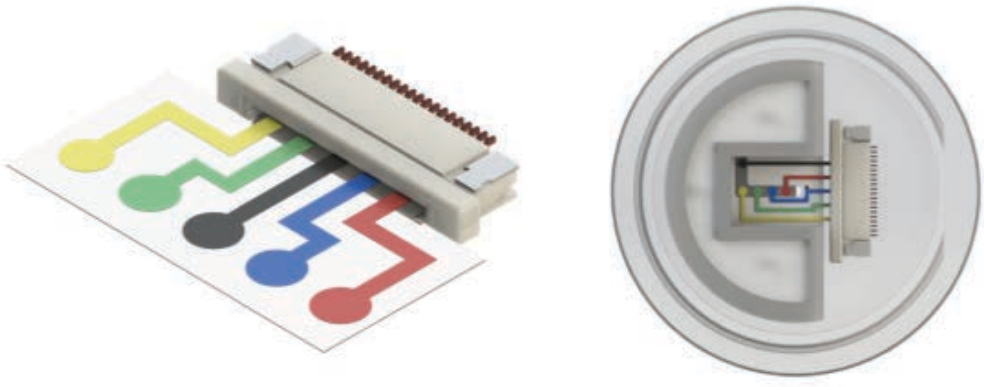

Figure 5-2: CAD rendered examples of strategies for incorporating multi analyte sensing in the SWEATCH sensing platform.

Future developments could include minimising the size of the device and adding flexibility through the incorporation of flexible electronics [15]. Exciting developments are being made in the incorporation of nanomaterials for miniaturised flexible electronics [16] as well as the integration of textile based wearable electronics [17]. The success of the work presented depends on the ability to further develop the SWEATCH platform by integrating advanced electronics and flexible battery technology (see section 1.4.2) to produce a

commercial wearable device able to compete with established and emerging non-invasive chemical sensors [3], [18], [19].

Minimally invasive wearable sensing devices such as the interstitial fluid glucose monitoring Abbott Freestyle Libre provide safer and less traumatic alternatives to traditional methods requiring blood samples [2]. However these methods require dermal penetration, which may still risk irritation and infection. An interesting optical approach to non-invasive chemical sensing can be seen in the BSXinsight which monitors muscle oxygenation through real-time dynamic changes in hemoglobin and myoglobin inside the calf muscle in order to calculate lactate threshold in cyclists [20]. This technology is effective but is currently only available for a very specific application while approaches targeting information rich bio-fluids such as saliva, tear fluid and sweat have a more diverse range of analytes and applications [6], [21], [22].

Gao *et al.* [18] and Rose *et al.* [19] have developed fully integrated devices for non-invasive monitoring of electrolytes and other analytes in sweat in real-time. These flexible and wearable devices monitor sweat with sensors in direct contact with sweat on the skin surface which may be susceptible to accumulation of analytes in the sensing area which may prevent accurate analysis of sweat samples in real-time. SWEATCH provides a means of removing the sweat from the sampling area as it accumulates moving it across the sensors located within the device, for real-time monitoring of electrolytes, into a sampling reservoir from which it can be removed for further analysis.

5.3 References

[1] ‘Smart contact lenses move closer to reality: Novartis and Google announce partnership to develop the new glucose-sensing technology’, *diaTribe*, 15-Jul-2014. [Online]. Available: https://diatribe.org/issues/65/new-now-next/11. [Accessed: 28-Nov-2016].

[2] ‘Abbott’s FreeStyle Libre – Transforming Glucose Monitoring Through Utter Simplicity, Fingersticks Aside!’, *diaTribe*, 09-Jan-2015. [Online]. Available: https://diatribe.org/abbott-freestyle-libre-transforming-glucose-monitoring-through-utter-simplicity-fingersticks. [Accessed: 28-Nov-2016].

[3] ‘Wearable Muscle Oxygen Monitor & Lactate Threshold’. [Online]. Available: https://www.bsxinsight.com/. [Accessed: 15-Dec-2016].

[4] A. J. Bandodkar and J. Wang, ‘Non-invasive wearable electrochemical sensors: a review’, *Trends Biotechnol.*, vol. 32, no. 7, pp. 363–371, Jul. 2014.

[5] G. Matzeu, L. Florea, and D. Diamond, ‘Advances in wearable chemical sensor design for monitoring biological fluids’, *Sens. Actuators B Chem.*, vol. 211, pp. 403–418, May 2015.

[6] T. Deepa and N. Thirrunavukkarasu, ‘Saliva as a potential diagnostic tool’, *Indian J. Med. Sci.*, vol. 64, no. 7, pp. 293–306, Jul. 2010.

[7] P. Düking, A. Hotho, H.-C. Holmberg, F. K. Fuss, and B. Sperlich, ‘Comparison of Non-Invasive Individual Monitoring of the Training and Health of Athletes with Commercially Available Wearable Technologies’, *Front. Physiol.*, vol. 7, Mar. 2016.

[8] M. H. Rosner and J. Kirven, ‘Exercise-Associated Hyponatremia’, *Clin. J. Am. Soc. Nephrol.*, vol. 2, no. 1, pp. 151–161, Jan. 2007.

[9] D. Diamond, G. Svehla, E. M. Seward, and M. A. McKervey, 'A sodium ion-selective electrodebased on methyl p-t-butylcalix[4]aryl acetate as the ionophore', *Anal. Chim. Acta*, vol. 204, pp. 223–231, Jan. 1988.

[10] C. Zuliani, G. Matzeu, and D. Diamond, 'A liquid-junction-free reference electrode based on a PEDOT solid-contact and ionogel capping membrane', *Talanta*, vol. 125, pp. 58–64, Jul. 2014.

[11] J. Hu, X. U. Zou, A. Stein, and P. Bühlmann, 'Ion-Selective Electrodes with Colloid-Imprinted Mesoporous Carbon as Solid Contact', *Anal. Chem.*, vol. 86, no. 14, pp. 7111–7118, Jul. 2014.

[12] B. Paczosa-Bator, 'Ion-selective electrodes with superhydrophobic polymer/carbon nanocomposites as solid contact', *Carbon*, vol. 95, pp. 879–887, Dec. 2015.

[13] L. van de Velde, E. d'Angremont, and W. Olthuis, 'Solid contact potassium selective electrodes for biomedical applications – a review', *Talanta*, vol. 160, pp. 56–65, Nov. 2016.

[14] N. Traeger, Q. Shi, and A. J. Dozor, 'Relationship between sweat chloride, sodium, and age in clinically obtained samples', *J. Cyst. Fibros.*, vol. 13, no. 1, pp. 10–14, Jan. 2014.

[15] S. H. Kang and S. W. Hong, 'Recent Progress in Flexible/Wearable Electronics', *J. Weld. Join.*, vol. 32, no. 3, pp. 34–42, 2014.

[16] D. Chen, J. Liang, and Q. Pei, 'Flexible and stretchable electrodes for next generation polymer electronics: a review', *Sci. China Chem.*, vol. 59, no. 6, pp. 659–671, Jun. 2016.

[17] L. M. Castano and A. B. Flatau, 'Smart fabric sensors and e-textile technologies: a review', *Smart Mater. Struct.*, vol. 23, no. 5, p. 53001, 2014.

[18] W. Gao *et al.*, 'Fully integrated wearable sensor arrays for multiplexed in situ perspiration analysis', *Nature*, vol. 529, no. 7587, pp. 509–514, Jan. 2016.

[19] D. P. Rose *et al.*, 'Adhesive RFID Sensor Patch for Monitoring of Sweat Electrolytes', *IEEE Trans. Biomed. Eng.*, vol. 62, no. 6, pp. 1457–1465, Jun. 2015.

[20] 'What is BSXinsight and how does it work?', *BSX Athletics*. [Online]. Available: http://support.bsxinsight.com/hc/en-us/articles/204394525-What-is-BSXinsight-and-how-does-it-work-. [Accessed: 01-Jan-2017].

[21] N. M. Farandos, A. K. Yetisen, M. J. Monteiro, C. R. Lowe, and S. H. Yun, 'Contact Lens Sensors in Ocular Diagnostics', *Adv. Healthc. Mater.*, vol. 4, no. 6, pp. 792–810, Apr. 2015.

[22] A. Mena-Bravo and M. D. Luque de Castro, 'Sweat: A sample with limited present applications and promising future in metabolomics', *J. Pharm. Biomed. Anal.*, vol. 90, pp. 139–147, Mar. 2014.

Appendix

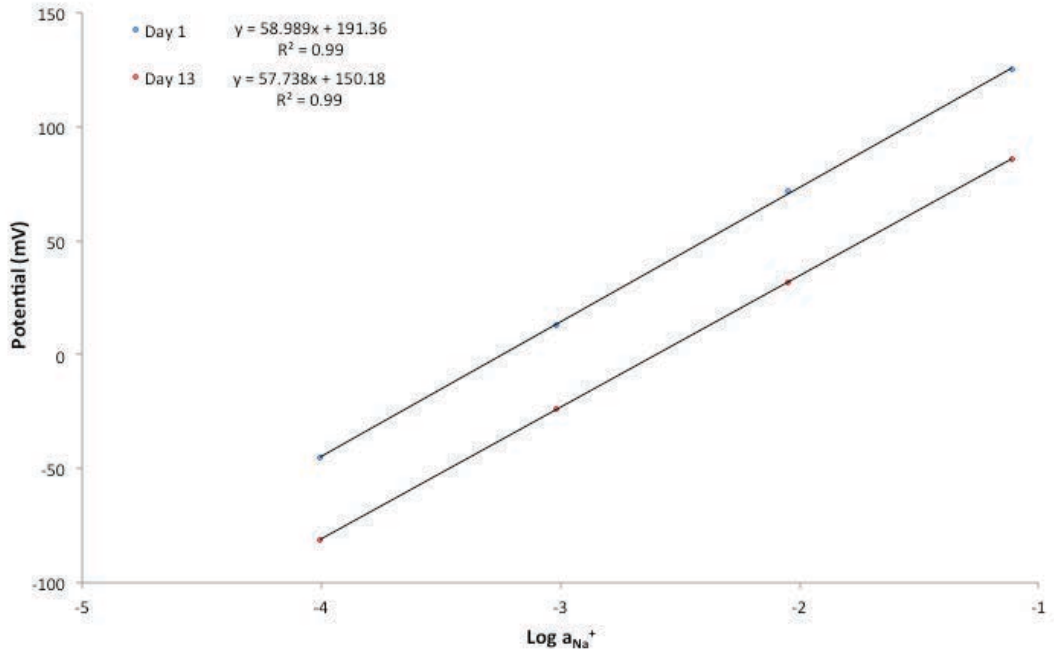

Figure A-1: Calibration data from a storage stability study of Sensor 1 on Day 1 and on Day 13 after storage in the dark at room temperature.

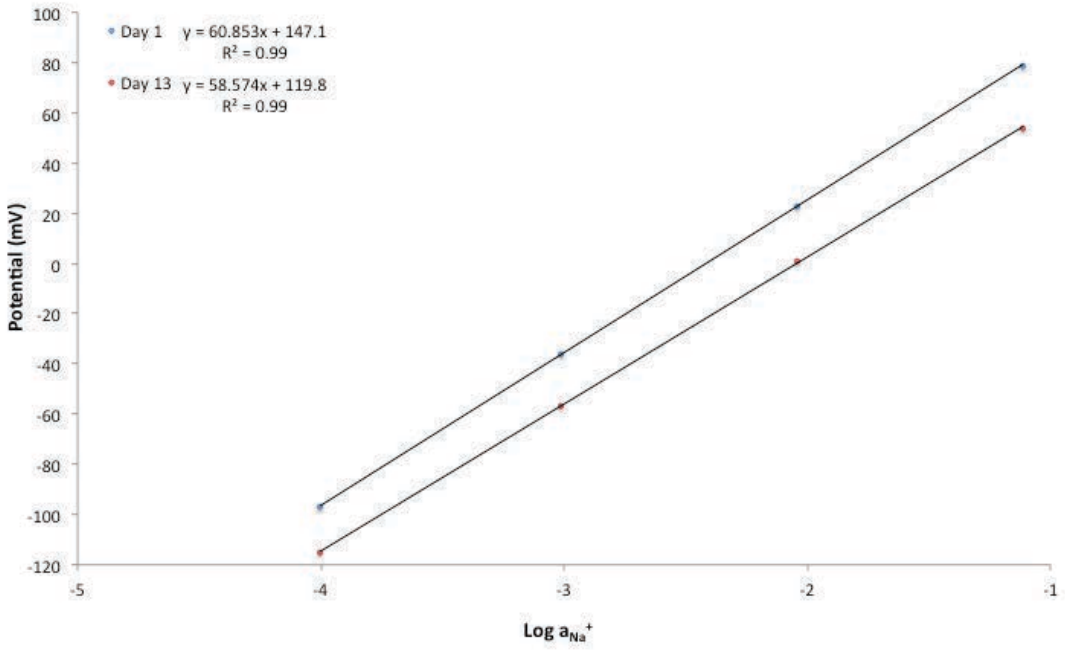

Figure A-2: Calibration data from a storage stability study of Sensor 2 on Day 1 and on Day 13 after storage in the dark at room temperature.

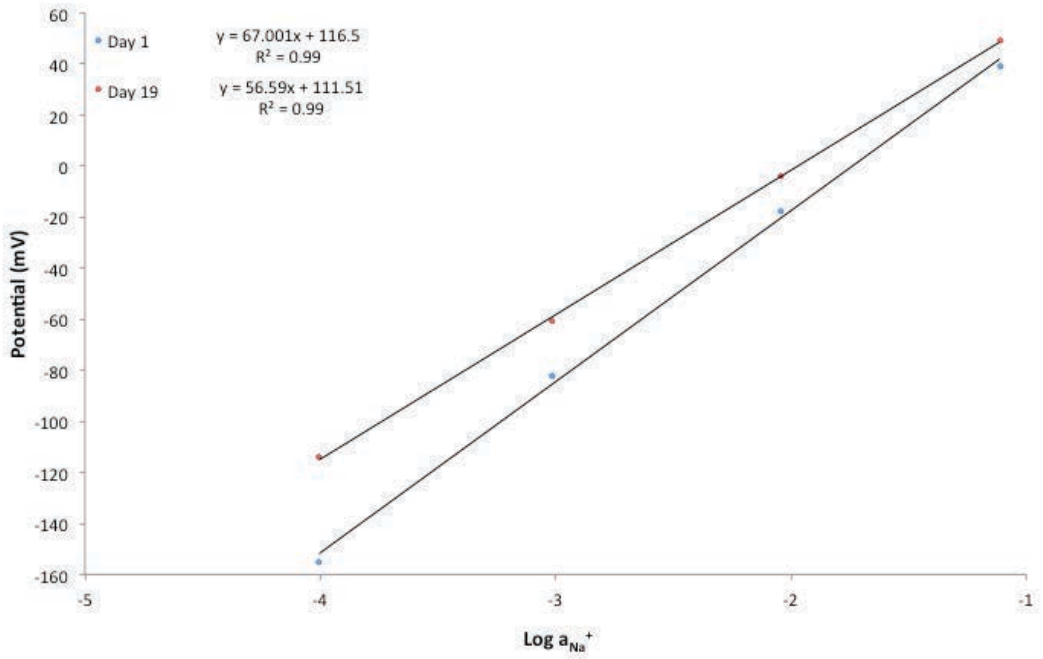

Figure A-3: Calibration data from a storage stability study of Sensor 3 on Day 1 and on Day 19 after storage in the dark at room temperature.

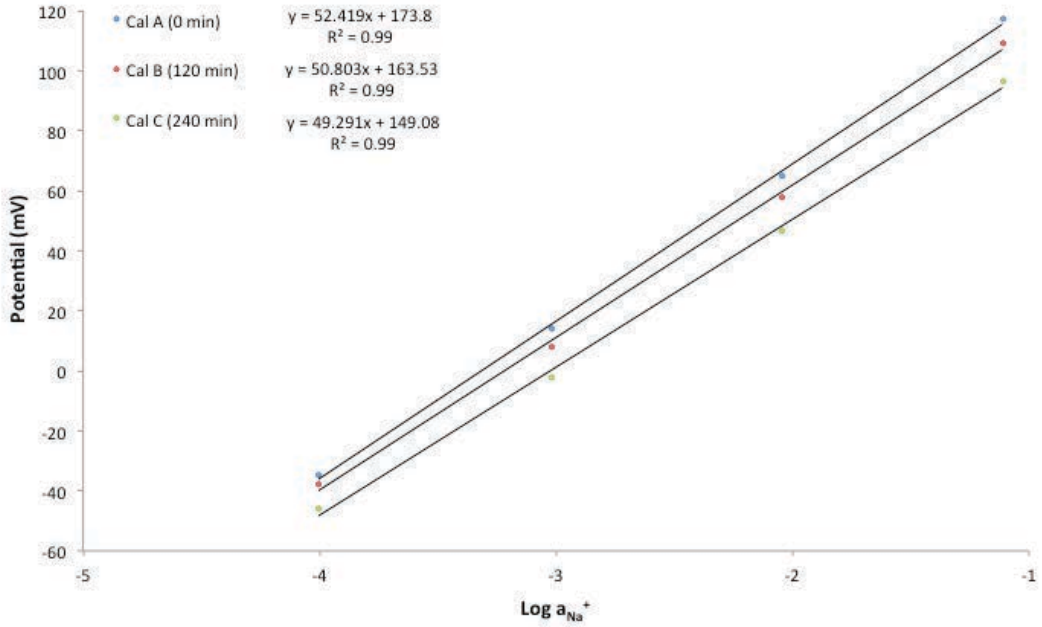

Figure A-4: Calibration data from a study into the effect of prolonged Na^+ exposure on Sensor 1 showing initial data (0min) compared to data after 120 min exposure to 10 mM NaCl (120 min) and an immediate 120 min subsequent exposure to 50 mM NaCl (240 min).

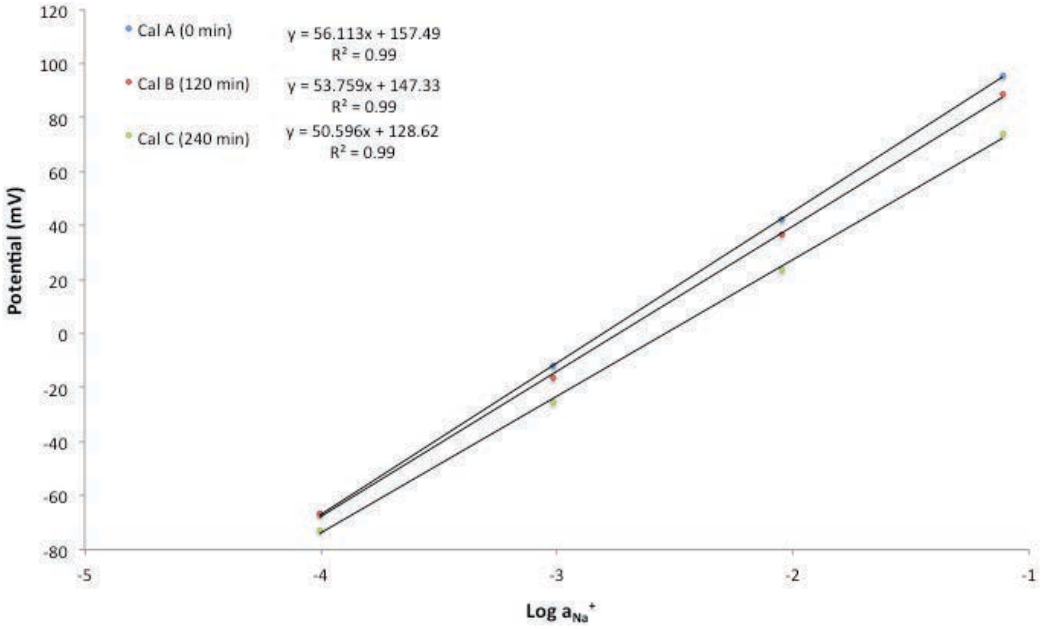

Figure A-5: Calibration data from a study of the effect of prolonged Na^+ exposure on Sensor 2 showing initial data (0min) compared to data after 120 min exposure to 10 mM NaCl (120 min) and an immediate 120 min subsequent exposure to 50 mM NaCl (240 min).